# SEISMIC INTERSTORY DRIFT DEMANDS IN STEEL FRICTION DAMPED BRACED BUILDINGS

A Thesis

by

LUIS EDUARDO PETERNELL ALTAMIRA

Submitted to the Office of Graduate Studies of
Texas A&M University
in partial fulfillment of the requirements for the degree of

MASTER OF SCIENCE

May 2009

Major Subject: Civil Engineering

# SEISMIC INTERSTORY DRIFT DEMANDS IN STEEL FRICTION DAMPED BRACED BUILDINGS

A Thesis

by

LUIS EDUARDO PETERNELL ALTAMIRA

Submitted to the Office of Graduate Studies of
Texas A&M University
in partial fulfillment of the requirements for the degree of

MASTER OF SCIENCE

Approved by:

| | |
|---|---|
| Chair of Committee, | Gary T. Fry |
| Committee Members, | Terry Creasy |
| | Terry Kohutek |
| Head of Department, | David Rosowsky |

May 2009

Major Subject: Civil Engineering

# ABSTRACT

Seismic Interstory Drift Demands in Steel Friction Damped Braced Buildings.

(May 2009)

Luis Eduardo Peternell Altamira, B.S., Universidad de las Américas, Puebla, Mexico

Chair of Advisory Committee: Dr. Gary T. Fry

In the last 35 years, several researchers have proposed, developed and tested different friction devices for seismic control of structures. Their research has demonstrated that such devices are simple, economical, practical, durable and very effective.

However, research on passive friction dampers, except for few instances, has not been given appropriate attention lately. This has caused some of the results of old studies to become out-of-date, lose their validity in the context of today's design philosophies or to fall short on the expectations of this century's structural engineering.

An analytical study on the behavior of friction devices and the effect they have on the structures into which they are incorporated has been undertaken to address the new design trends, codes, evaluation criteria and needs of today's society.

The present study consists of around 7,000 structural analyses that are used to show the excellent seismic performance and economic advantages of Friction Damped Braced Frames. It serves, at the same time, to improve our understanding on their dynamic behavior. Finally, this thesis also sets the basis for future research on the application of this type of seismic energy dissipating systems.

# ACKNOWLEDGEMENTS

I would like to acknowledge the technical guidance and constant motivation provided by my thesis advisor and Chair of Committee Dr. Gary T. Fry.

I appreciate the financial support provided by the Mexican National Council for Science and Technology (CONACyT) and the Texas Transportation Institute (TTI) without which the completion of this stage of my academic life at Texas A&M University would have represented additional challenges.

Finally, I also would like to make use of this opportunity to recognize and thank all those who, among professors and students, contributed with their ideas, experience and/or moral support to the conclusion of this work.

# TABLE OF CONTENTS

Page

Page

# LIST OF FIGURES

Page

Page

Page

Page

Page

Page

# LIST OF TABLES

Page

# 1. INTRODUCTION

The vibration of structures causes damage and destruction; those generated by earthquakes are at the top of the scale (Mead 1998) and have exposed our vulnerability to them even in advanced countries (Soong and Dargush 1997). To cope with earthquake induced forces, the design philosophy is that of providing the structural elements with the necessary strength and ductility. By providing ductility, incursions in the nonlinear range of structural materials will dissipate energy in the form of inherent damping and the amount of energy input into a structure will be limited. However, inelastic deformations will cause a certain level of damage, which has to be kept within acceptable limits.

The nature of earthquake engineering problems can be very complex (Krinitzsky et al. 1993); therefore, understanding of their basics is absolutely necessary to be able to find solutions. A common way to simplify the seismic analysis of structures has been to treat the seismic excitations as a set of equivalent static lateral forces (Soong and Dargush 1997). However, consideration of the dynamic characteristics of earthquake excitations allows more accurate analyses, more efficient designs and has permitted the development of different innovative concepts for seismic protection of structures. These concepts can be categorized into three groups: seismic isolation, passive energy dissipation and active control.

---

This thesis follows the style of the *American Society of Civil Engineers.*

The objective of these technologies is to reduce the energy dissipation demand and the damage caused in the primary structural members. This is achieved through the installation of special devices that will dissipate, at least, part of the energy that is input into a building during a seismic event.

There are four general approaches to achieve passive energy dissipation (Mead 1998):

1. Control by structural design,
2. Control by localized additions,
3. Control by added damping,
4. Control by resilient isolation,

and combinations thereof.

The simple addition of passive structural control devices modifies the stiffness and inherent damping in a structure; when in action, these devices additionally oppose the earthquake generated forces without requiring external control or energy (Mead 1998).

The development of passive energy dissipation devices for structural applications has approximately 35 years of history (Soong and Dargush 1997). These devices were either created specifically for structural engineering applications or were adapted from already available technologies that were used in the automotive, military and/or aerospace industries (Soong and Constantinou 1994).

Practical applications of passive energy dissipation devices have demanded considerable research. During their development, changes have been induced in the way

structural engineering is executed. For instance, (nonlinear) dynamical methods are necessary to model and analyze structures that incorporate passive control devices (Soong and Dargush 1997).

# 2. BACKGROUND

## 2.1 History of Friction Devices

For years, various devices that utilize friction for energy dissipating purposes have been developed and tested (Soong and Constantinou 1994). Although various forms of friction can be used to reduce vibrations and the damage they cause to structures, the most popular type is solid friction (Soong and Dargush 1997).

Thus, the theory of solid friction constitutes the basis for most of the research that has been done on friction dampers. It relies upon the following hypotheses (Soong and Dargush 1997):

1. The friction force is independent of the surface area of contact.
2. The friction force is proportional to the normal force that acts across the sliding interface.
3. The friction force is independent of the sliding velocity.
4. The friction force acts tangentially within the interfacial plane opposing motion.

At the instant just before sliding occurs and while sliding, the friction force $F$ is given by

$$F = \mu N$$

where $N$ is the normal force acting across the sliding interface, and $\mu$ is the coefficient of friction. Since it is common that the coefficient of friction is higher before slippage occurs than it is during sliding, separate static ($\mu_s$) and kinetic ($\mu_k$) coefficients of friction have been defined.

Friction devices do not change the inherent properties of the structure (Chopra 2001), their cost is relatively low, and their installation and maintenance are simple (Mualla and Belev 2002).

In the United States, the earliest work on friction devices appears to be the one of Keightley (1977; 1979) at Montana State University. He proposed friction dampers constructed by clamping together steel plates with bolts and Belleville washers, but did not assess relaxation of the bolts, stability of the system and corrosion within the sliding surfaces.

Around that time, the firm of Severud, Perrone, Sturn and Bendel of New York installed two large friction dampers between the Gorgas hospital and two exterior concrete pylons in the Panama Canal Zone (Soong and Constantinou 1994).

Pall et al. (1980) developed passive friction dampers based upon the automotive brake. They performed a series of static and dynamic tests on various sliding materials with different surface treatments with the objective of identifying those that provided a consistent and predictable response. They found that heavy duty brake lining pads inserted between steel plates showed this desired type of behavior and, later, Pall invented the Limited Slip Bolted (LSB) joint for seismic control of panel structures, which incorporated the brake lining pads (Fig. 2.1). The LSB joints are placed in the joint lines between precast concrete panels; during a seismic event, the concrete wall panels slide relative to each other and energy dissipation and structural protection is achieved through the joints.

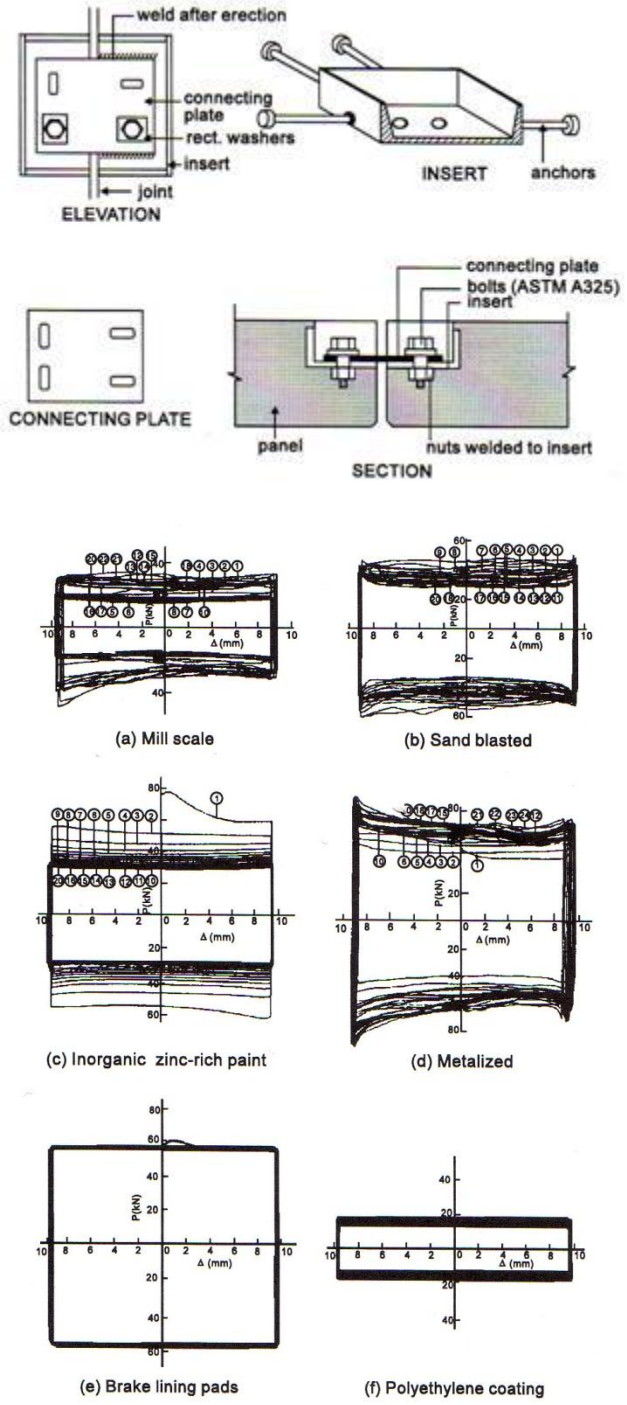


**Figure 2.1:** Hysteresis loops of limited slip bolted joints (Soong and Dargush 1997)

Two years later, Pall and Marsh (1982) developed an alternate design to the LSB (Figs. 2.2 and 2.3) for its use in conjunction with cross braces. It also incorporated brake lining pads and a very peculiar and effective mechanism where the braces do not have to be designed to resist compression forces to work in both lateral directions of movement. When tension in one of the braces forces the joint to slip, it activates the four links which force the joint in the other brace to slip at the same time. Hence, energy is dissipated in both braces in each half cycle of motion, which reciprocrates in the next half cycle. Moreover, in each cycle, the mechanism straightens the buckled "compression" brace and sets it ready for the next half cycle of motion. Filiatrault and Cherry (1987) and Aiken (1988) led studies that showed a superior performance of friction damped braced frames (FDBFs) using this device compared to traditional earthquake resisting systems.

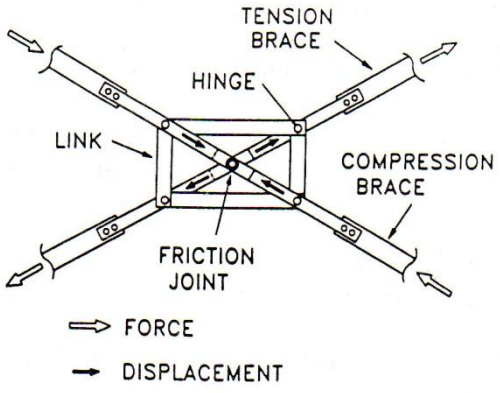


**Figure 2.2:** Friction Damper of Pall (1982)

In Japan, Sumitomo Metal Industries developed another friction damper for structural engineering applications (Fig. 2.4). An experimental study by Aiken (1990) on their device showed a better performance of frames incorporating this device than that of bare moment resisting frames (MRFs). Furthermore, in their experiments, energy dissipation was concentrated in the dampers rather than due to the inelastic action of the structural members.

Fitzgerald (1989) proposed a friction device that utilized slotted bolted connections in concentrically braced frames. One end of the brace is connected to the building frame gusset plate using the channel bracing members shown in Fig 2.5. His device also showed predictable and consistent behavior. Later, Grigorian (1993) tested a slightly different slotted bolted connection that showed more stable frictional characteristics (Fig 2.6).

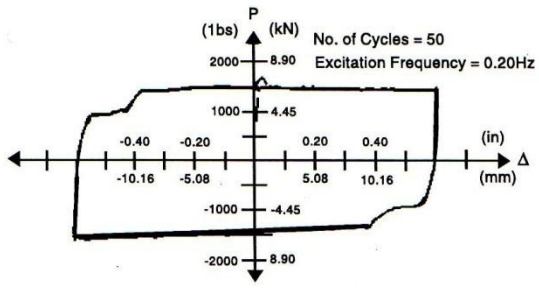


**Figure 2.3:** Hysteresis loops for X-braced friction damper (Soong and Dargush 1997)

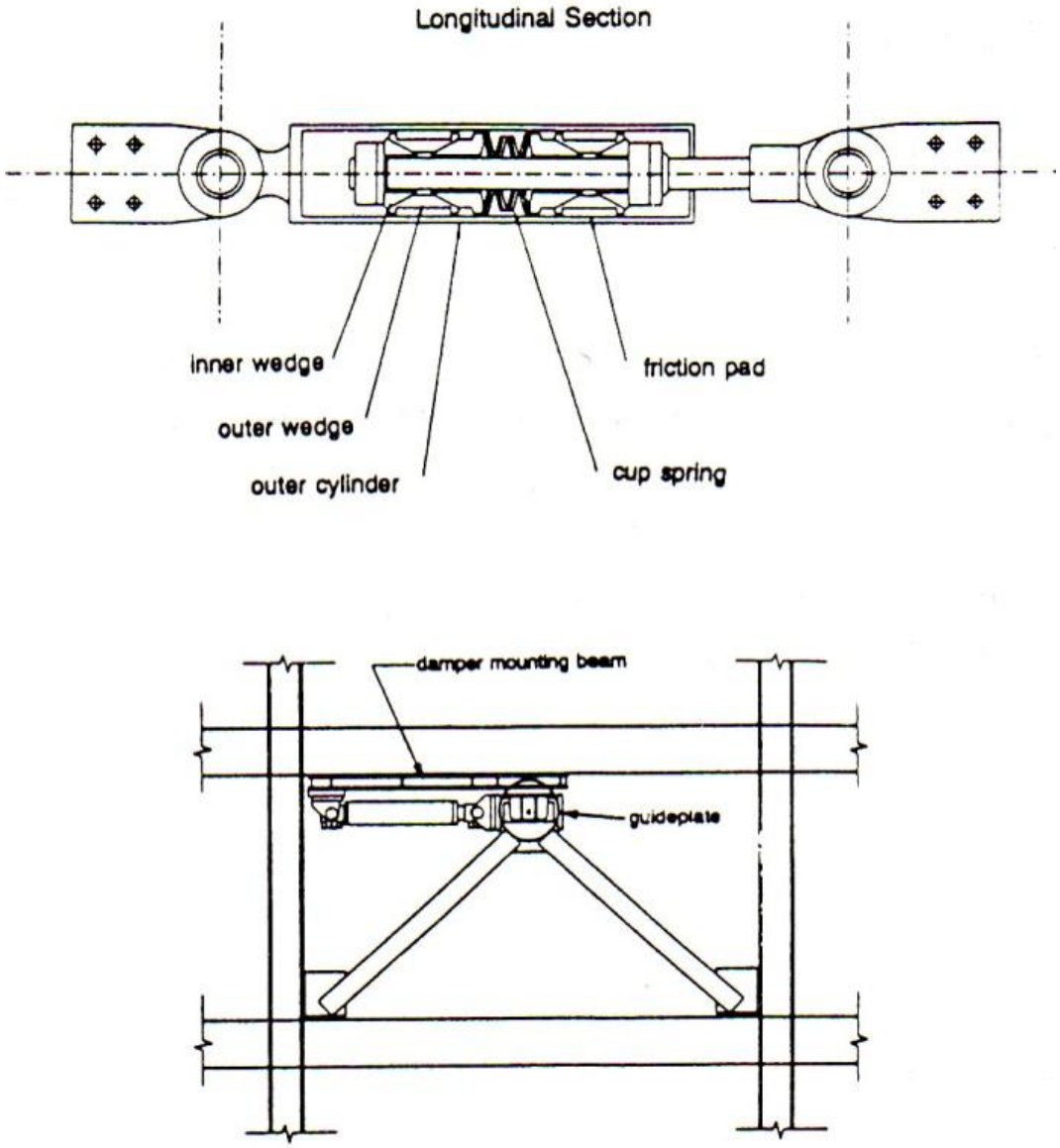


**Figure 2.4:** Sumitomo friction damper and installation detail (Aiken and Kelly 1990)

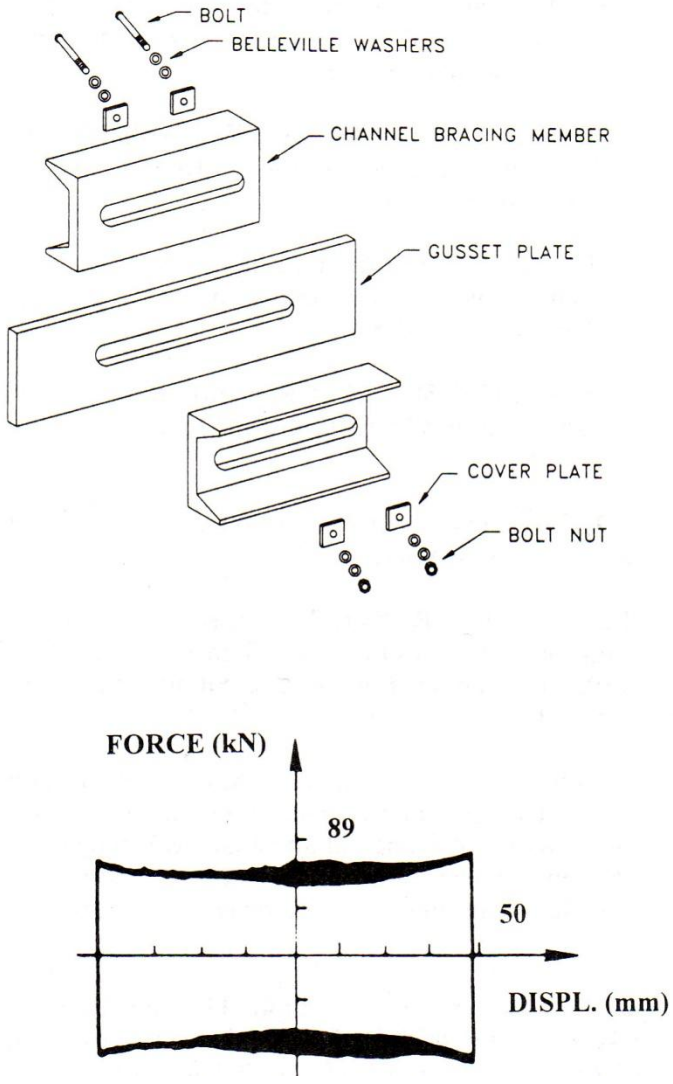


**Figure 2.5:** Slotted bolted connection of Fitzgerald (1989) and typical force-displacement loop

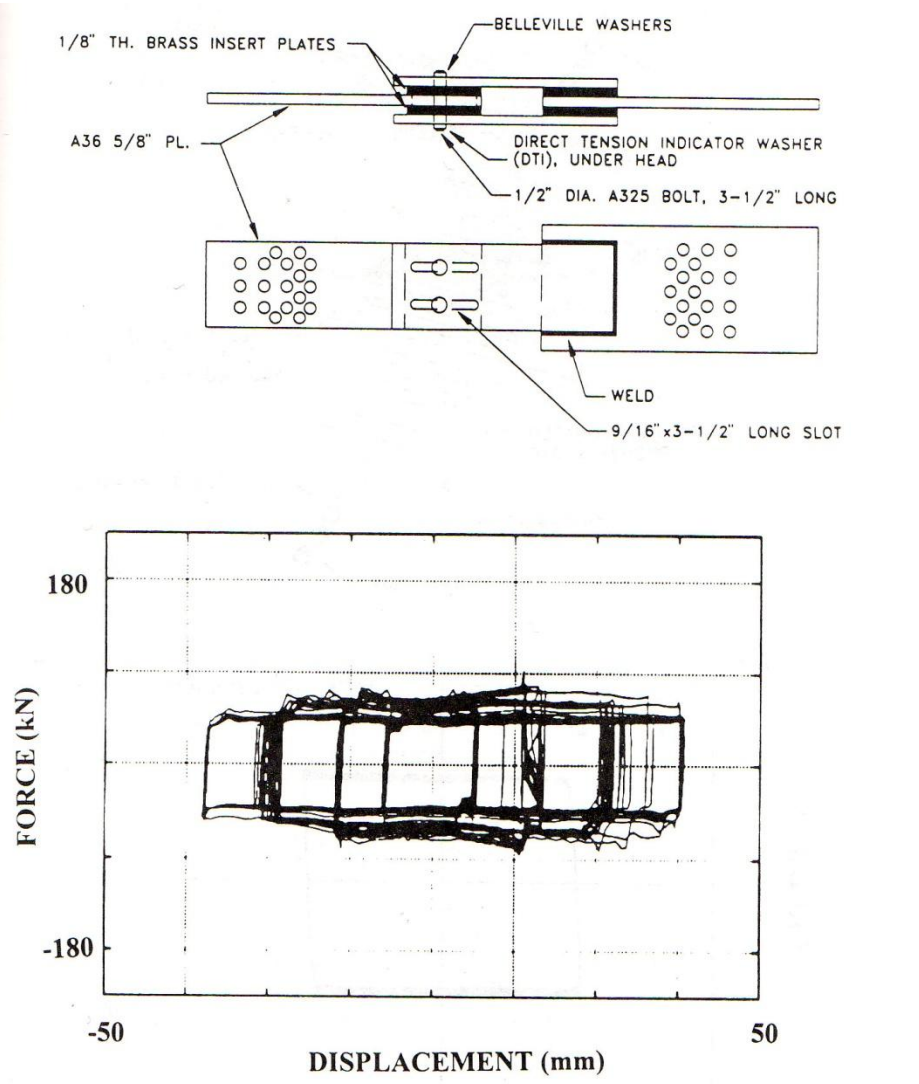


**Figure 2.6:** Slotted bolted connection of Grigorian (1993) and typical force displacement loop

Constantinou (Constantinou et al. 1991a; Constantinou et al. 1991b) developed a very stable friction device for bridge seismic isolation applications (Fig. 2.7) and Fluor Daniel invented a device with self-centering characteristics called Energy Dissipating Restraint (EDR) (Fig 2.8) (Soong and Constantinou 1994). Researchers coincided in the ease of construction of their friction devices.

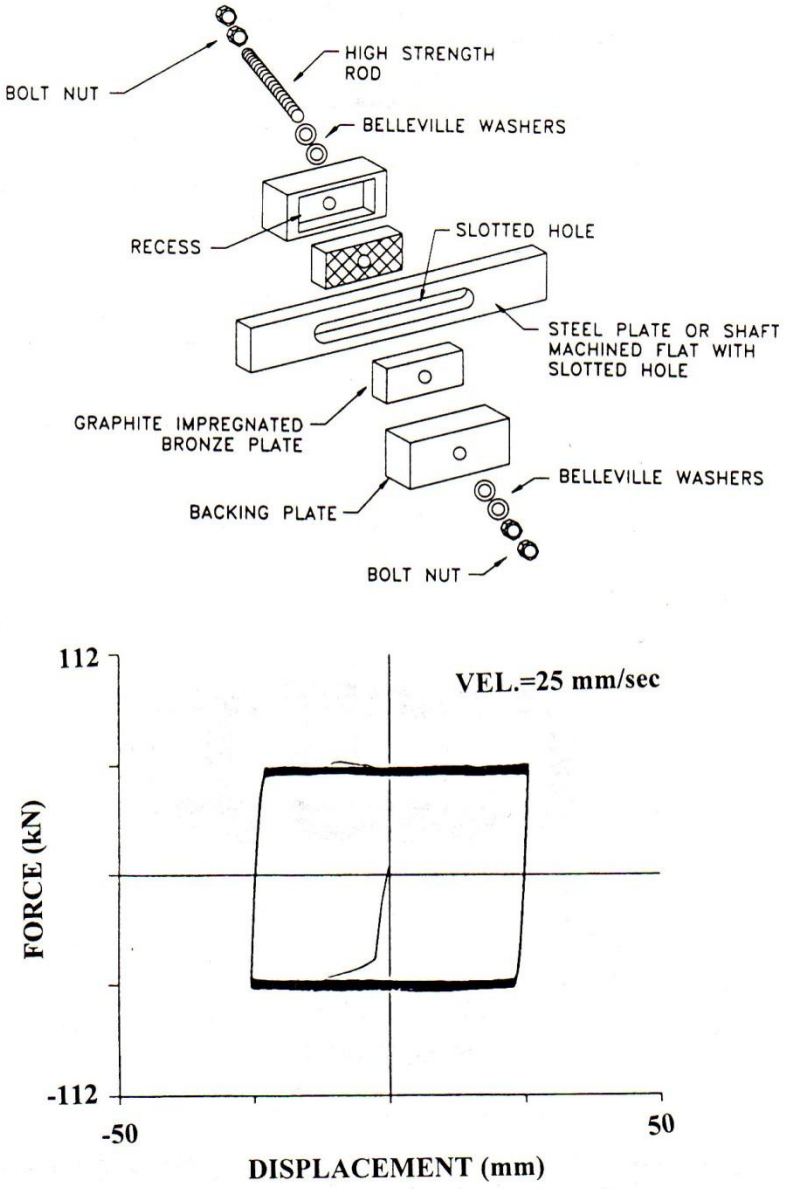


**Figure 2.7:** Friction device of Constantinou (1991a) and force-displacement loop in 200-cycle test

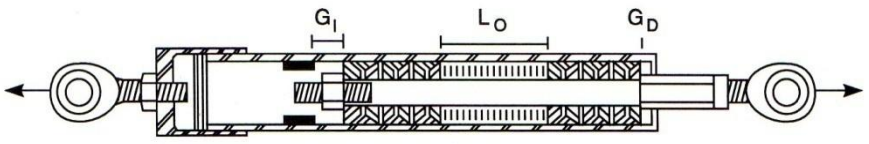


**Figure 2.8:** EDR configuration schematic (Soong and Dargush 1997)

Since metallic surfaces are prone to corrosion, a major problem that researchers faced with friction dampers was that of maintaining the original properties of the sliding materials over time. Also, since relaxation in the clamping parts is to be expected, maintaining of the normal load on the sliding interfaces became an issue; however, as will be shown later, small variations in the clamping (normal) force on the sliding interfaces will have very little effect on the performance of FDBFs, thus, it is possible to anticipate this relaxation by initially applying an adequately chosen larger clamping force which later relaxes to the friction force determined in design.

Research and actual applications around the world have demonstrated that friction dampers represent an inexpensive and effective way to reduce seismic response parameters while the integrity of the structural elements is protected. Conclusions by Pall and Marsh (1982) serve to describe the general characteristics of friction devices. These are:

1. Energy is dissipated by the friction devices rather than by the inelasticity of structural members.
2. The structure in question is softened with a relatively small loss of elasticity and recovers leaving little or no residual deformations.
3. The friction devices act like a fuse that limits the forces that act on the structure.
4. The amplitude of displacements and accelerations is considerably reduced.
5. The devices limit the amount of energy that is input into the structure.

6. The building can be tuned for optimum response without resorting to expensive devices.

Many of these advantages motivated continuous research and application of friction dampers as a means of passive and (semi) active control of structures (Mualla and Belev 2002).

## 2.2 Pall Friction Dampers

Pall friction dampers are manufactured by Pall Dynamics Ltd (PDL) and are available for tension-only cross bracing (Fig. 2.9), single diagonal tension/compression bracing (Fig. 2.10) and chevron bracing (Fig. 2.11).

Pall dampers consist of a series of steel plates that are clamped together and treated to offer consistent and predictable friction properties. They possess rectangular hysteresis loops with negligible fade (Fig. 2.12) and their performance is independent of the sliding velocity and temperature (Pall and Pall 2004).

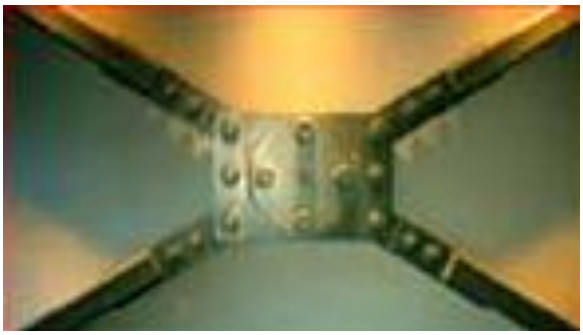

**Figure 2.9:** X-braced friction damper (PDL)

**Figure 2.10:** Diagonal tension/compression braced friction damper (PDL)

**Figure 2.11:** Chevron-braced friction damper (PDL)

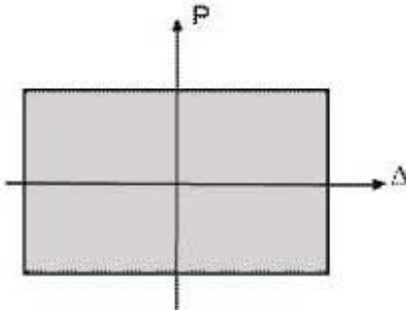


**Figure 2.12:** Hysteresis loop (Pall and Pall 2004)

With Pall friction dampers stiffness is also added to the buildings and a bigger amount of energy can be dissipated through friction than any other method like yielding of steel or viscous and viscoelastic dampers (damping of 20 to 50% of critical can be achieved). They do not need any energy source to operate and they do not require maintenance or replacement after earthquakes. (Pall and Pall 2004).

Several parametric studies have shown that the slip load of a friction damper is the principal variable. If the slip load is too low or too high, the response will be relatively high; that is, if the slip (friction) force is too high, the damper may not slide at all times and, thus, energy dissipation will be low if not nil (Nishitani et al. 1999). On the other hand, if the slip force is too low, the energy dissipation will also be low, even during large deflections (Pall and Pall 2004). As can be expected, an optimized slip load will give a minimum response (Fig. 2.13).

Variations of up to ±20% in the optimum slip load of the dampers will not affect the dynamic response significantly. Therefore, the less than 20% decrease in slip load that will occur in the devices due to the relaxation of the bolts over the life of the structure will not imply maintenance or replacement (Pall and Pall 2004).

ASCE-41/FEMA-356 (ASCE 2007; FEMA 2000) guidelines require that friction dampers are designed for 130% the displacements under BSE-2 earthquakes (defined later) and that all bracing and connections are designed to resist 130% of the damper slip load. Also, the variations in slip load from the design value should not be more than ±15% to guarantee the design response.

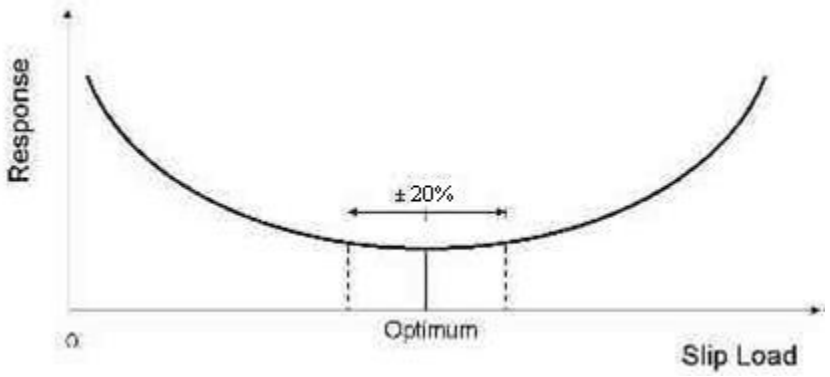


**Figure 2.13:** Response versus slip-load (Pall and Pall 2004)

## 2.3 Seismic Strengthening of Structures

The protection of civil structures is a global priority (Ohtori et al. 2004). Awareness of seismic risk, advancement of new seismic protection concepts and changes in codes may require additional protection of existing structures. This protection can be achieved through replacement or strengthening of inadequate structures (Coburn and Spence 2002).

Replacement of unsafe structures is very slow: new construction rates reach 1% per year in advanced nations and up to 8% per year in some emerging countries (Booth and Key 2006). Meanwhile, a great part of the rest of the building stock cannot be considered safe.

On the other hand, Coburn and Spence (2002) state that, for most types of buildings, strengthening is a less expensive way of increasing earthquake resistance than replacement. They discuss the application of cost-benefit analysis to strengthening and mention additional factors to be taken into account when considering strengthening a building.

Apart from serving for economically increasing the level of seismic resistance, strengthening can also be used for rehabilitation and extension of the lifespan of buildings (Booth and Key 2006). The convenience of strengthening versus rebuilding has increased its popularity around the world.

The ASCE-31 standard (ASCE 2003) provides guidelines for the determination of the necessity for strengthening of buildings. If the decision of retrofitting a structure has already been taken, ASCE-41 (ASCE 2007), which is the latest generation of a

series of performance based seismic rehabilitation (pre) standards, will serve for extensive and complete guidance on the process.

## 2.4 Performance Based Design

Performance based design (PBD) is a design philosophy in which the design criteria are expressed in terms of established structural performance objectives (Fig. 2.14) when the structure is subjected to different levels of seismic hazard (Ghobarah 2001).

In PBD, the displacement response of a structure is related to a strain-based limit state which, in turn, is related to a level of damage (strains and deformations are better damage indicators than the more commonly used stresses (Moehle 1996)). The level of damage is related to a probability of failure under a probability of seismic demand and serves to measure the structural performance.

Specific values of interstory drift ratios have been associated with the different structural performance/damage levels for different structural systems and materials. For steel MRFs these values and their structural performance/damage equivalences are given in Fig. 2.15.

ASCE-41 defines two basic Earthquake Hazard Levels: the Basic Safety Earthquake 1 (BSE-1) and the Basic Safety Earthquake 2 (BSE-2). For their definition, reference is made to the 10%/50-year probabilistic maps and the Maximum Considered Earthquake (MCE) maps developed in Project 97. The BSE-1 are taken from the 10%/50-year maps, which have a 10% probability of exceedance in 50 years, and the

BSE-2 shall be obtained from the MCE maps which, in most areas of the United States, have a 2% probability of exceedance in 50 years.

ASCE-41 also defines 3 general rehabilitation objectives for buildings; namely, reduced, basic and enhanced rehabilitation objectives. For the elaboration of the present work, the Basic Safety Objective (BSO) was chosen. The BSO is a rehabilitation objective that achieves the dual rehabilitation goals of Life Safety Building Performance Level (3-C) for the BSE-1 Earthquake Hazard Level and Collapse Prevention Building Performance Level (5-E) for the BSE-2 Earthquake Hazard Level (Table 2.1). The BSO is intended to approximate the earthquake risk to life safety traditionally considered acceptable in the United States. Buildings meeting the BSO are expected to experience little damage from relatively frequent, moderate earthquakes, but significantly more damage and potential economic loss from the most severe and infrequent earthquakes (ASCE 2007).

| | Target Building Performance Levels | | | |
|---|---|---|---|---|
| | **Collapse Prevention Level (5-E)** | **Life Safety Level (3-C)** | **Immediate Occupancy Level (1-B)** | **Operational Level (1-A)** |
| **Overall Damage** | Severe | Moderate | Light | Very Light |
| General | Little residual stiffness and strength, but load-bearing columns and walls function. Large permanent drifts. Some exits blocked. Infills and unbraced parapets failed or at incipient failure. Building is near collapse. | Some residual strength and stiffness left in all stories. Gravity-load-bearing elements function. No out-of-plane failure of walls or tipping of parapets. Some permanent drift. Damage to partitions. Building may be beyond economical repair. | No permanent drift. Structure substantially retains original strength and stiffness. Minor cracking of facades, partitions, and ceilings as well as structural elements. Elevators can be restarted. Fire protection operable. | No permanent drift. Structure substantially retains original strength and stiffness. Minor cracking of facades, partitions, and ceilings as well as structural elements. All systems important to normal operation are functional. |
| Nonstructural components | Extensive damage. | Falling hazards mitigated but many architectural, mechanical, and electrical systems are damaged. | Equipment and contents are generally secure, but may not operate due to mechanical failure or lack of utilities. | Negligible damage occurs. Power and other utilities are available, possibly from standby sources. |
| Comparison with performance intended for buildings designed under the *NEHRP Provisions,* for the Design Earthquake | Significantly more damage and greater risk. | Somewhat more damage and slightly higher risk. | Less damage and lower risk. | Much less damage and lower risk. |

**Figure 2.14:** Damage control and building performance levels (FEMA 2000)

| | | Structural Performance Levels | | |
|---|---|---|---|---|
| **Elements** | **Type** | **Collapse Prevention S-5** | **Life Safety S-3** | **Immediate Occupancy S-1** |
| Steel Moment Frames | Primary | Extensive distortion of beams and column panels. Many fractures at moment connections, but shear connections remain intact. | Hinges form. Local buckling of some beam elements. Severe joint distortion; isolated moment connection fractures, but shear connections remain intact. A few elements may experience partial fracture. | Minor local yielding at a few places. No fractures. Minor buckling or observable permanent distortion of members. |
| | Secondary | Same as primary. | Extensive distortion of beams and column panels. Many fractures at moment connections, but shear connections remain intact. | Same as primary. |
| | Drift | 5% transient or permanent | 2.5% transient; 1% permanent | 0.7% transient; negligible permanent |

**Figure 2.15:** Structural performance levels and damage (FEMA 2000)

**Table 2.1:** ASCE-41 Basic Safety Objective (ASCE 2007)

| Performance level | Overall damage | Drift | Hazard level |
|---|---|---|---|
| Life Safety | Moderate | 2.5% | BSE-1 |
| Collapse Prevention | Severe | 5% | BSE-2 |

## 2.5 The Benchmark Buildings

Several control strategies have been studied for more than 20 years; some of which are referenced in (Ohtori et al. 2004). These studies, however, differ from each other not only in the control algorithms and devices that were tested, but also in the experimental and analytical models, the evaluation criteria and in the objectives that were pursued with the application of the different control concepts.

An obvious necessity for control benchmark structures was therefore recognized by the *American Society of Civil Engineers Committee on Structural Control* which, consequently, undertook a benchmark study for the comparison of control algorithms that considered three-story building models (Spencer et al. 1998a; Spencer et al. 1998b).

Later, the *Working Group on Building Control* (Chen 1996) worked towards the development of a systematic and standardized means to evaluate and compare different control strategies. The result of their work was the *Next Generation Benchmark Control Problem for Seismically Excited Buildings* (Spencer et al. 1999). In it, inelasticity of the structural materials was not considered; however, strong earthquakes cause yielding of

the frame elements even in controlled structures. That is why, later, the inclusion of the material nonlinear behavior was necessary.

The *Benchmark Control Problems for Seismically Excited Nonlinear Buildings* (Ohtori et al. 2004) are an extension of the *Next Generation Benchmark Control Problem* that includes the nonlinear behavior of 3 different steel buildings that were designed for the SAC Steel Project (SAC_Steel_Project 1994) along with several evaluation criteria and control design constraints.

## 2.6 Earthquake Records

The ground accelerations that are used for the time-history analyses of the building frames were developed by Somerville et al. (1997) from historical recordings and simulations for the FEMA project on steel moment-resisting frames (SAC_Steel_Project 1994). They constitute 2 suites of records for Los Angeles, California with seismic hazard levels corresponding to probabilities of exceedance of 10% in 50 years (BSE-1) and 2% in 50 years (BSE-2). Each suite consists of 20 horizontal ground acceleration records, which correspond to fault-parallel and fault-normal orientations of 10 recordings, rotated 45 degrees to preclude excessive near-fault effects. The ground accelerations were adjusted so that their mean response spectrum matched the 1997 NEHRP design spectrum.

# 3. RESEARCH OBJECTIVE

As has been stated before, friction devices constitute a simple, economic and effective means for reducing the seismic response of structures and the damage in their elements. When they are installed in a structure as part of a structural strengthening strategy, additional practical, technical and economic benefits are obtained. These added advantages motivated the consideration of the application of this type of passive energy dissipation system for continuing research aiming at improved subsequent designs.

Recent research done on friction dampers has focused mainly on their utilization as a means of (semi) active control. As such, different (semi) active friction dampers have been tested and appropriate control approaches have been developed (Chen and Chen 2002; Chen and Chen 2004; Chen and Chen 2003; Guglielmino and Edge 2003; Lane et al. 1992; Ng and Xu 2004; Nishitani et al. 1999). However, since the studies of Pall, Filiatrault, Aiken, Constantinou, Fitzgerald, etc. presented in the past chapter, and with the exception of the introduction of a couple of new variations of the already existing friction devices, little has been researched on passive friction energy dissipaters.

Furthermore, even though some of the past studies on friction devices are already somewhat conclusive, design codes, philosophies and trends have considerably changed in recent years. This has limited their validity to the historical context in which they were made and a revision of the results and conclusions that were obtained at that time seems appropriate. For instance, Performance Based Design (PBD) has been introduced, nonlinear time-history analyses are now required when considering the application of

control devices and reliance on ductility of structural members for seismic energy dissipation is a constant these days.

The introduction of the nonlinear benchmark buildings now allows a more up-to-date, standardized measurement and evaluation of the results of the dynamic analyses. It also facilitates a more direct and fair comparison of the performance of friction devices with other structural control concepts. It is worth mentioning that, sometimes, the results obtained in previous research done on friction devices were not evaluated in a formal and standard manner and that, in many of the cases, the analytical models and procedures employed to arrive to such results were linear.

With the aforementioned in mind, a study on the application of friction devices in buildings has been designed to update, enhance, improve, and supplement results and conclusions of previous research on the topic. This will be achieved by the consideration of current analysis and design philosophies and techniques, and the new evaluation and comparison criteria.

This study is also intended to provide further insight and knowledge on the theoretical dynamic behavior of friction damped braced frames and its relationship with the particular design parameters. The economic benefits of using friction damped braced frames instead of the traditional moment-resisting frames will also be assessed indirectly.

# 4. MODELING AND ALGORITHM

The building models used in this study are those given in (Ohtori et al. 2004) and introduced in the benchmark buildings section. They were originally designed to be used as benchmarks for the SAC Phase II Steel Project (SAC_Steel_Project 1994) and represent typical 3-, 9-, and 20-story buildings designed for the Los Angeles, California region. The friction dampers that are incorporated into the friction damped braced frame models are the Pall single diagonal tension/compression friction damped braces briefly described before in section 2.2.

## 4.1 Analytical Modeling of the Frames

Since friction devices and the structures into which they are incorporated behave in a highly nonlinear manner, friction damped braced frames should always be analyzed using nonlinear dynamic time-history methods (Aiken and Kelly 1990; ASCE 2007; Fu and Cherry 1999; Moreschi and Singh 2003). In this thesis, the modeling and nonlinear dynamic time-history analyses of the building frames were carried out using the computer program SAP2000 (CSI 2007b).

All building models use clear span dimensions for their beams and columns in order to avoid the overestimation of the contributions of the structural elements to interstory drifts that are possible when centerline-to-centerline dimensions are used.

Panel zones are considered using the panel zone definitions available in SAP2000. Rigid floor diaphragms are assumed at all floors, thus, all nodes lying at a same horizontal plane were constrained together in the lateral direction.

Beams and columns are modeled using frame elements considering all their deformational degrees of freedom (axial, flexural and shear) with their strength and stiffness based on the material definitions of the computer program. Nonlinear hinges, as defined in ASCE-41 (Fig. 4.1), are specified at both ends of the structural elements; in the beams, M3 hinges (bending about the strong axis) were placed and, in the columns, either P-M3 (axial load plus bending about the strong axis), or P-M2 (axial load plus bending about the weak axis) hinges depending on the orientation of the element. The rigid beam-to-column connections are idealized as fully restrained and their fracture is not considered.

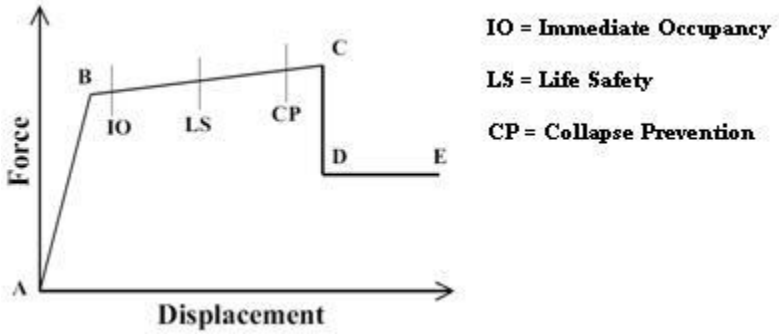


**Figure 4.1:** Post-yield behavior of ASCE-41 nonlinear hinges (CSI 2007a)

Seismic masses for each frame are calculated by dividing the total seismic mass at each floor by 2 (the number of frames in that direction). Since p-delta effects can have a great influence on the response of steel structures (Gupta and Krawinkler 1999), they as well as large displacements are considered in the analyses. The seismic masses are not directly applied to the structural elements; they are only used as mass source for the dynamic analyses. This allows a more appropriate assessment of the p-delta effects and potential collapse hazards.

In recognition of the portion of inherent damping that is due to the inelastic behavior of steel structural members and in order to achieve a fair inclusion of the modes that contribute to the dynamic response of the frames, 2% Rayleigh damping was enforced at the first mode period and at a period of 0.2 seconds, except for the 20-story building where the same amount of damping was assigned to the first and fifth mode periods (Gupta and Krawinkler 1999).

Due to the complexity increase in computational effort and uncertainty, other factors like the contributions to strength and stiffness of the floor slabs, shear connections, gravity columns and the weak axis columns of the orthogonal moment resisting frames were ignored.

## 4.2 Analytical Modeling of the Friction Damped Braces

As mentioned before, the friction damped braces that are modeled in all frames are Pall single diagonal tension/compression braces with a friction device at one end. Before accepting the proposed analytical model for the damped braces, it was validated for its use in the analyses.

The friction damped braces were modeled using link elements assigned with an appropriate plasticity model. Based upon the behavior obtained by Pall et al. (1980), the characterization of their brake lining frictional system in terms of an elastic-perfectly plastic model is appropriate.

The plasticity model that was assigned to the friction damped braces (FDBs) is based on the hysteretic behavior proposed by Wen (1976) where the nonlinear force-deformation relationship is given by (Fig. 4.2):

$$F = r \cdot k \cdot d + (1 - r) \cdot Fy \cdot z$$

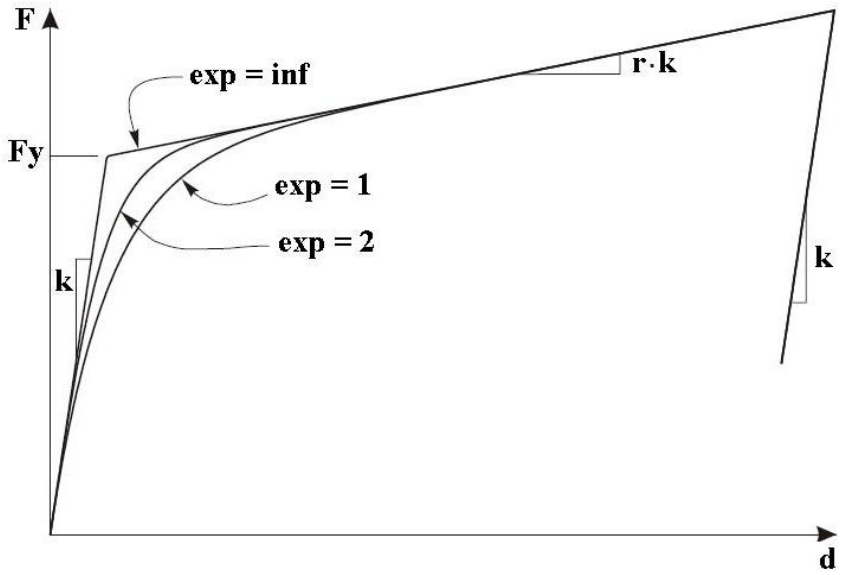


**Figure 4.2:** Definition of parameters for the Wen plasticity property (CSI 2007a)

where $k$ is the elastic spring constant, $Fy$ is the yield force, $r$ is the specified ratio of post-yield stiffness to elastic stiffness $k$ and $z$ is an internal hysteretic variable. This variable has a range of $|z| \leq 1$, with the yield surface represented by $|z| = 1$. The initial value of $z$ is zero, and it evolves according to the differential equation:

$$\dot{z} = \frac{k}{Fy} \begin{Bmatrix} \dot{d}(1 - |z|^{\exp}) & if \ \dot{d}z > 0 \\ \dot{d} & otherwise \end{Bmatrix}$$

where *exp* is an exponent greater than or equal to unity. Larger values of this exponent increase the sharpness of yielding as shown in Fig. 4.2. The practical limit for *exp* is about 20 (CSI 2007a). The equation for $\dot{z}$ is equivalent to Wen's model with $A$ =1 and $\alpha = \beta = 0.5$.

As suggested by Dr. Avtar Pall, president of Pall Dynamics Ltd, in personal communication, the values of the Wen plasticity property parameters that were assigned to the model of the friction damped braces are $k$ = brace stiffness, $Fy$ = slip load of the friction device, post-yield stiffness ratio $r$ = 0.0001 and yielding exponent $exp$ = 10.

## 4.3 Validation of Models

In order to guarantee the correctness of the results and conclusions presented in this thesis, validation of the SAP2000 analytical building models is indispensable. For acceptance of the computer models that were constructed, two main things are identified as subject of validation: the building models and the friction-damped brace model.

For the validation of the SAP2000 steel frame models, eigenvalue analyses were performed to them to obtain and compare their mode shapes and natural frequencies with those of the benchmark buildings as defined in (Ohtori et al. 2004).

Eigenvalue analyses are the best option for validation of the SAP2000 frame models, since this type of analyses uses a very well established standard mathematical procedure, whose results do not depend on possible different (inelastic) material definitions and/or numerical methods, among other things, used to obtain solutions to problems. These differences can be a source of discrepancies in the results obtained

when one seeks to obtain the solution to a "same" problem using different means. For example, if the solutions to the equations of motion are chosen as the corroboration parameter for validation, it is not possible to obtain the exact same results and, thus, the doubtless acceptance of a model is also not possible. Furthermore, the unique characteristics of the eigenvalue analyses allow a very direct, straightforward and strict comparison between the values of the eigen-properties of the created SAP2000 building models and those of the given benchmark structures. This permits one to easily confirm the validity of the models that have been constructed.

Results of the eigenvalue analyses that were performed with the purpose of validation of the models of the benchmark buildings are shown in Table 4.1 and Fig. 4.3. It is important to mention that at the time of carrying out the analyses, the SAP2000 models of the frames had exactly the same modeling assumptions of the frames of Ohtori et al. (2004), i.e. centerline to centerline elements, no nodes at splices, no panel zones, etc. After these (simplistic) models were validated, they were updated with all the additional geometric, material, and analytical characteristics mentioned in the Analytical Modeling section.

**Table 4.1:** Modal frequencies for the 3-, 9-, and 20-story building models

| | *3-Story* | | *9-Story* | | *20-Story* | |
|---|---|---|---|---|---|---|
| | Ohtori | SAP2000 | Ohtori | SAP2000 | Ohtori | SAP2000 |
| 1st mode | 0.99 Hz | 0.99 Hz | 0.44 Hz | 0.44 Hz | 0.26 Hz | 0.26 Hz |
| 2nd mode | 3.06 Hz | 3.06 Hz | 1.18 Hz | 1.18 Hz | 0.75 Hz | 0.75 Hz |
| 3rd mode | 5.83 Hz | 5.83 Hz | 2.05 Hz | 2.05 Hz | 1.30 Hz | 1.30 Hz |

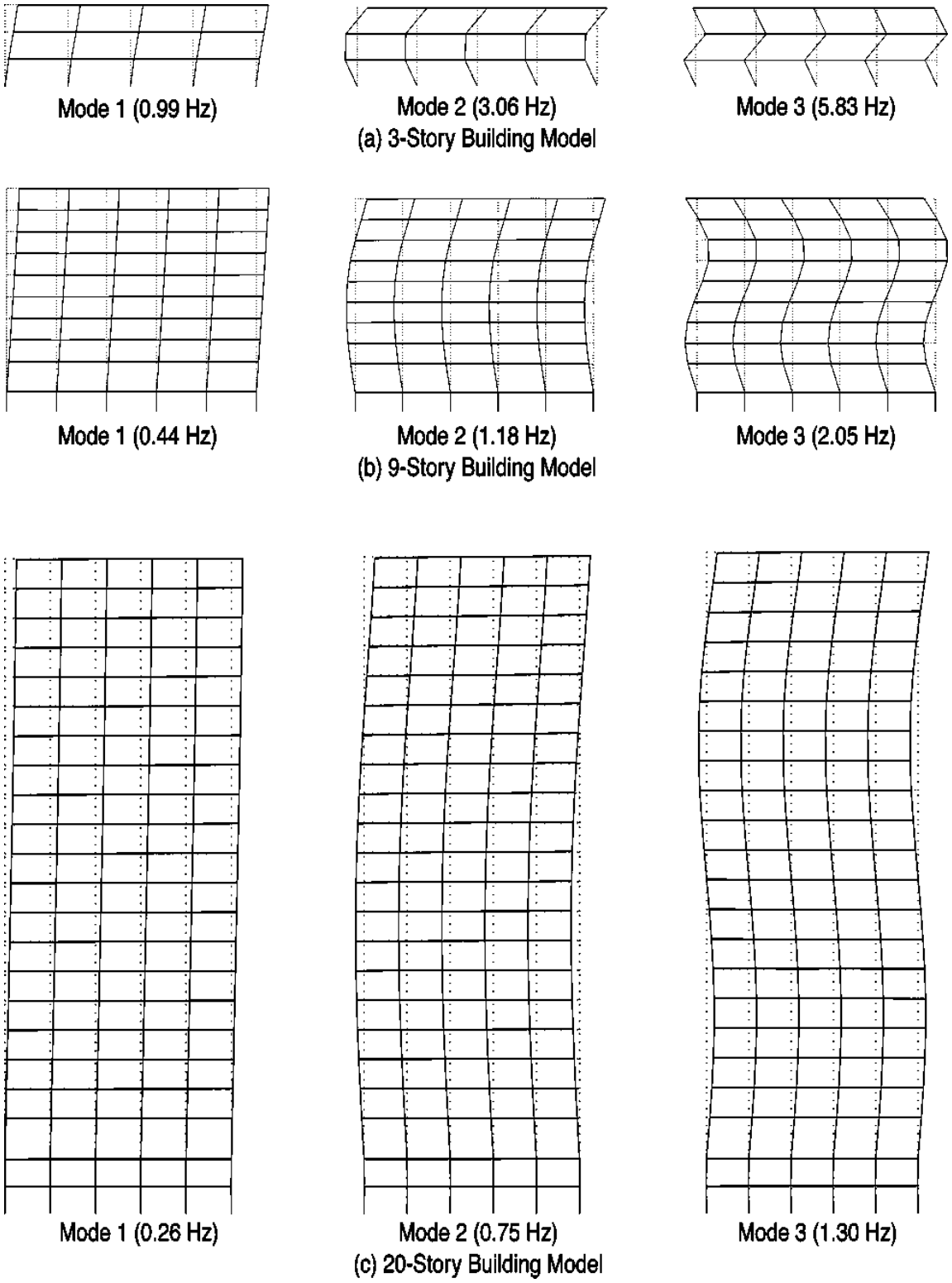


**Figure 4.3:** Mode shapes for the 3-, 9-, and 20-story building models (Ohtori et al. 2004)

On the other hand, for validation of the SAP2000 friction-damped brace model a SIMULINK® (TheMathWorks 2008) model was created to simulate the dynamic response of up to 3- degree-of-freedom shear buildings with friction devices installed. The model is shown in Fig. 4.5. The friction devices were modeled using the *Coulomb and Viscous Friction* block (Fig. 4.4) which, as it name implies, it is intended to model dry and viscous friction; however, its characteristics make it adequate to model the friction damped braces, since it represents, in its most basic form, a bilinear model. The slope of the first part (line) of the model can be specified and the slope of the second line has a fixed value of zero, but its offset with respect of the x-axis can be specified. This behavior is exactly that of an elastic-perfectly plastic material which, as mentioned before, mimics the behavior of friction damped braces quite appropriately. Thus for the sake of validating the SAP2000 model of the damped brace, the slope of the first part of the bilinear model was given the value of the elastic stiffness of the steel brace in the lateral direction and the slip force of the friction device was specified for the offset of the second part of the bilinear model. The model in SIMULINK uses the *State-Space* block to find the solutions to the equations of motion.

For validation of the brace model, 2 structures were considered, the single degree of freedom system shown in Fig. 4.6a, and the 3-degree of freedom shear building shown in Fig. 4.6b. Their properties are given in Table 4.2. Both were subjected to sinusoidal forces at each of their left nodes acting in the x-direction for 10 seconds and the solutions to the equations of motion given by both SIMULINK and SAP2000 were compared to validate the SAP2000 friction damped brace model (Fig. 4.7).


**Figure 4.4:** Coulomb and Viscous Friction block (TheMathWorks 2008)

**Table 4.2:** Structural and loading properties of the FDBFs used for validation of the SAP2000 analytical model of the FDB

| **SDF System** | |
|---|---|
| Height: | 3.28 ft |
| Bay width: | 3.28 ft |
| Frame elements: | Only translational DOFs in the x-direction without consideration of shear stiffness. All solid steel 2 in x 2 in sections. |
| Mass: | 4,111 slugs |
| Damping: | 0% |
| Friction brace: | Solid steel 2 in x 2 in section with slip force equal to 787 lb |

| **MDF System** | |
|---|---|
| Height: | 3.28 ft per story |
| Bay width: | 3.28 ft |
| Frame elements: | Only translational DOFs in the x- direction without consideration of shear stiffness. All solid steel 2 in x 2 in sections. |
| Mass: | 4,111 slugs at each story level. |
| Damping: | 0% |
| Friction braces: | All solid steel 2 in x 2 in sections. with slip force equal to 787 lb |

| **Sinusoidal loading** |
|---|
| Amplitude: 11.2 kips |
| Period: 1 sec |
| Phase: 0 |

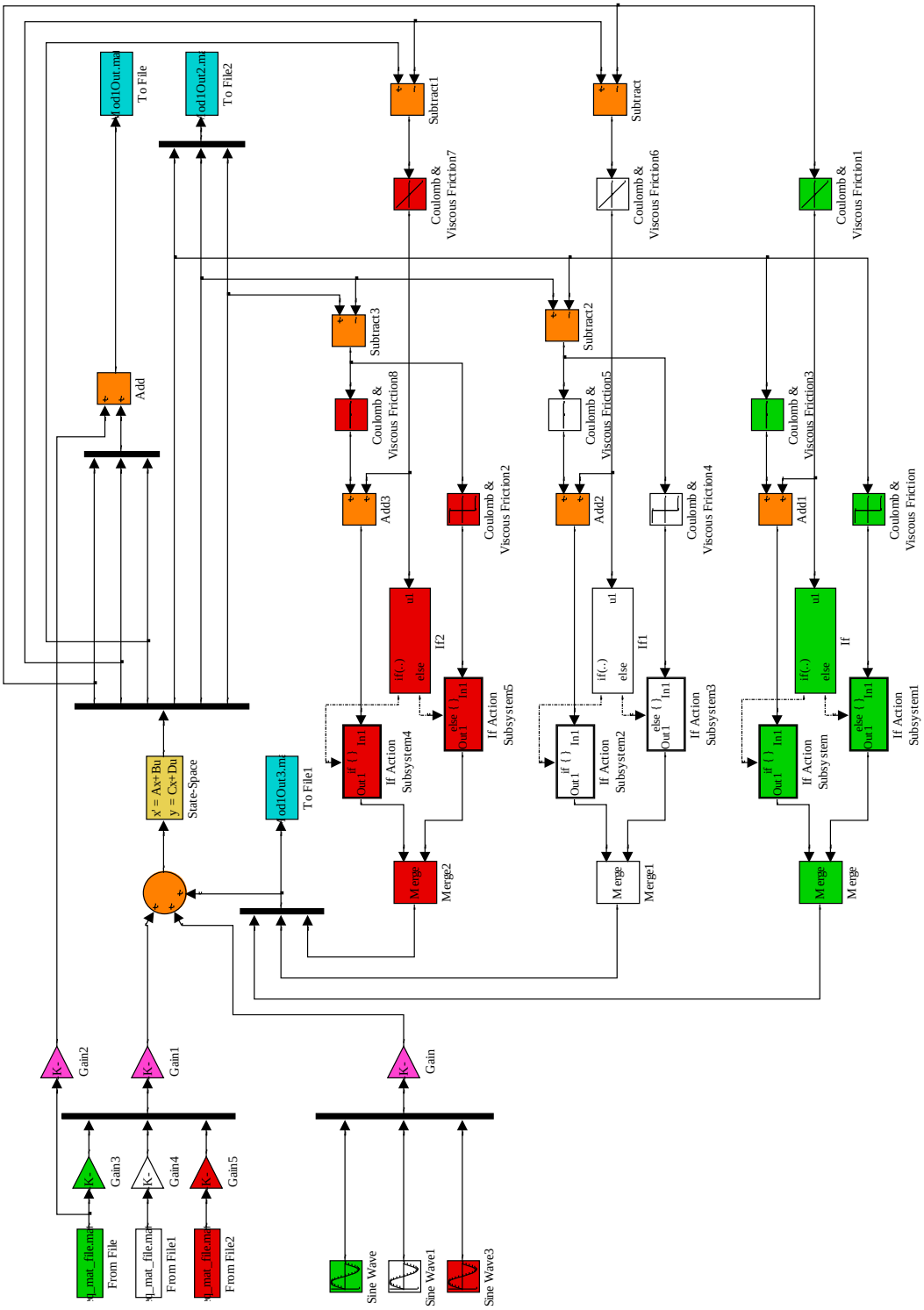


**Figure 4.5:** SIMULINK model for verification of the SAP2000 friction damped brace model behavior

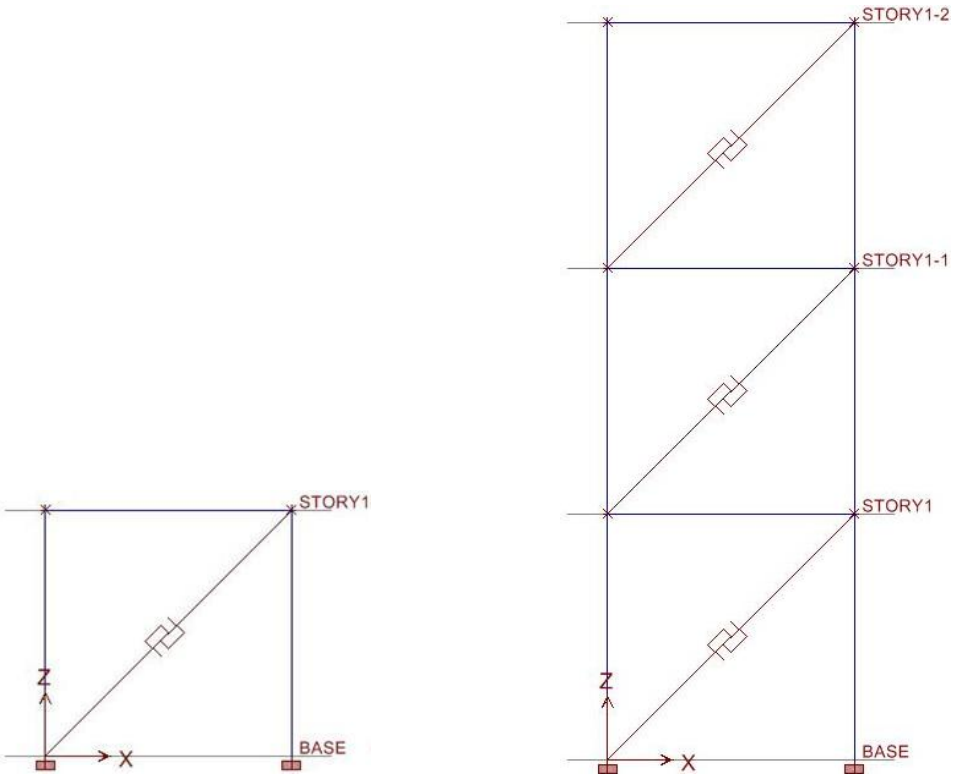


**Figure 4.6:** a) SDF structure with friction damped brace, b) MDF structure with friction damped braces

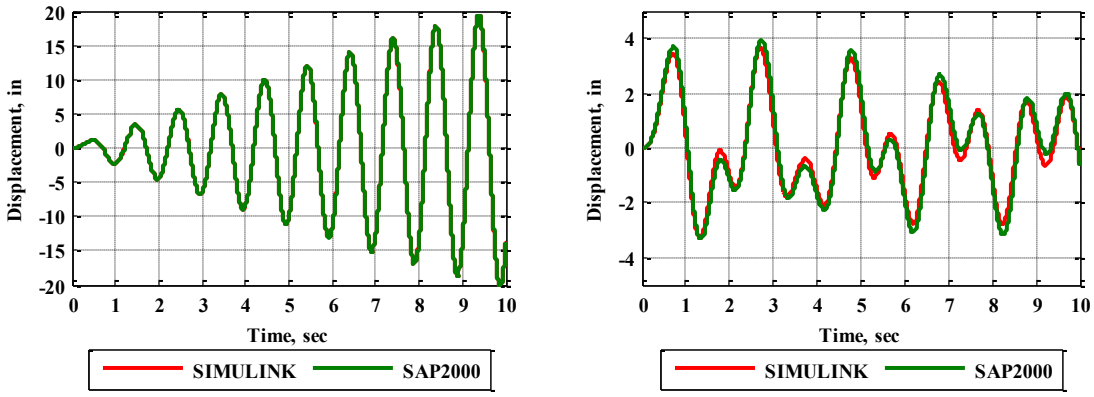


**Figure 4.7:** a) Response of SDF structure to the sinusoidal force, b) Response of the MDF to the sinusoidal forces

## 4.4 Philosophy and Algorithm

The ever present intention in the development of this thesis was that of considering it a design/rehabilitation problem. In order to update the results obtained in previous research, use formal measurement and evaluation criteria and relate the values to practical situations, conventions and definitions, use was made of the guidelines and parameters given in the *Seismic Rehabilitation of Existing Buildings* [ASCE-41] standard (ASCE 2007) and related documents. The reader is, therefore, referred to those documents for a broader understanding of the design philosophies and the knowledge of definitions, criteria, parameters and assumptions made throughout this work.

The intention of this thesis is to use friction dampers to achieve interstory drift reductions, for it is the main parameter used for seismic structural performance evaluation. The interstory drift ratio is defined as the quotient of the relative horizontal displacement between two construction levels and the construction level height. Although other response parameters may also be positively (or negatively) affected by the incorporation of the dampers to the buildings, they are not addressed in the present study.

By following the guidelines, suites of earthquake records with 10 and 2% probability of exceedance in 50 years specific for the site of the buildings (Los Angeles, California) are used in the analyses. In this sense, this thesis follows the stream of the benchmark studies by Kiggins and Uang (2006), Sabelli et al. (2003), and Zhu and Zhang (2008) which follow the Performance Based Design philosophies and diverges

from the concept of Ohtori et al. (2004) who define particular evaluation criteria for the assessment of the performance of different control strategies.

The general steps that are taken in the development of this thesis and are followed for each of the 3 frames are enlisted next and described later in more detail.

1. Evaluation of the capacity of the original benchmark frame under the BSE-1 and BSE-2 earthquake records.
2. Optimization of the number and location of the friction-damped braces using the BSE-1 records that caused the benchmark frame to exceed the Life Safety (LS) limit.
3. Optimization of the design parameters of the friction-damped braces using the BSE-1 records that caused the benchmark frame to exceed the Life Safety (LS) limit.
4. Evaluation of the capacity of the resulting FDBF under the suite of BSE-2 records.
5. Optimization of the design parameters of the friction-damped braces using the BSE-2 records that caused the FDBF to exceed the Collapse Prevention (CP) limit.
6. Evaluation of the capacity of the updated (final) version of FDBF under the suites of BSE-1 and BSE-2 records.
7. Comparison of the “before and after” interstory drift demands in the building.
8. Redesign of the original moment-resisting frame (MRF) to achieve compliance with the BSO requirements.

9. Comparison between the incremental weight of the FDBF and that of the redesigned MRF compared to the weight of the original benchmark to indirectly assess the potential economical benefit of using FDBFs.

In order to measure the reductions in the interstory drifts that are expected after the FDBs are incorporated into the MRFs, an evaluation of the bare benchmark frames has to initially be done. The ASCE-41 will require subjecting the rehabilitated building to at least 3 earthquake records, but for a more complete set of results and for concordance of my work with that of Kiggins and Uang (2006), Sabelli et al. (2003), and Zhu and Zhang (2008), the bare frames are subjected to a series of 20 earthquake records with probability of exceedance of 10% in 50 years (BSE-1), and a series of 20 with probability of exceedance of 2% in 50 years (BSE-2).

Next, the BSE-1 hazard level earthquake records that cause the benchmark frame in question to exceed the limits of the performance level of Life Safety are used, each one separately, to find a sub-optimal configurations of the friction damped braces that minimize the interstory drift response under the earthquake considered in the corresponding optimization process. The optimization algorithm used for this purpose is the sequential heuristic procedure given in (Chen and Chen 2002) which works as follows: At each step, a damper is considered on all possible locations of the building and the peak interstory drift ratio is calculated. That particular damper is finally left at the location where it achieved the maximum reduction of the peak interstory drift ratio. The same process is repeated at all the remaining empty locations with more damped

braces until the proposed number of devices has been placed or until the interstory drift ratio is reduced by a predetermined percentage or below a specified limit.

At the end of the last step, different sub-optimal arrays of dampers for the frame in question are available; each minimizes the peak interstory drift ratio under the action of a particular earthquake. These different combinations of dampers are then subjected to the series of 20 BSE-1 records. The maximum interstory drifts yielded by each sub-optimal configuration under the 20 records are averaged and compared with the average peak interstory drift ratios that resulted from testing of the remaining configurations. The array which yields the lowest average peak interstory drift ratio response is finally selected to continue with the study.

Further optimization of the selected damper configuration is carried out. This time, the design parameters of the friction damped braces, namely, the slip load of the friction device and the stiffness of the brace on which it is placed (Moreschi and Singh 2003), are the subject of this subsequent optimization.

For the optimization of the damped brace parameters, the building with the sub-optimal array of dampers chosen before is again subjected to the BSE-1 (10% in 50 years) earthquake records that caused the bare building to exceed the Life Safety (LS) limit. Monte Carlo simulations are undertaken under the action of each of those earthquakes varying the values of the brace stiffness and the slip load of the friction device to come up with a combination of values that minimizes the response. When a maximum reduction in interstory drift ratio is sought, the combination of brace stiffness and slip load that minimize such parameter is selected and, when maximum economy is

sough, the smallest combination of values that brings the peak interstory drift ratio below the LS limit is chosen.

The result of the last step, combined with the other actions taken previously, is a sub-optimized damper configuration with sub-optimized design parameters. The friction force of the devices as well as the brace stiffness values are adjusted to match those of actual rolled steel shapes and practical slip loads.

The updated structure is subsequently analyzed under the series of 20 BSE-2 (2% in 50 years) earthquake records. The objective is to make sure the strengthened building satisfies the requirements of the Collapse Prevention structural performance level too. For those BSE-2 records that took the frames beyond the Collapse Prevention performance level limit, the same approach as for optimization of the FDB parameters for the BSE-1 records is again followed, this time, considering the 2% in 50 years set of earthquakes for which the FDBF is not yet adequate. Monte Carlo simulations are again run to find a combination of slip force and brace stiffness that minimizes the response or at least brings the structure into compliance with the BSO requirements of ASCE-41. Finally, after choosing the new combination of values for the damper parameters, these are again adjusted to take practical values and this definitive version of the FDBF is subjected to the 40 BSE-1 and BSE-2 earthquake records to assess and compare the expected reductions in the interstory drift ratios.

In real life situations, economics play a decisive role at the moment of choosing a rehabilitation or seismic control strategy. Thus, in order to provide an indirect measure any economic benefits that can be achieved when passive friction dampers are installed

for energy dissipation and seismic protection purposes, the benchmark building in question is redesigned to comply with the BSO of ASCE-41. The incremental weight of the redesigned MRF with reference to the original benchmark is compared with the incremental weight that results from incorporating friction damped braces into the benchmark frame.

# 5. RESULTS

## 5.1 3-Story Building

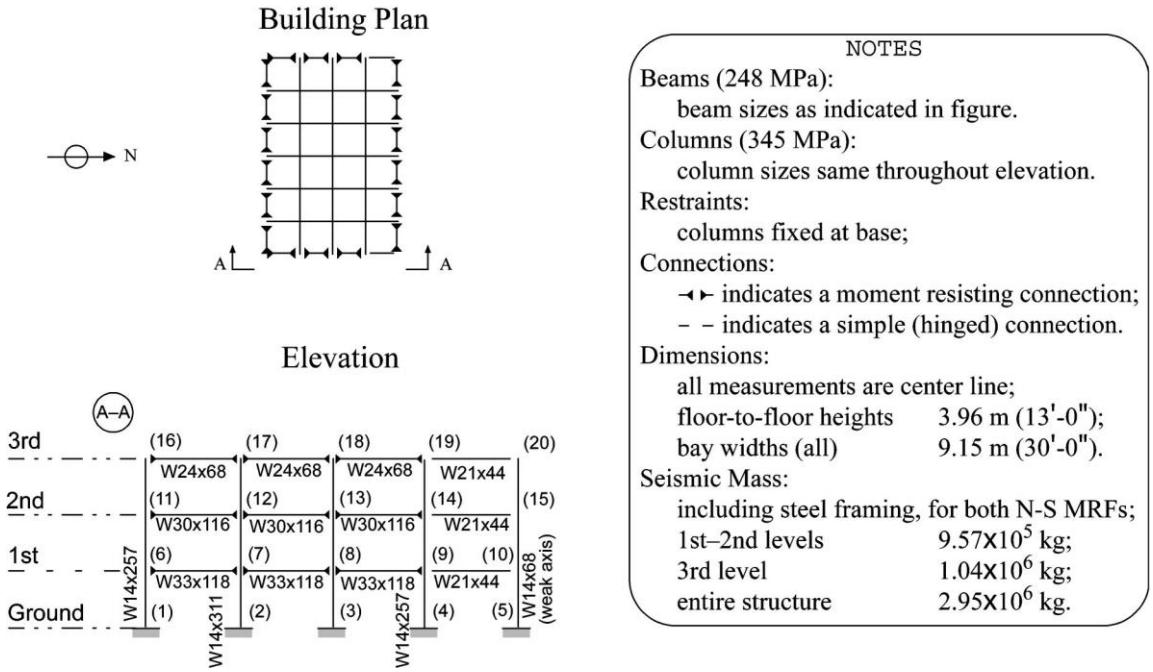


**Figure 5.1:** Three-story benchmark building north-south moment-resisting frame (Ohtori et al. 2004)

As outlined before, first, the (bare) 3-story benchmark frame (Fig. 5.1) is subjected to the action of the series of 20 10% in 50 years earthquake records (LA01 to LA20) and the series of 20 2% in 50 years records (LA21 to LA40) to assess the capacity of the original benchmark frame. The results are shown in Fig. 5.2.

Note for all graphs throughout this thesis: If the value(s) of a particular parameter corresponding to a particular earthquake, combination of brace stiffness, etc. is not shown, it means that value was not obtained from the corresponding analysis. If it is the case, the reason for the absence of the result is the non-convergence of the numerical

method which occurs due to the collapse of the structure. The consequent lack of numerical values is caused by the physical and numerical instability that arises from the sudden and abrupt degradation in strength of the localized plasticity models that are assigned to the structural elements. This big loss of strength happens close after the plastic hinge passes the Collapse Prevention (CP) performance limit (Fig. 4.1).

As can be seen in Fig. 5.2a, there are 12 records for which the building is not adequate, i.e. the peak interstory drift-ratio exceeds the limit of the Life Safety (LS) performance level. At the same time, the frame is only complying with the Collapse Prevention requirements for the case of 3 earthquake records; namely, LA23, LA29, and LA39. Recall that, under the BSE-1 records, the building should not exceed the LS limit and, under the BSE-2 records, the interstory drifts have to be kept below the Collapse Prevention (CP) limit.

It is the BSE-1 earthquake records that caused the frame to exceed the LS limit, the ones are first used to optimize the frame for seismic resistance using the friction devices.

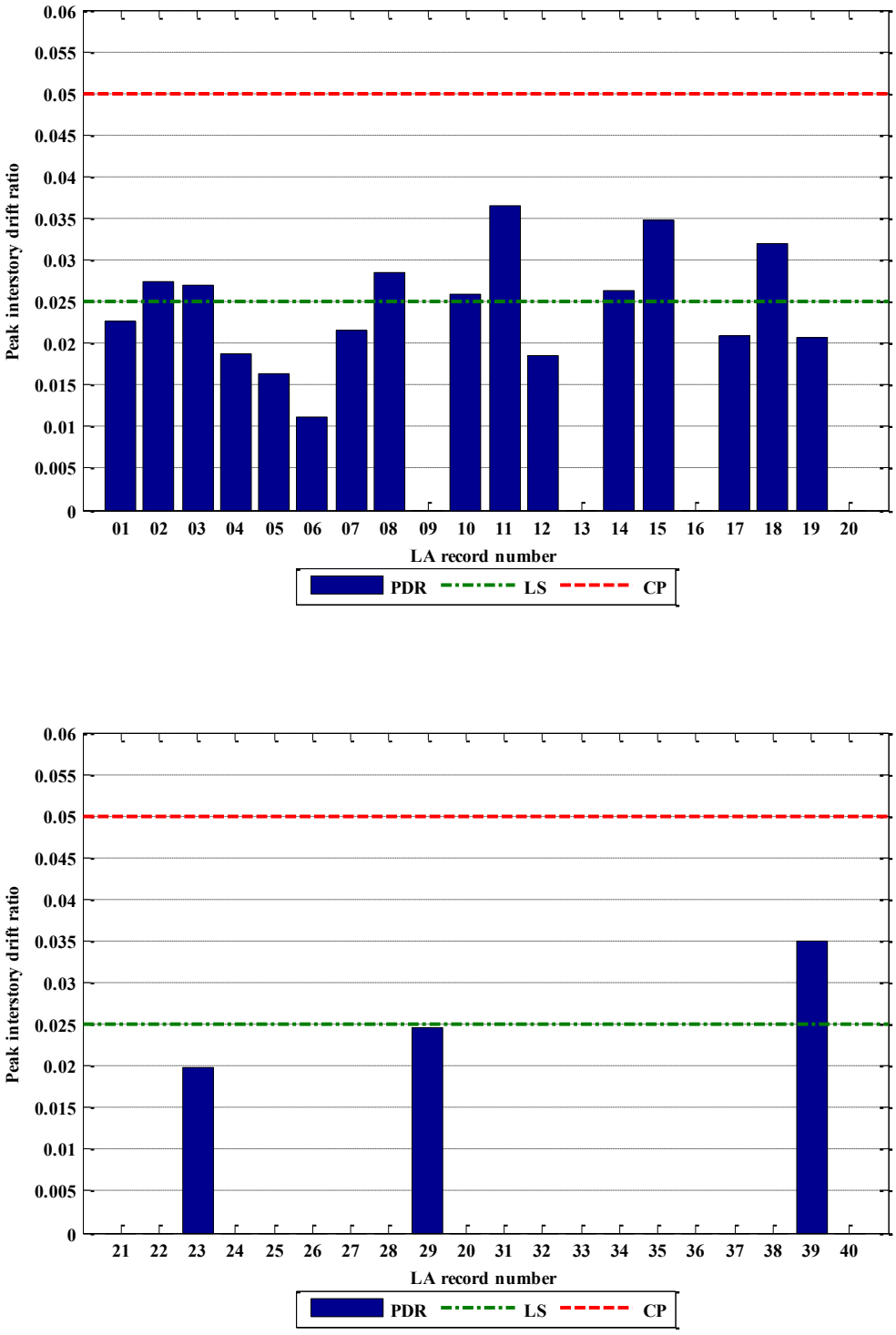


**Figure 5.2:** BSE-1 and BSE-2 interstory drift demands in the 3-story building

The optimization algorithm for the placement of the friction-damped braces of Chen and Chen (2002) described before is used to determine braced configurations that bring the peak interstory drift ratios to a minimum value under the action of a particular earthquake record. For the purpose of symmetry, a maximum of 6 friction braces is proposed to be installed inside the left and right bays of the 3-bay moment frame of the building (the braces showed to perform better inside the rigidly connected elements than inside the hinged bays). For symmetry, the friction damped braces (FDBs) are tested in couples at a same story each time with provisional brace stiffness equal to 1600 kips/in and slip force of 300 kips. The results of the optimization of the number and location of the dampers are given in Figs 5.3 to 5.5.

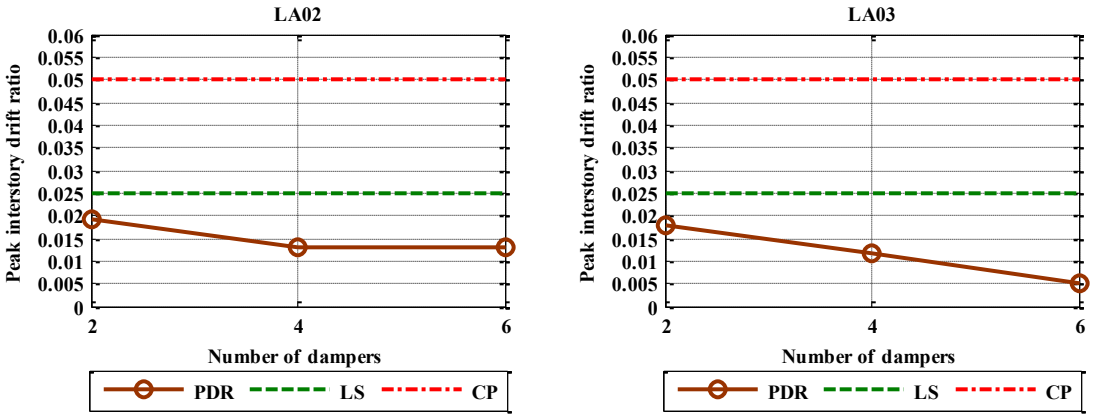


**Figure 5.3:** Performance of interstory drift ratio criterion in the 3-story building (part 1)

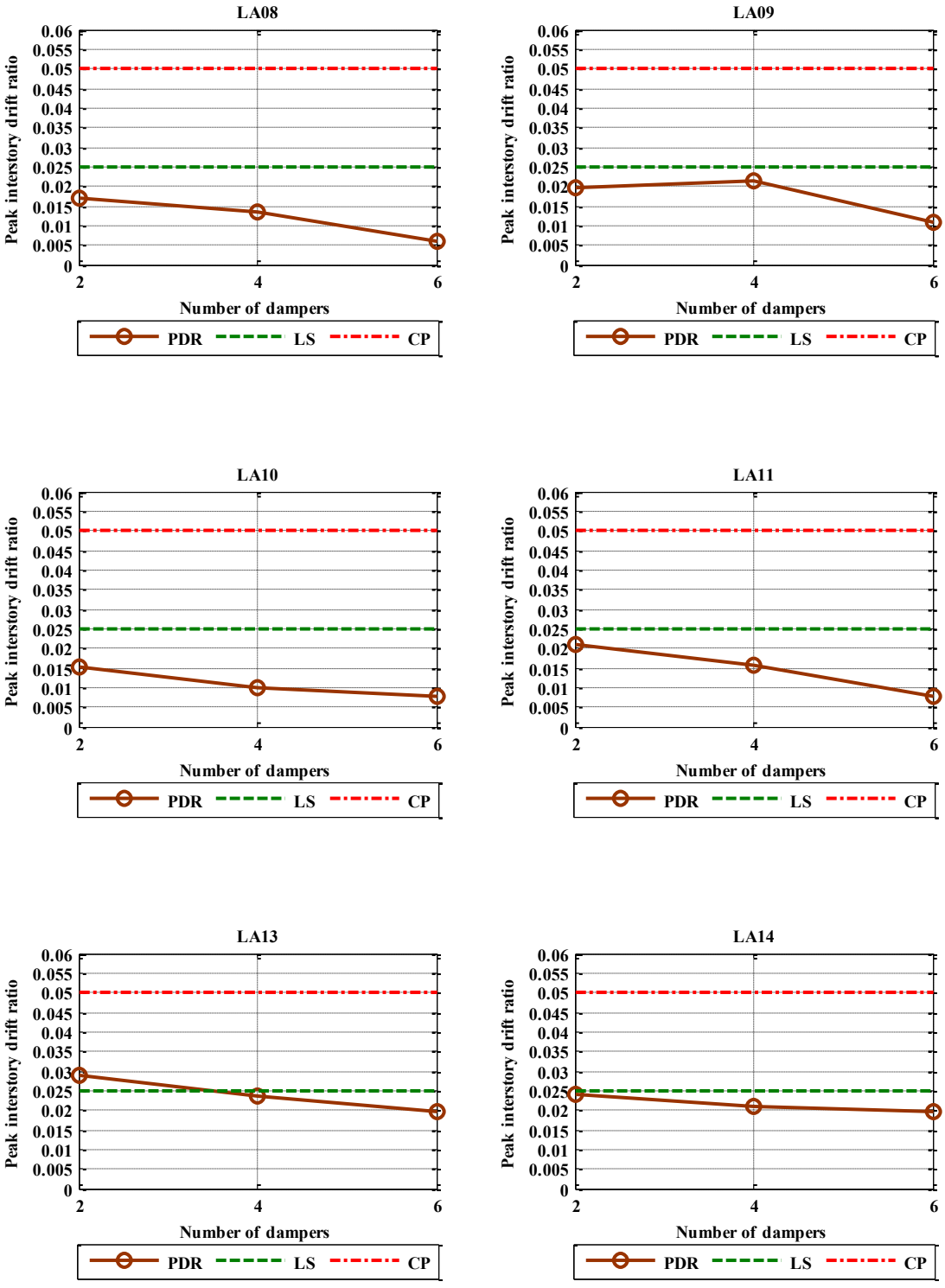


**Figure 5.4:** Performance of interstory drift ratio criterion in the 3-story building (part 2)

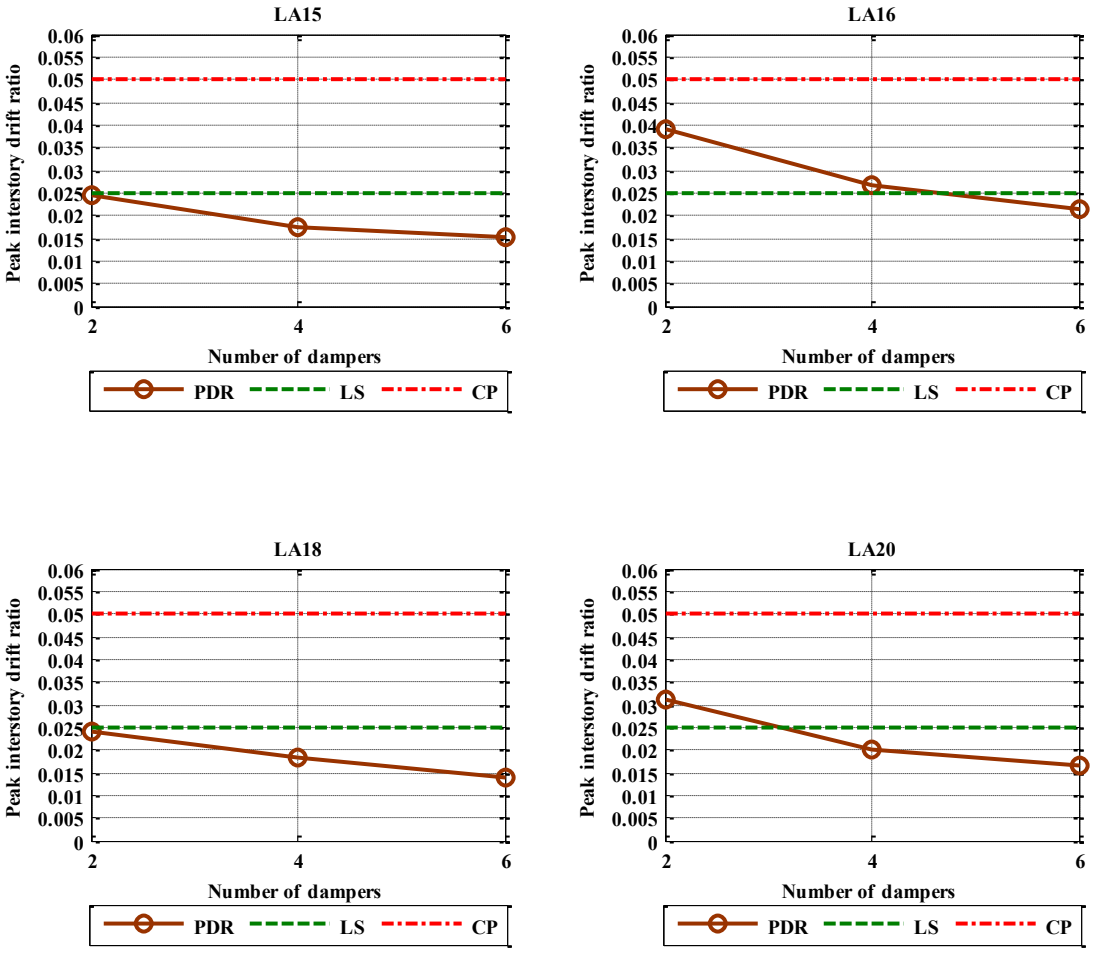


**Figure 5.5:** Performance of interstory drift ratio criterion in the 3-story building (part 3)

As the plots show, in all the cases the number of FDBs that yielded the lowest response was 6. Thus, according to the originally proposed location of the braces (the 3-bay moment frame), the 6 dampers are set in the configuration shown in Fig. 5.6.

Once the configuration was selected, the determination of the design parameters of the friction-damped braces (slip force of device and brace stiffness), was undertaken. For this, several analyses of the bare frame trying different combinations of brace stiffness and device slip load were run under the action of those BSE-1 earthquakes that caused the bare frame to exceed the LS limit. The results of these analyses are shown below in Figs. 5.7 to 5.12.

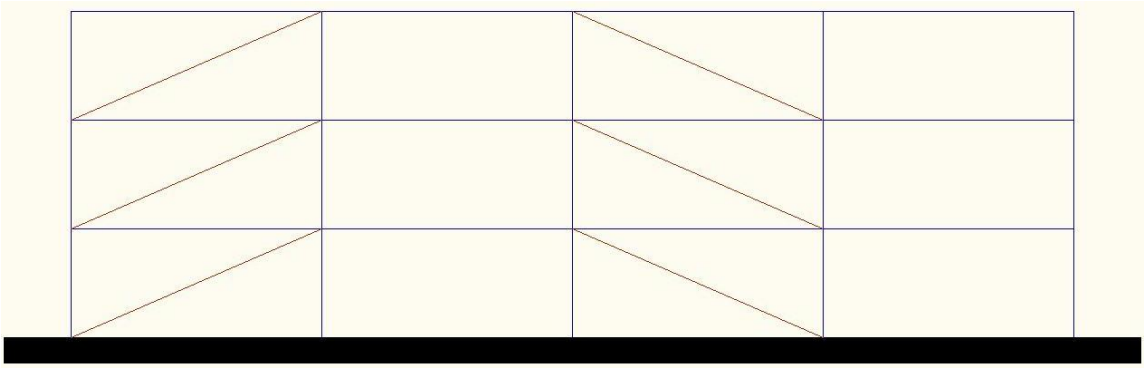

**Figure 5.6:** Sub-optimal FDB configuration determined after the consideration of the BSE-1 earthquake records

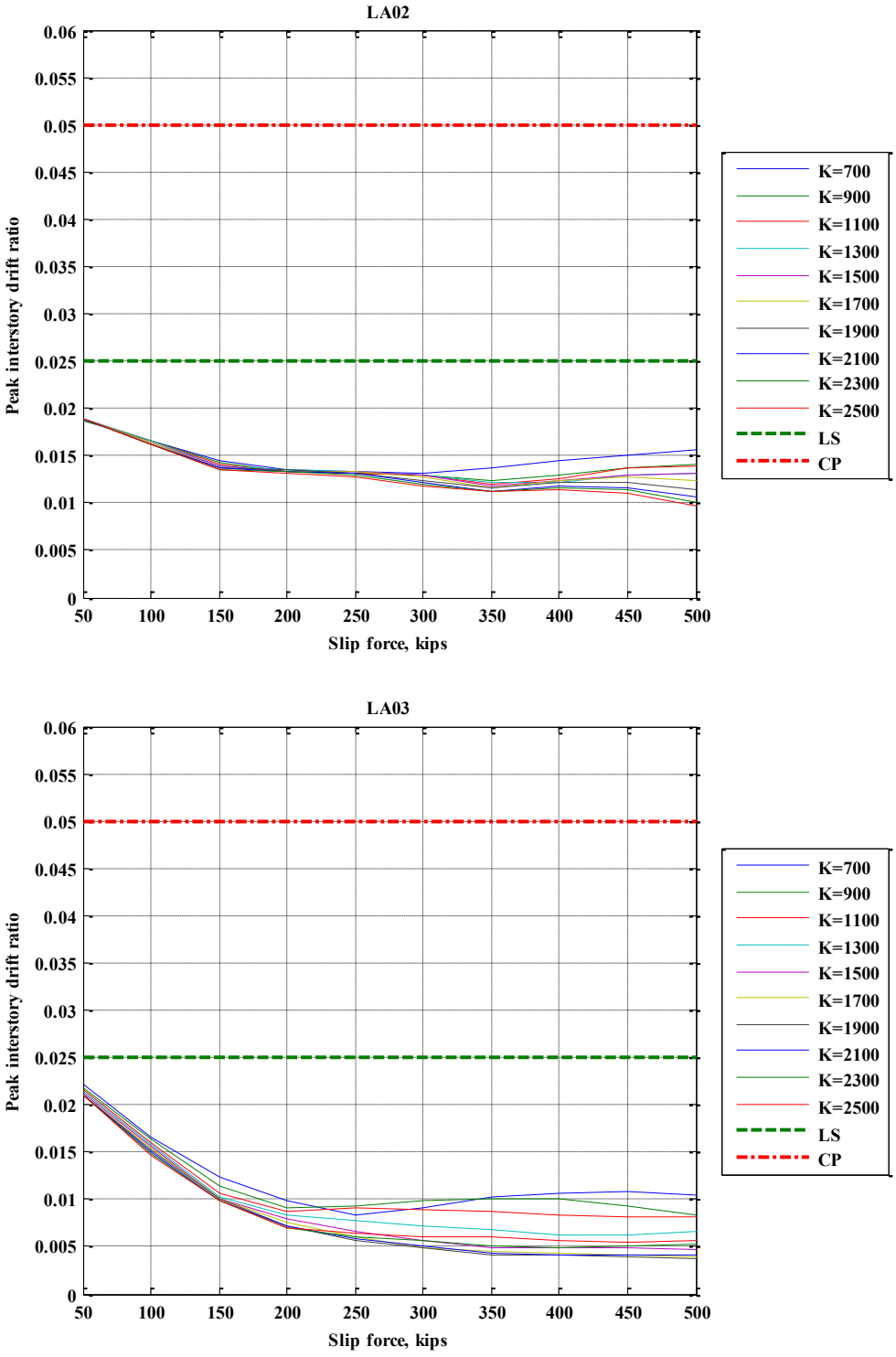


**Figure 5.7:** Effect of FDB parameters on the 1st FDB 3-story building (part 1)

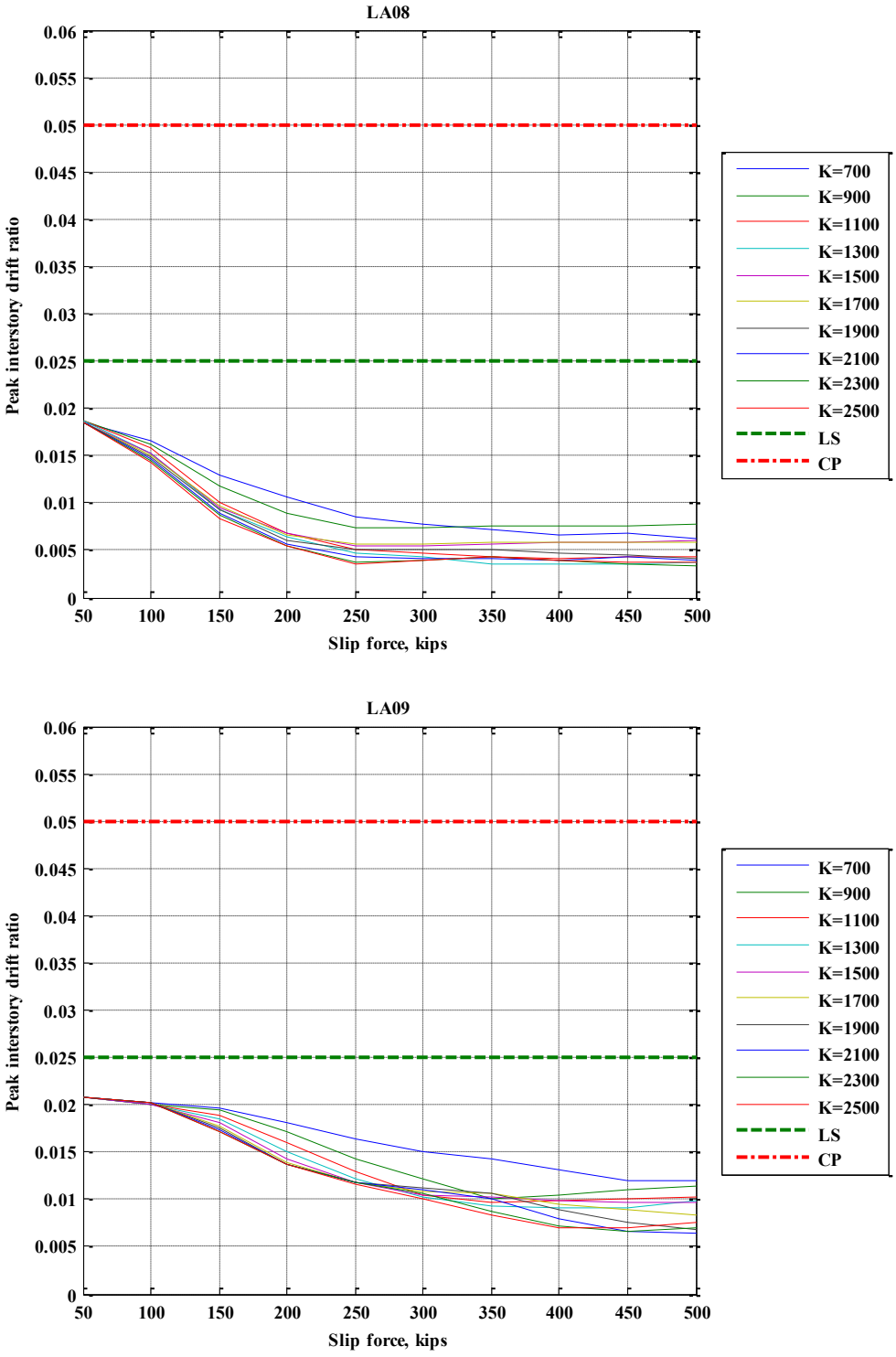


**Figure 5.8:** Effect of FDB parameters on the 1st FDB 3-story building (part 2)

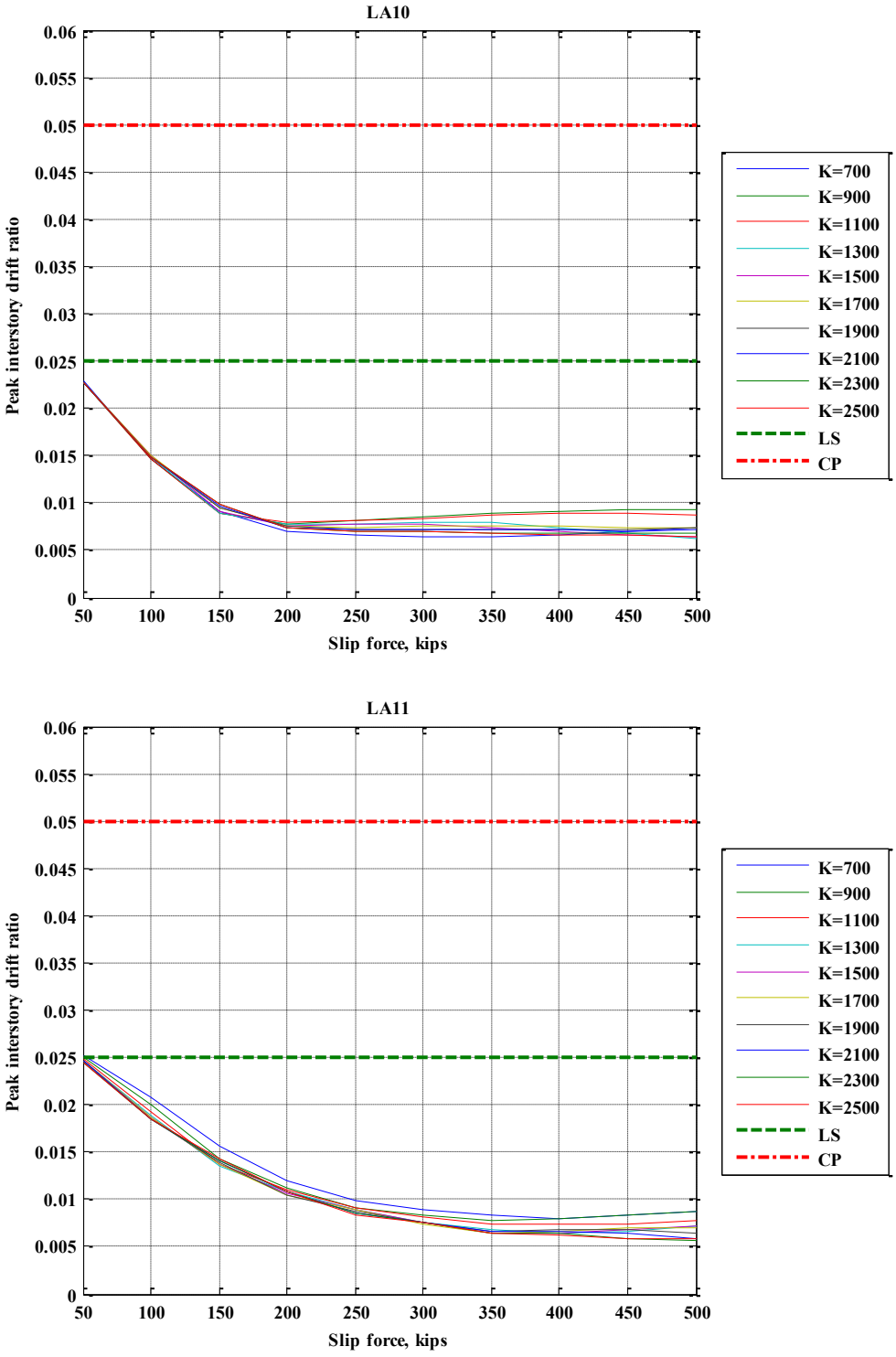


**Figure 5.9:** Effect of FDB parameters on the 1st FDB 3-story building (part 3)

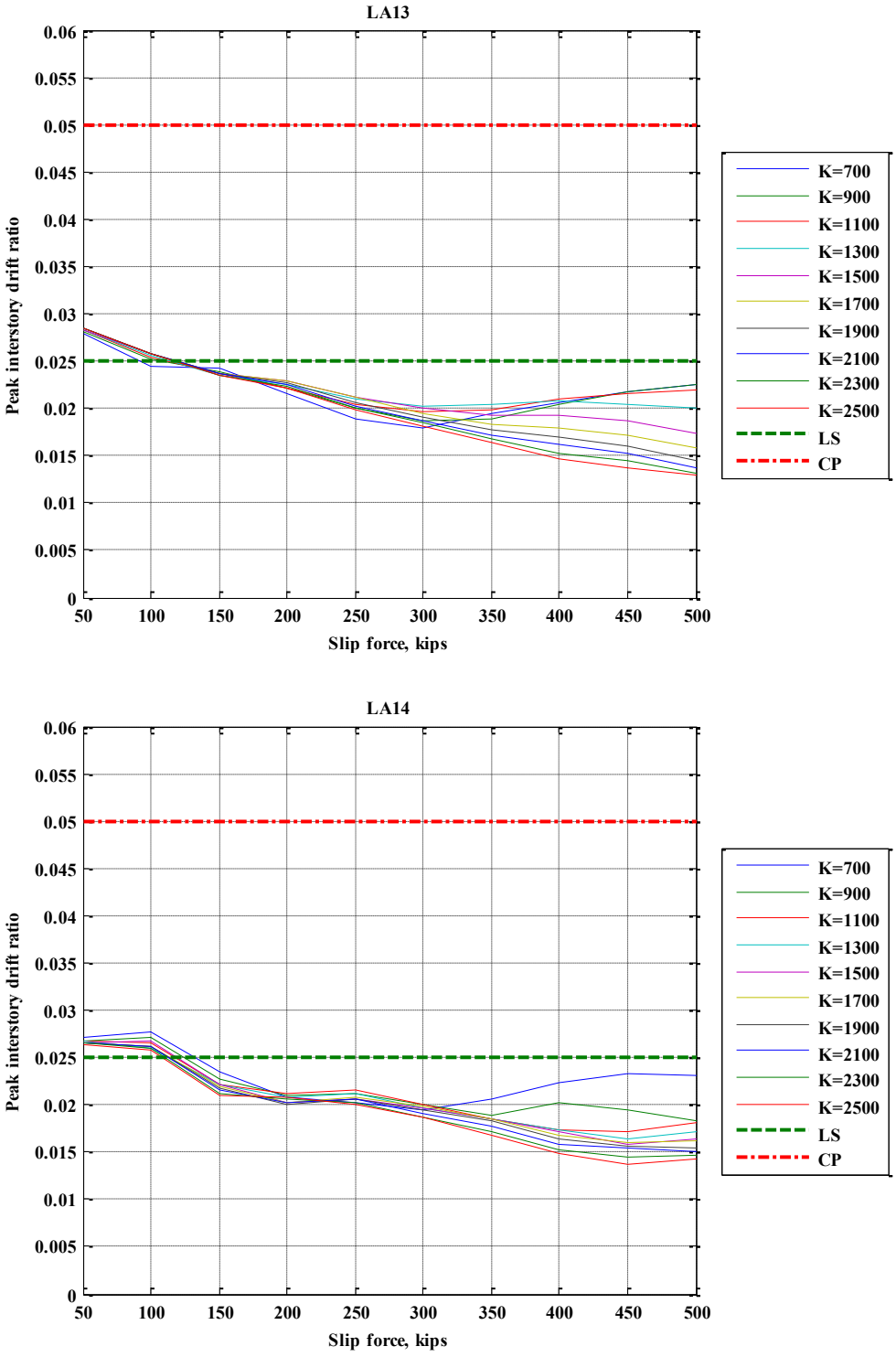


**Figure 5.10:** Effect of FDB parameters on the 1st FDB 3-story building (part 4)

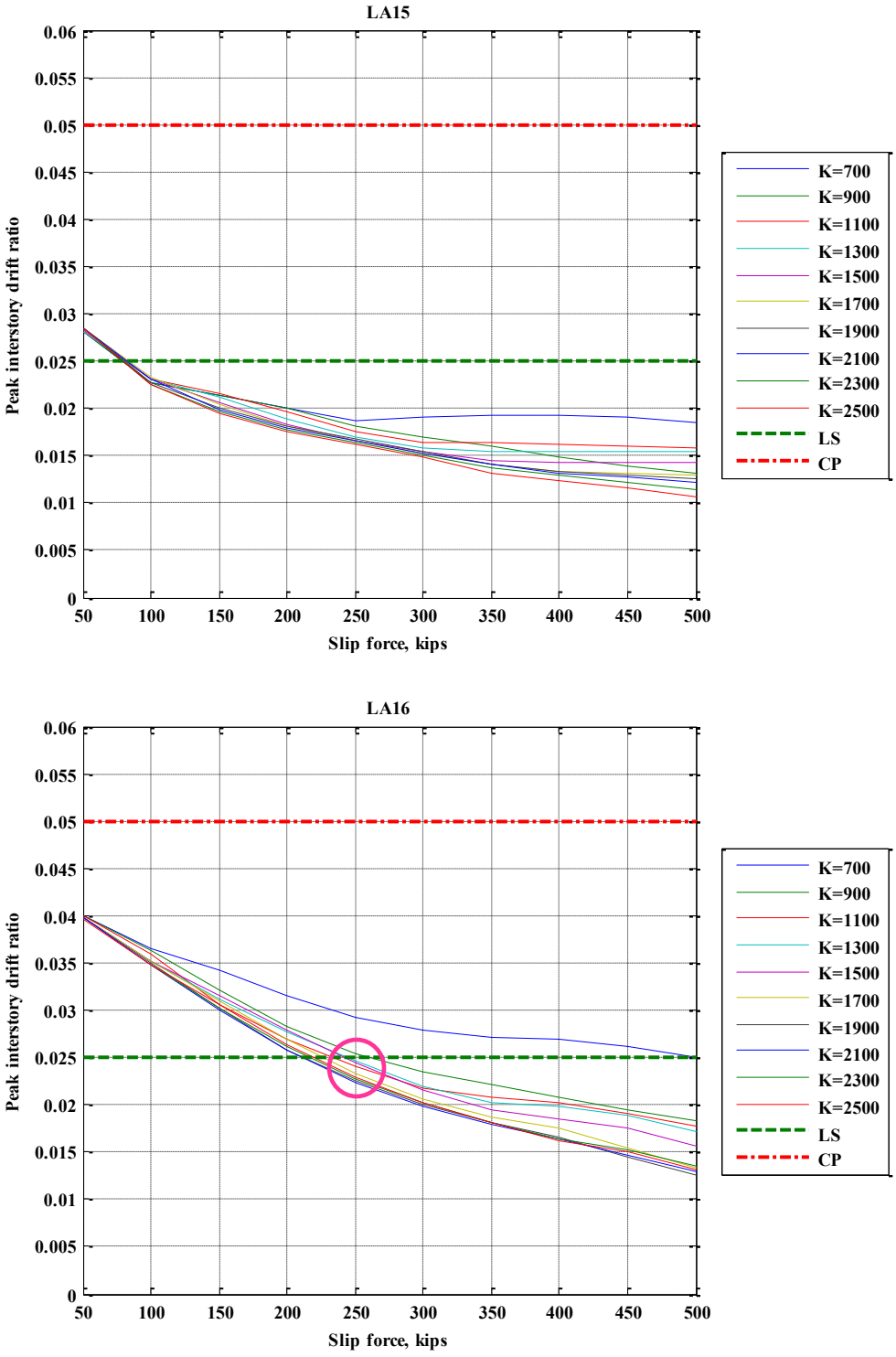


**Figure 5.11:** Effect of FDB parameters on the 1st FDB 3-story building (part 5)

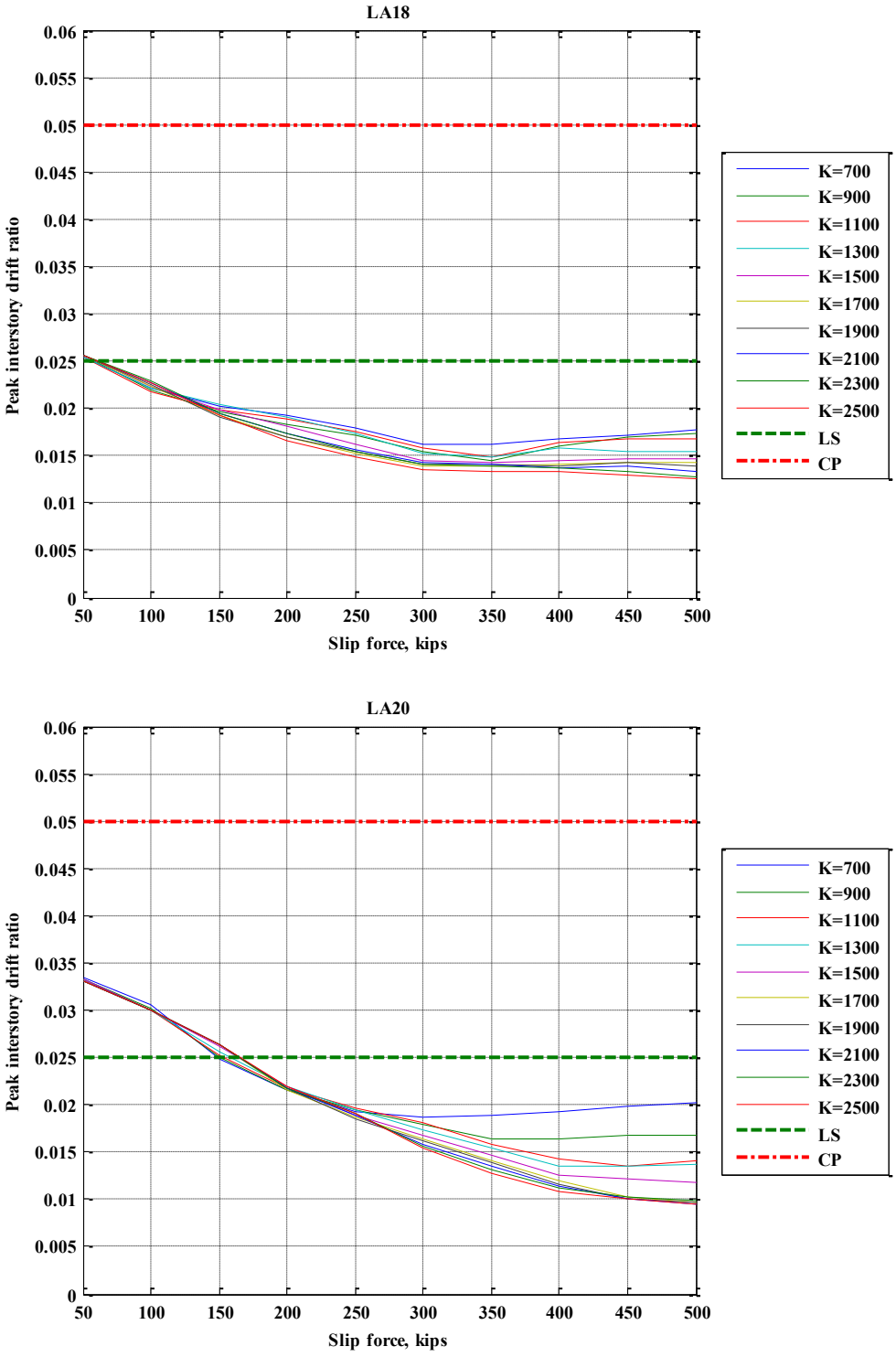


**Figure 5.12:** Effect of FDB parameters on the 1st FDB 3-story building (part 6)

The plots show that larger values of stiffness together with high slip forces will yield lower peak interstory drifts. This result seems logical, since all stories in the frame are equally braced. In practice, however, it might not be necessary, convenient or even possible to provide such large values. That is why, in this case, only the most economical combination of stiffness and slip force capable of bringing the frame into compliance with the LS limit was chosen. The most economical combination is the one that implies the lowest brace stiffness and device slip load.

By looking at the graphs, it can be found out that any brace stiffness combined with a slip force of 250 kips or larger will bring the maximum interstory drift ratio below the LS limit of 2.5%. So, this slip load was chosen and it only became necessary to find a steel section that would resist the maximum compression force that will be generated in the brace, that is, the 250 kip slip load. For this, HSS12×12×5/16 sections were selected, which provide a value of axial stiffness equal to 990 kips/in.

Now that the FDB configuration, brace stiffness, and slip load of the device required to bring the original frame into compliance with the LS limits are available, the next step is to make the building comply with CP requirements too. Consequently, the recent design is first subjected to the 2% in 50 years series of earthquakes to assess its performance. The results are presented in Fig 5.13.

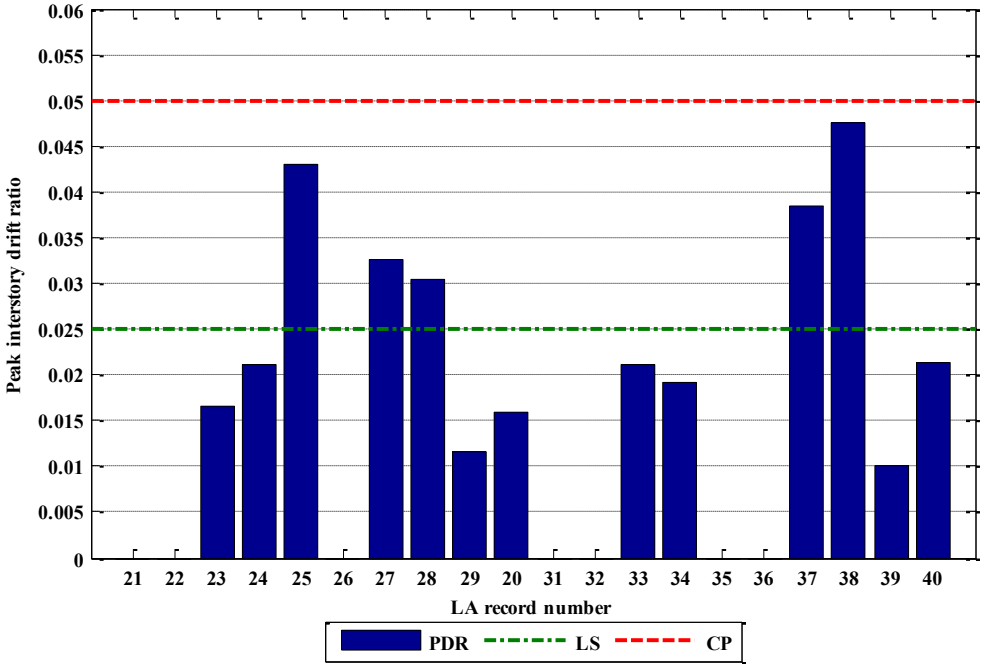


**Figure 5.13:** BSE-2 peak interstory drift ratios of the first proposed FDBF

According to the information displayed in the graph, while the braced frame complies with the CP limit for most of the earthquakes in the series, there are still 7 records for which it is not yet good. Since, at this point, it is still practical to vary the parameters of the FDBs, action is taken to find new values for the brace stiffness and slip force of the friction device that will achieve the compliance of the frame with the CP requirement.

The same procedure of trying several combinations of brace stiffness and slip load under the action of each of the earthquakes that caused collapse of the frame is again followed only considering BSE-2 records this time. It was found that, except for the case of the LA31 and LA36 earthquakes (Fig. 5.14), all other earthquakes continued to cause the collapse of the structure even when higher combinations were tested.

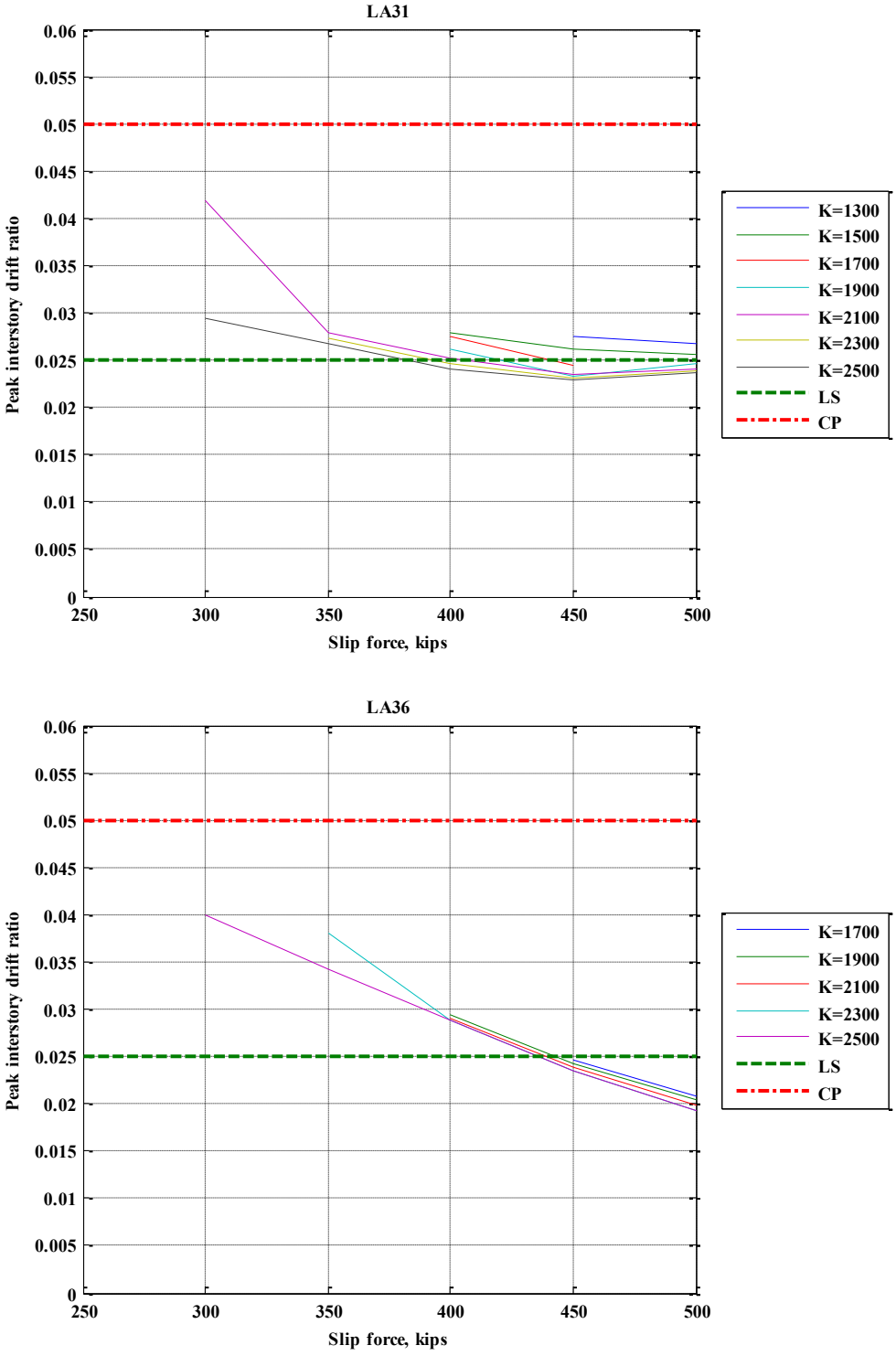


**Figure 5.14:** Effect of FDB parameters on the 1st FDB 3-story building (part 7)

To deal with the consistent problem of collapse, the addition of at least one more damper was necessary. Thus, the new brace configuration shown in Fig. 5.15 was proposed.

The new configuration is again subjected to the procedure of "randomly" trying different brace stiffness and slip load values to generate the plots that could not be created with the previous array of dampers due to the consistent collapse of the structure. In this case, the attempt of avoiding the collapse of the 3-story frame is successful and the plots that were drawn from the analyses are given below.

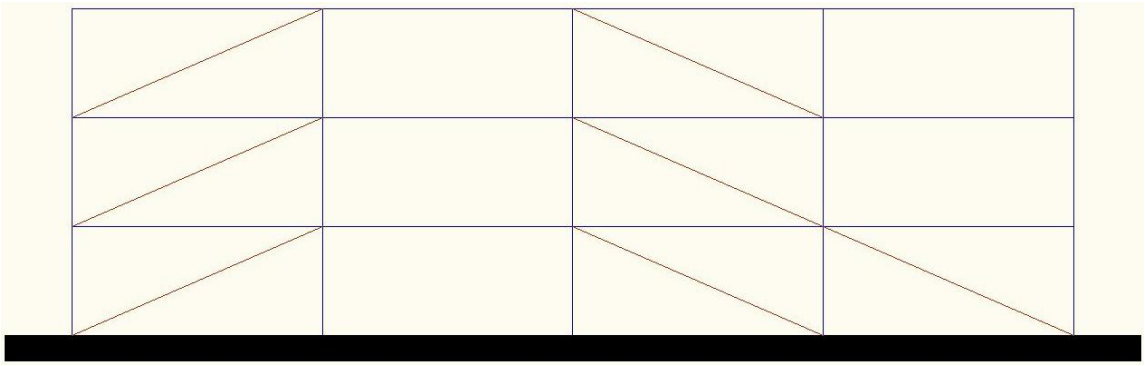

**Figure 5.15:** Second proposed FDBF

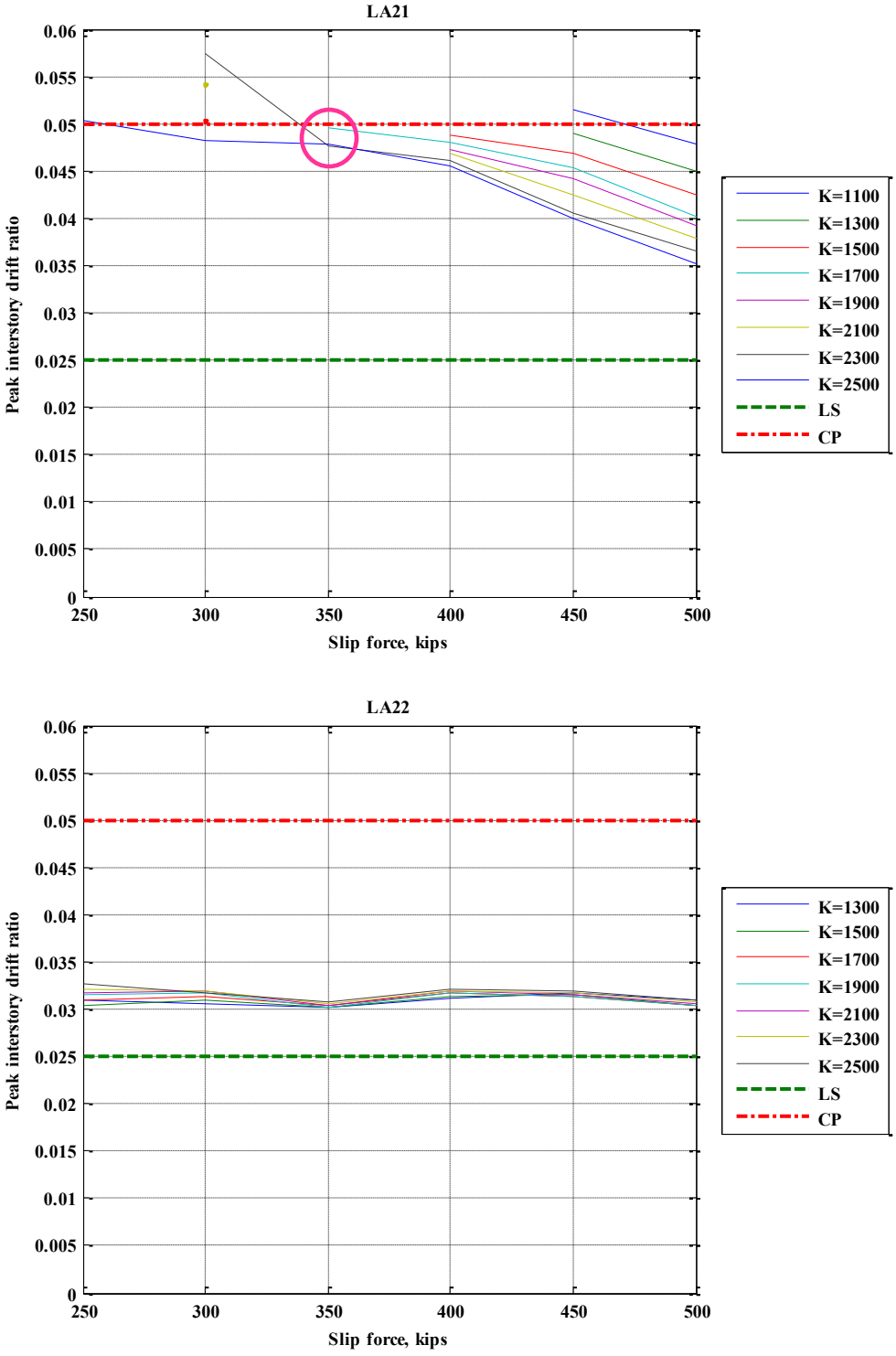


**Figure 5.16:** Effect of FDB parameters on the 2nd FDB 3-story building (part 1)

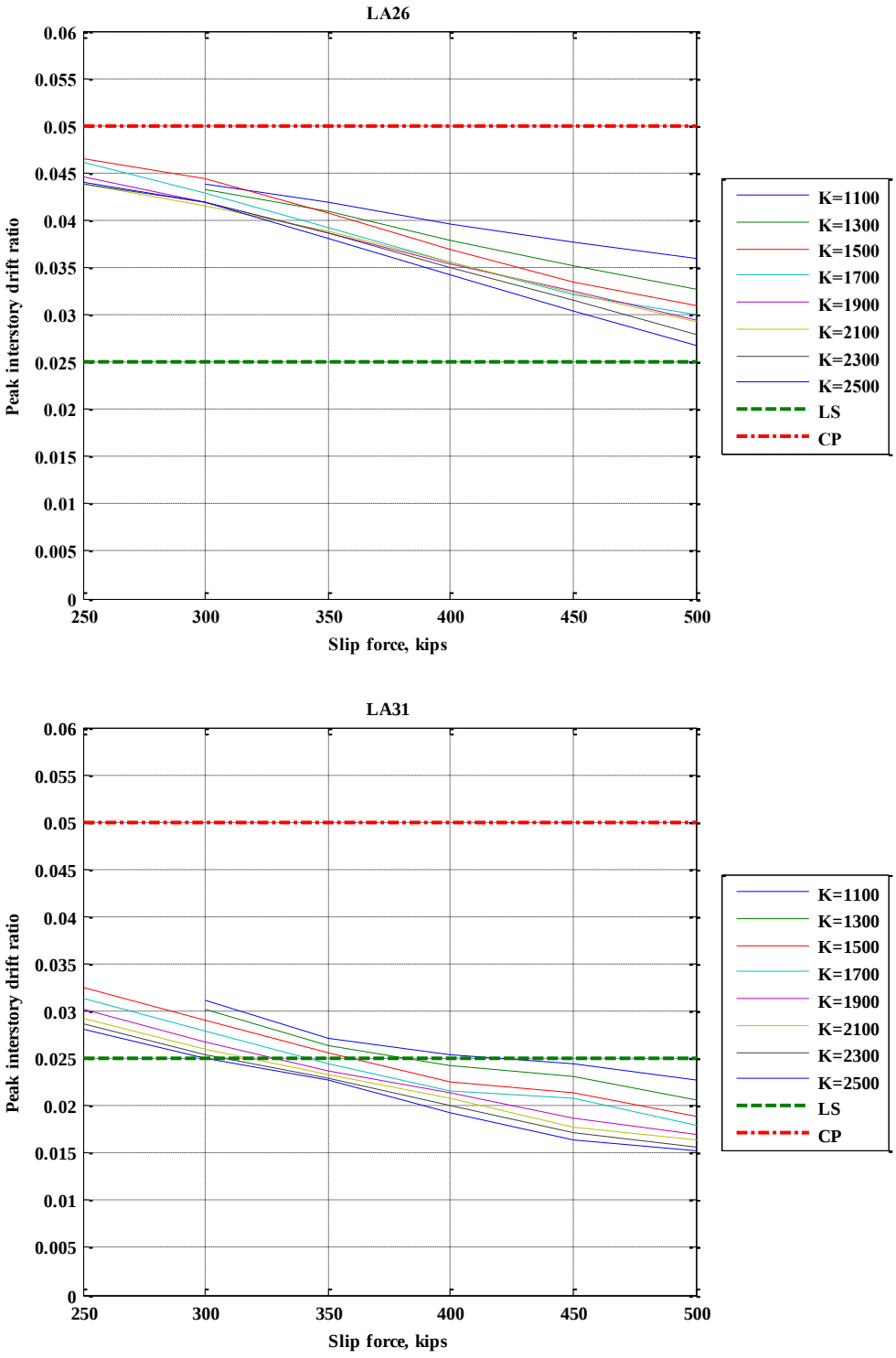


**Figure 5.17:** Effect of FDB parameters on the 2nd FDB 3-story building (part 2)

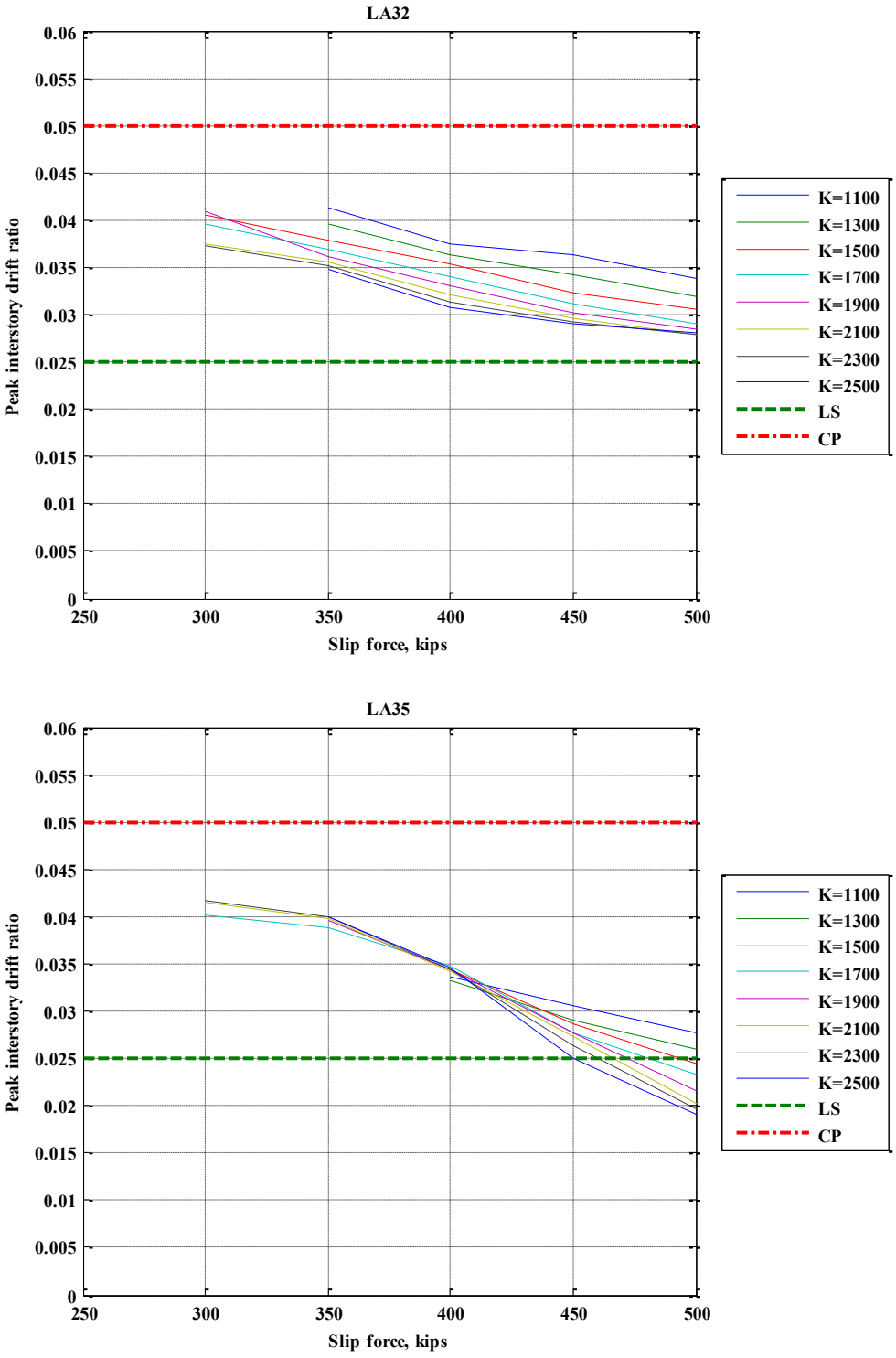


**Figure 5.18:** Effect of FDB parameters on the 2nd FDB 3-story building (part 3)

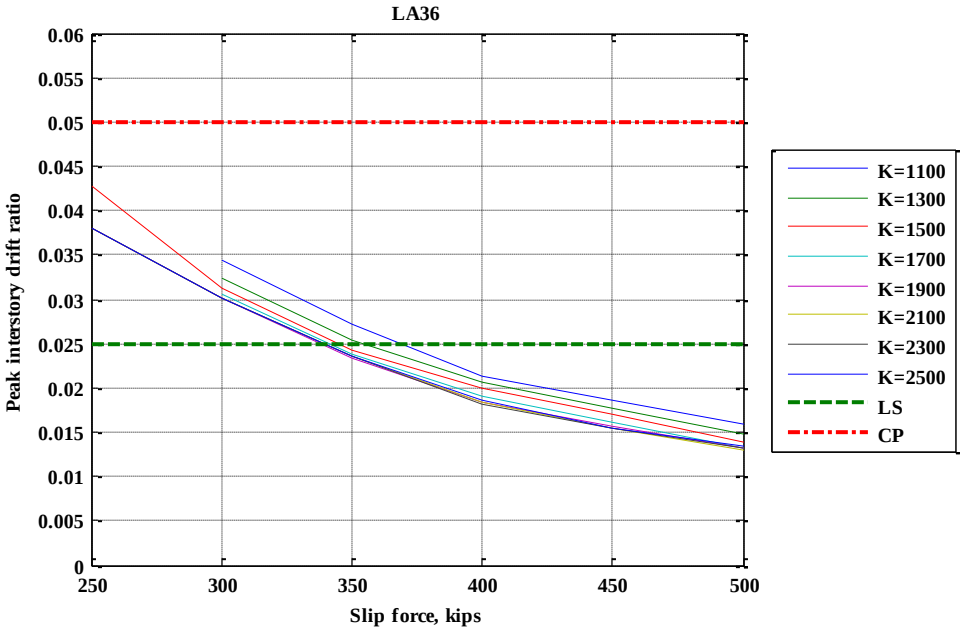


**Figure 5.19:** Effect of FDB parameters on the 2nd FDB 3-story building (part 4)

The conclusion of the revision of the graphs is that the use of friction devices with a slip force of 350 kips combined with stiff braces is enough to do the job to achieve compliance of the frame. The chosen section has to fulfill this stiffness requirement as well as be able to sustain the larger 350 kip force that is generated in the brace as the friction devices slip.

HSS14×14×5/8 sections (K = 2240 kips/in) fulfill both the stiffness and the strength requirements. Thus, such section is proposed to work together with 350 kip force devices in the last brace configuration.

Finally, this design is checked, i.e. the FDBF is evaluated under the action of all 40 earthquake records used in this thesis. The results are shown next together with a comparison with the original interstory drift ratios that were obtained for the original benchmark frame.

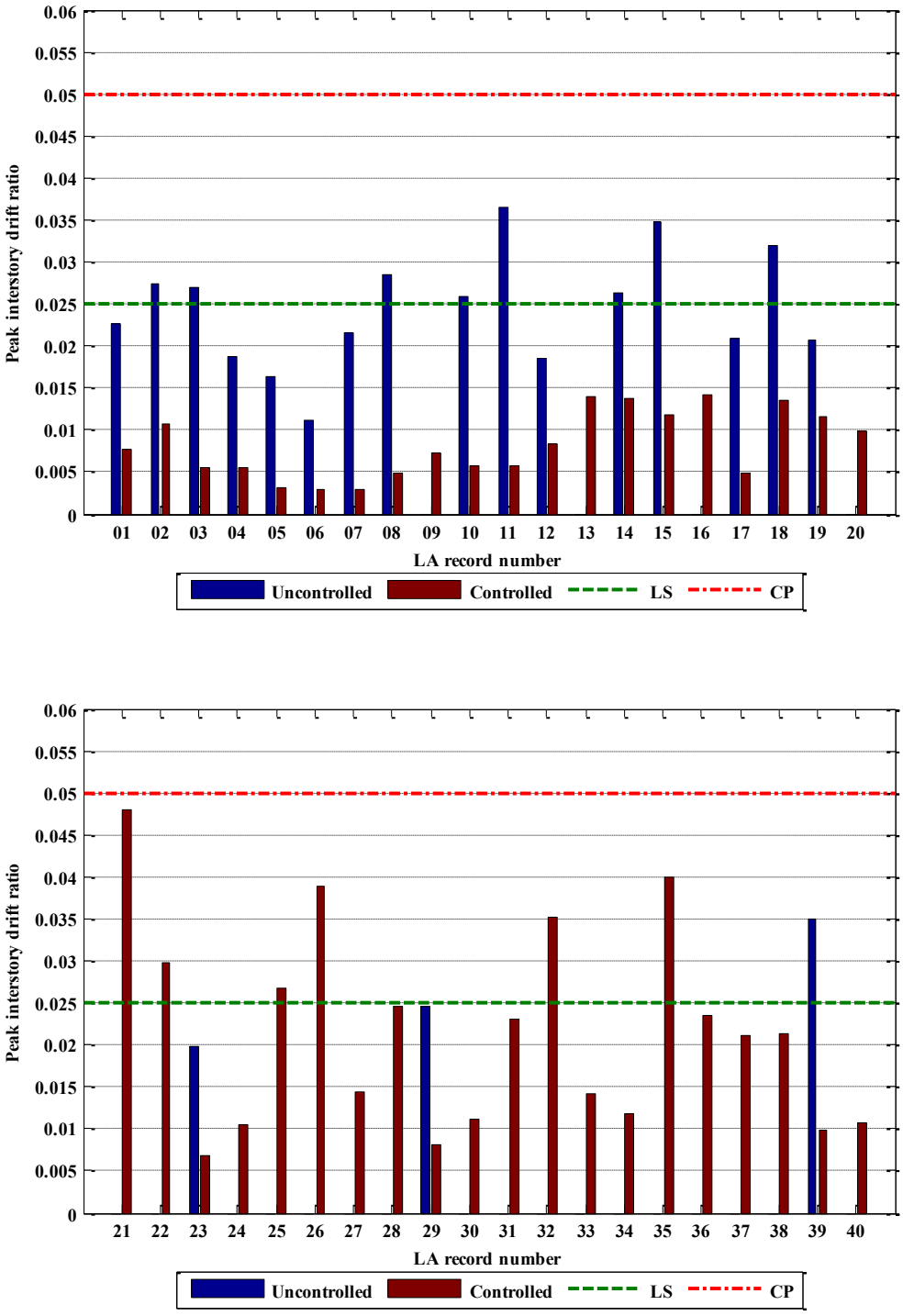


**Figure 5.20:** Comparative peak interstory drift ratios of 3-story FDBF and benchmark

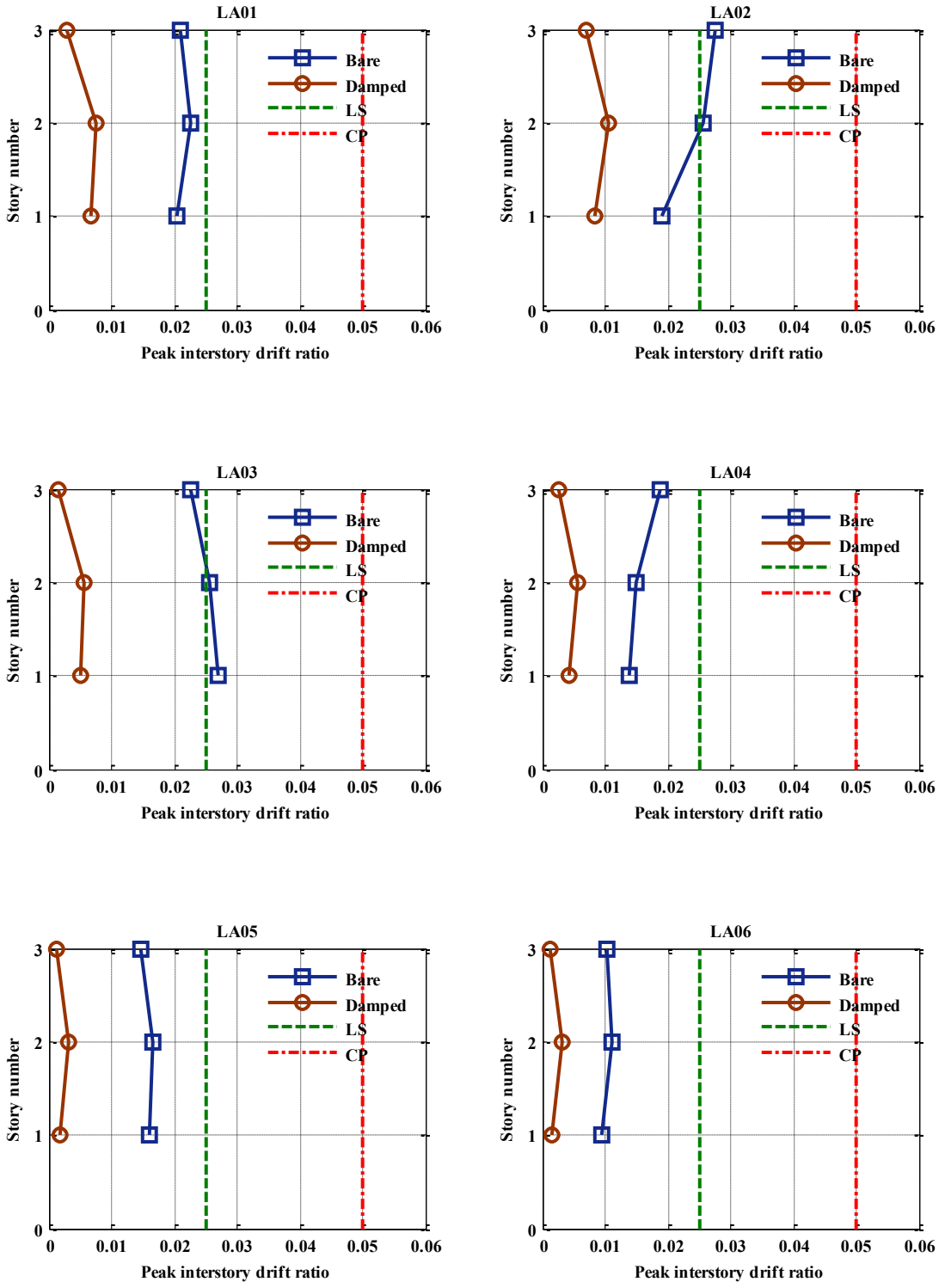


**Figure 5.21:** Comparative interstory drift ratios of 3-story FDBF and benchmark (part 1)

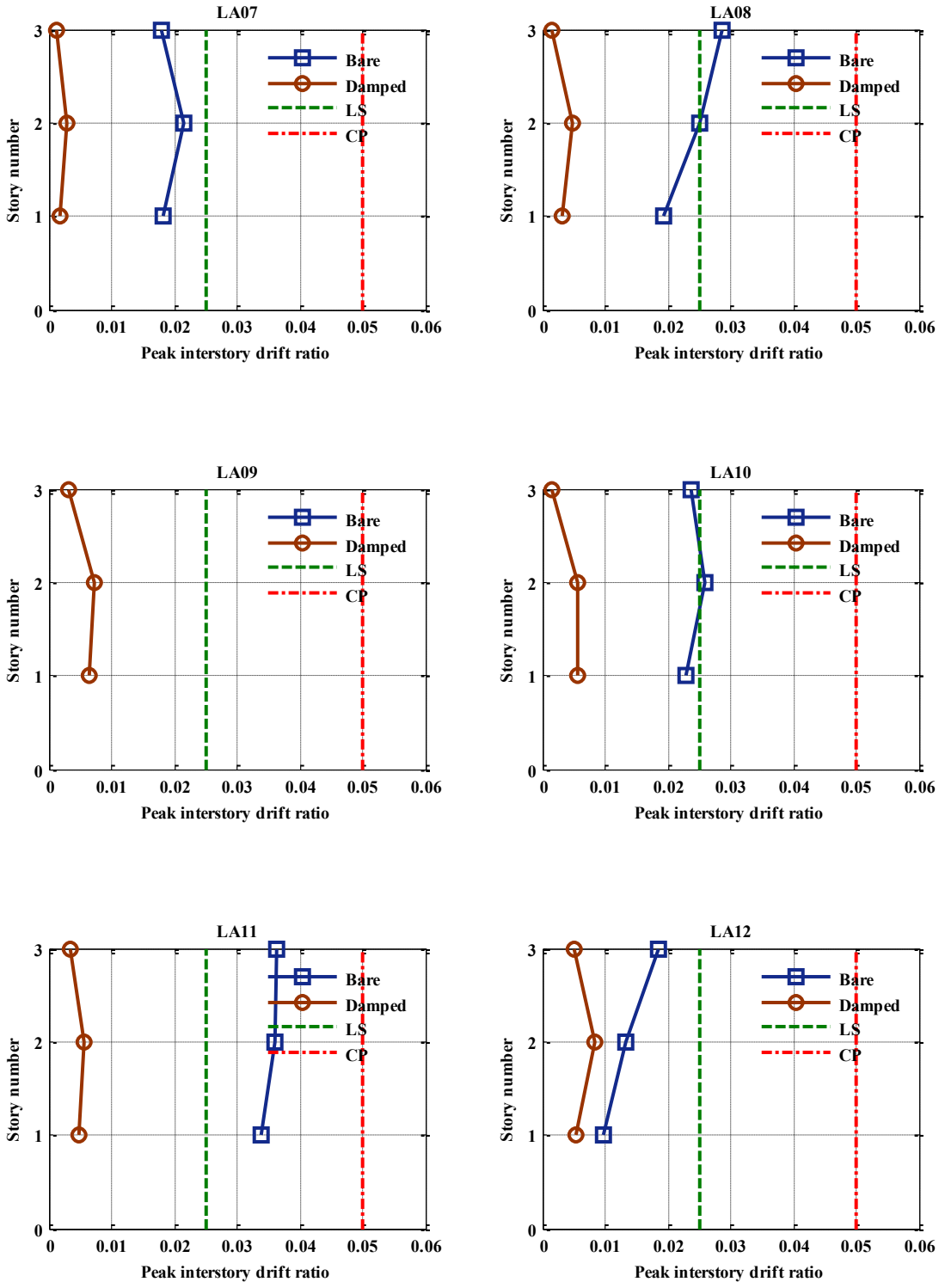


**Figure 5.22:** Comparative interstory drift ratios of 3-story FDBF and benchmark (part 2)

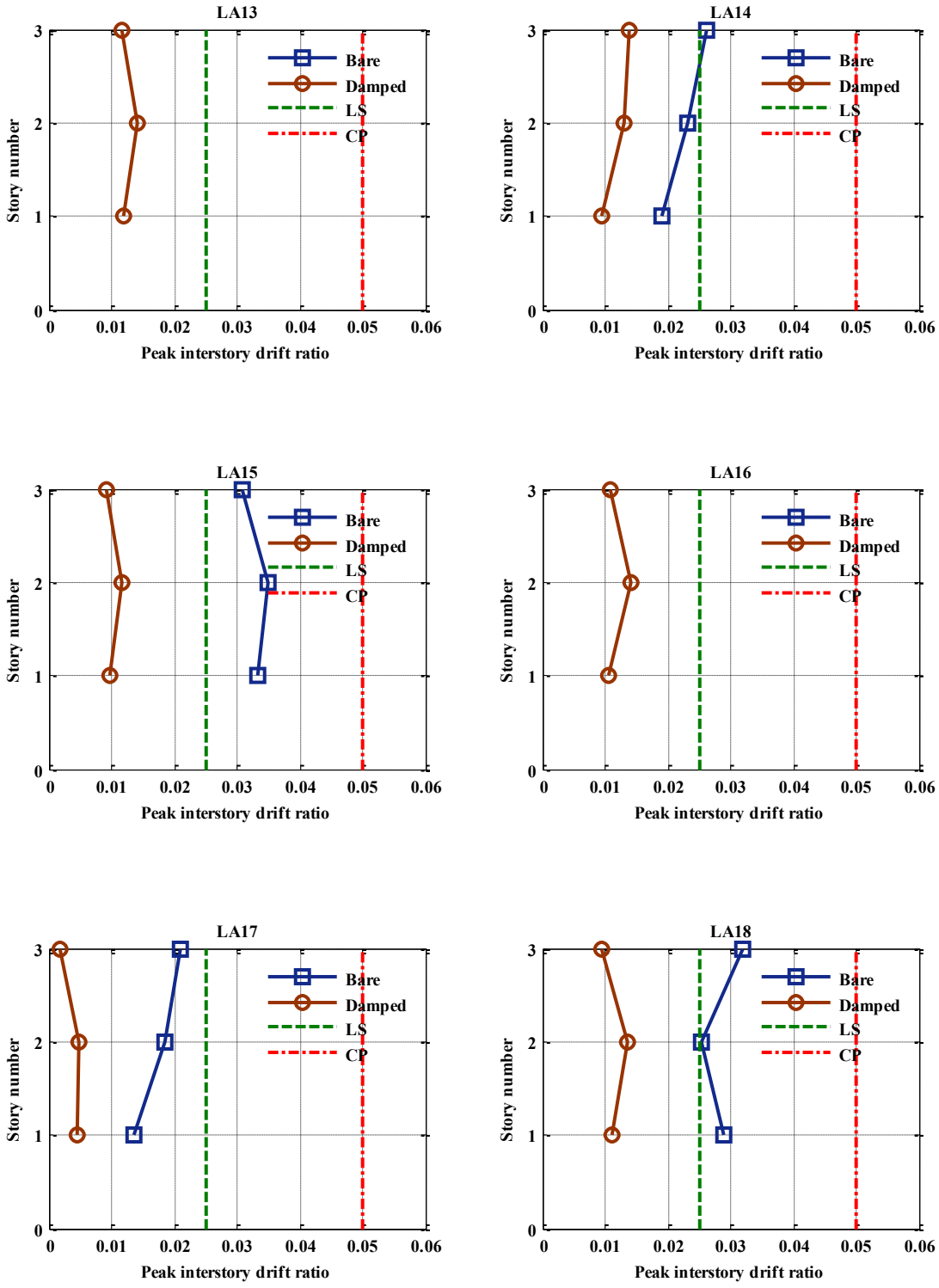


**Figure 5.23:** Comparative interstory drift ratios of 3-story FDBF and benchmark (part 3)

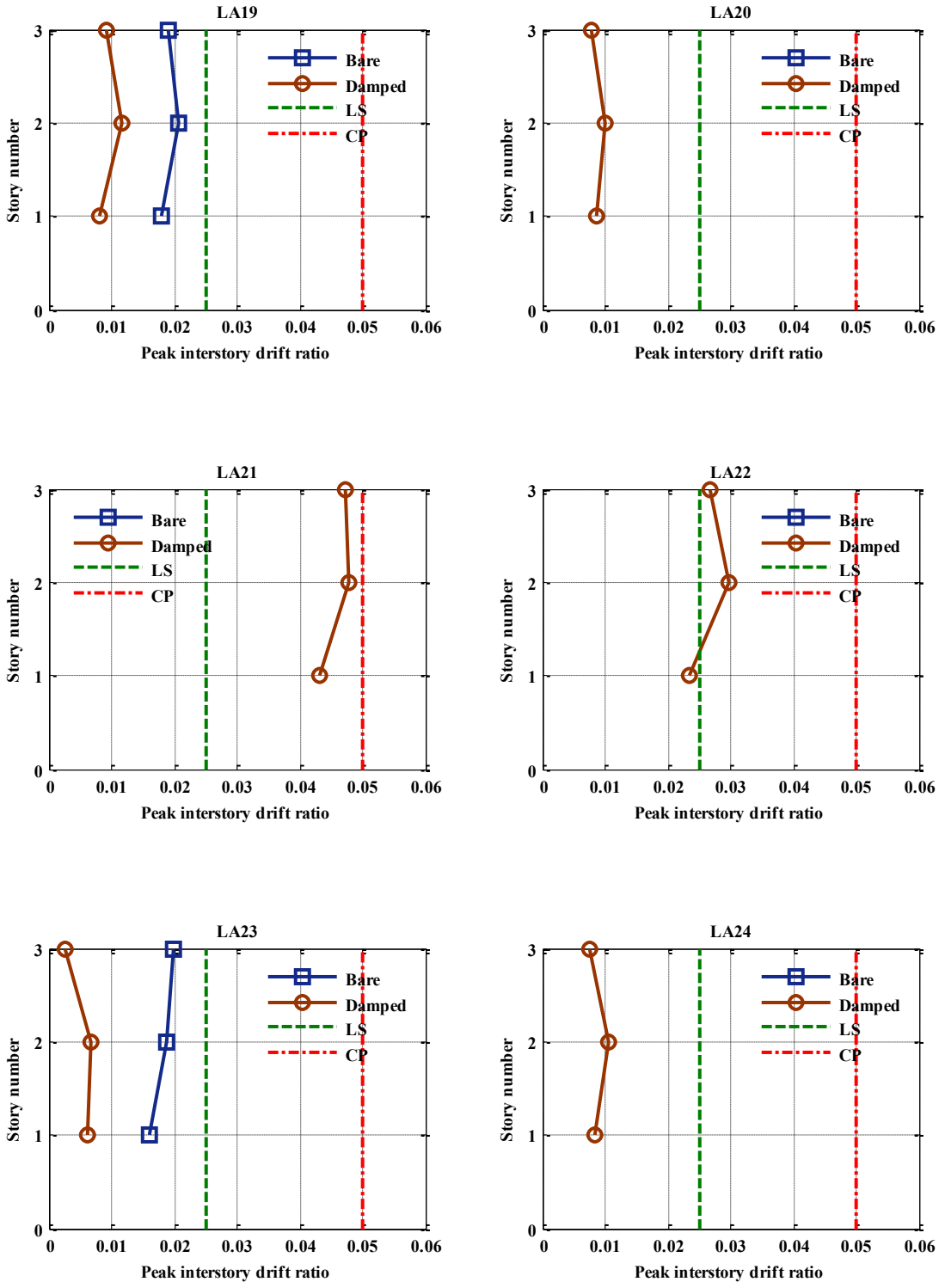


**Figure 5.24:** Comparative interstory drift ratios of 3-story FDBF and benchmark (part 4)

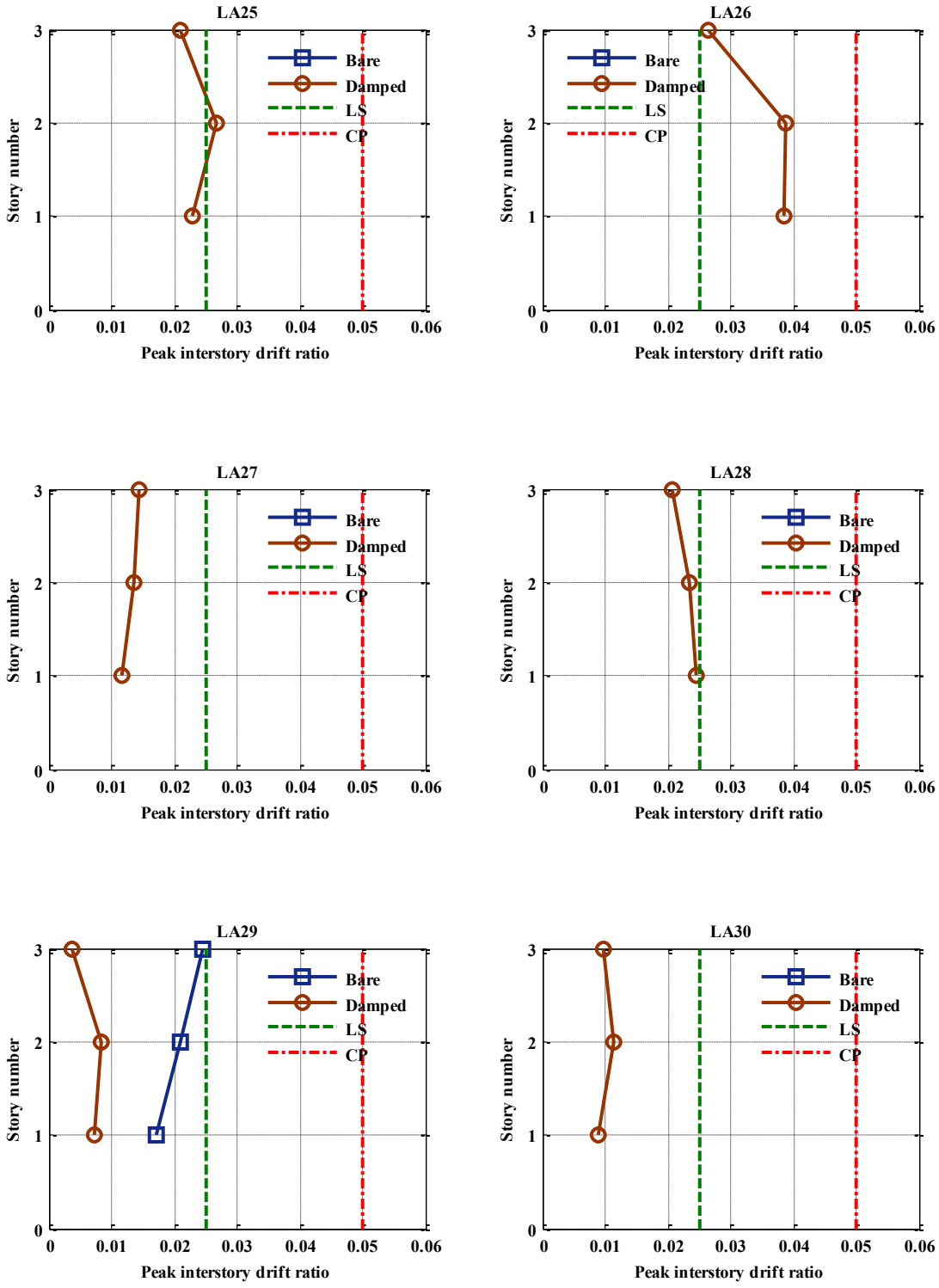


**Figure 5.25:** Comparative interstory drift ratios of 3-story FDBF and benchmark (part 5)

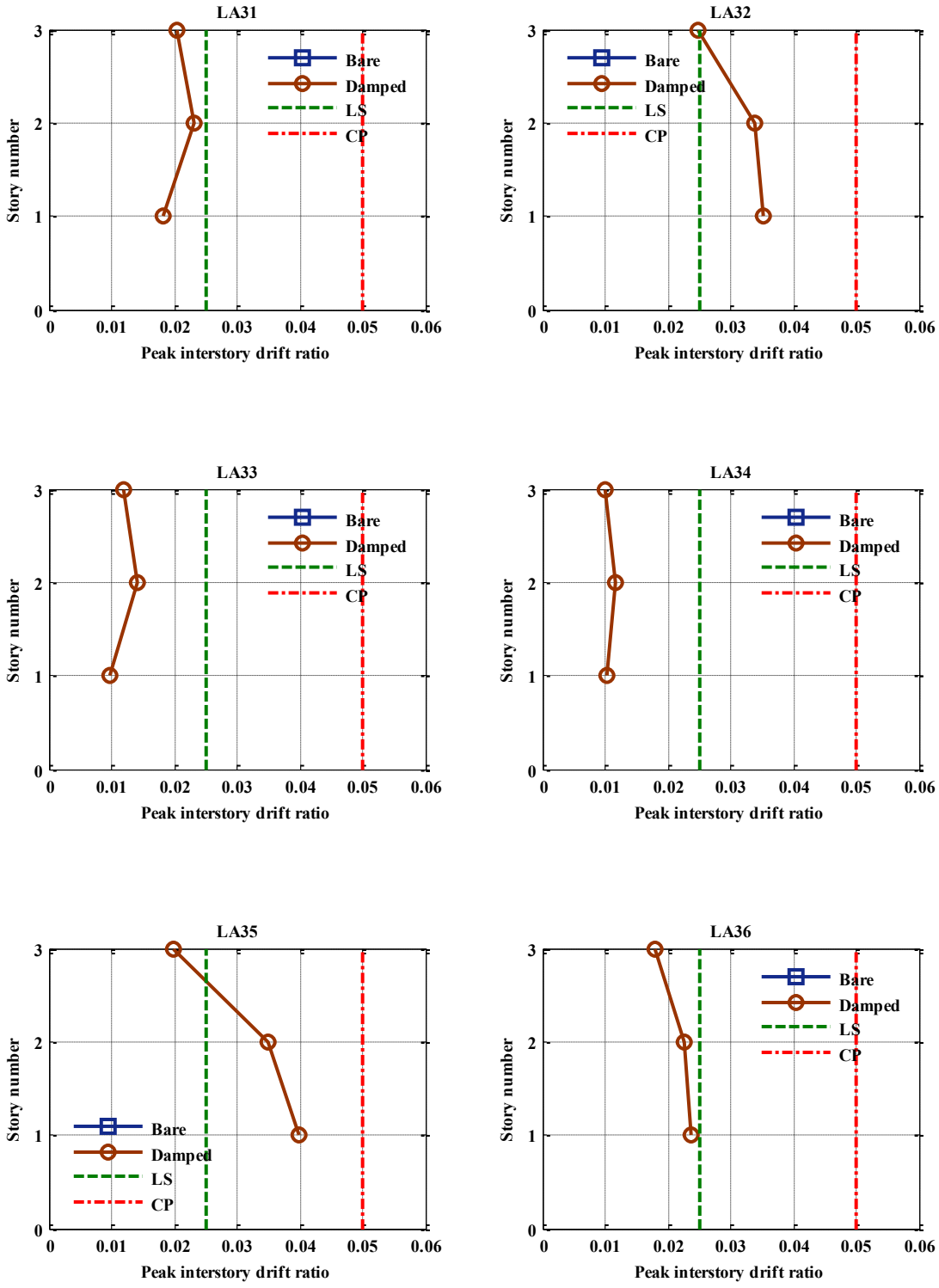


**Figure 5.26:** Comparative interstory drift ratios of 3-story FDBF and benchmark (part 6)

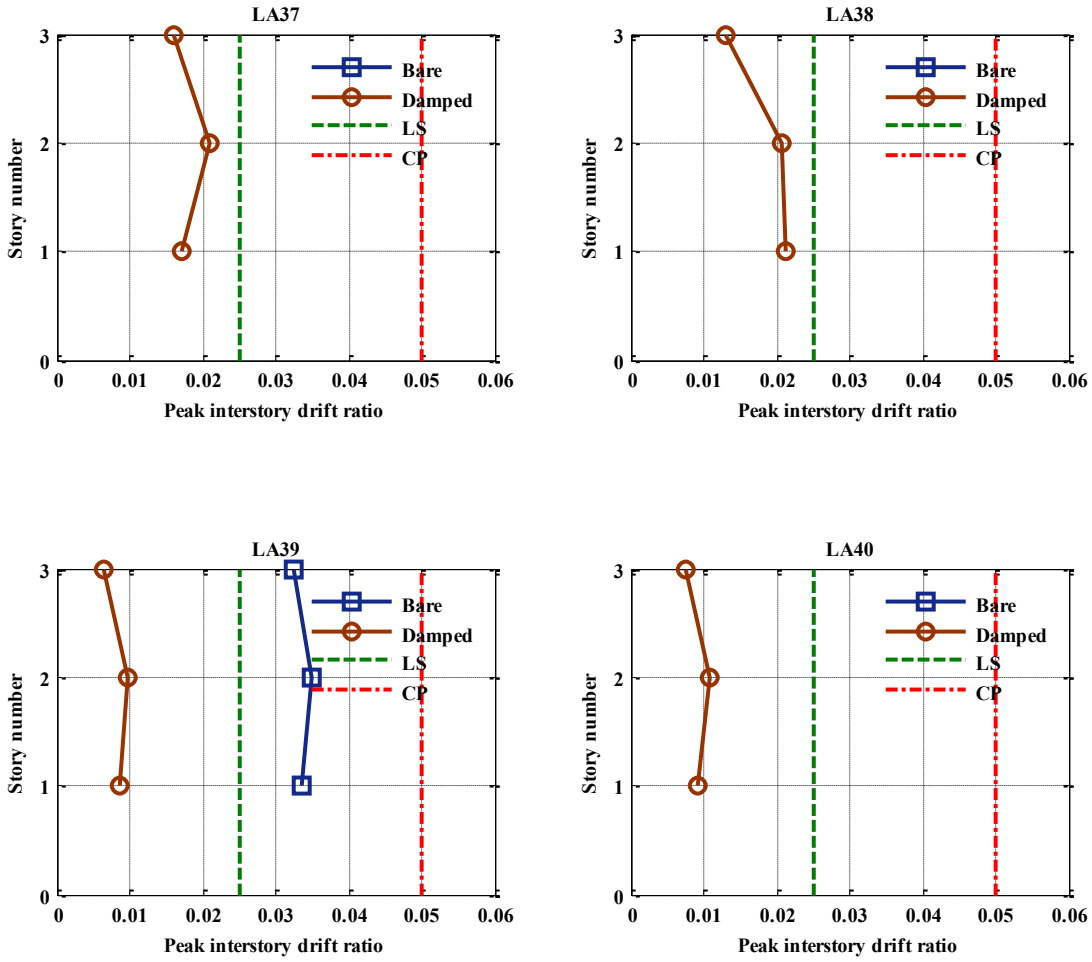


**Figure 5.27:** Comparative interstory drift ratios of 3-story FDBF and benchmark (part 7)

## 5.2 9-Story Building

Like in the case of the 3-story building, first, the capacity of the bare 9-story benchmark building was calculated in order to assess it and have a starting point for the strengthening process. The frame is subjected, again, to the total of 40 earthquakes (20 BSE-1 and 20 BSE-2) considered in this thesis. The maximum interstory drift ratios resulting from these analyses are depicted in the next bar plots.

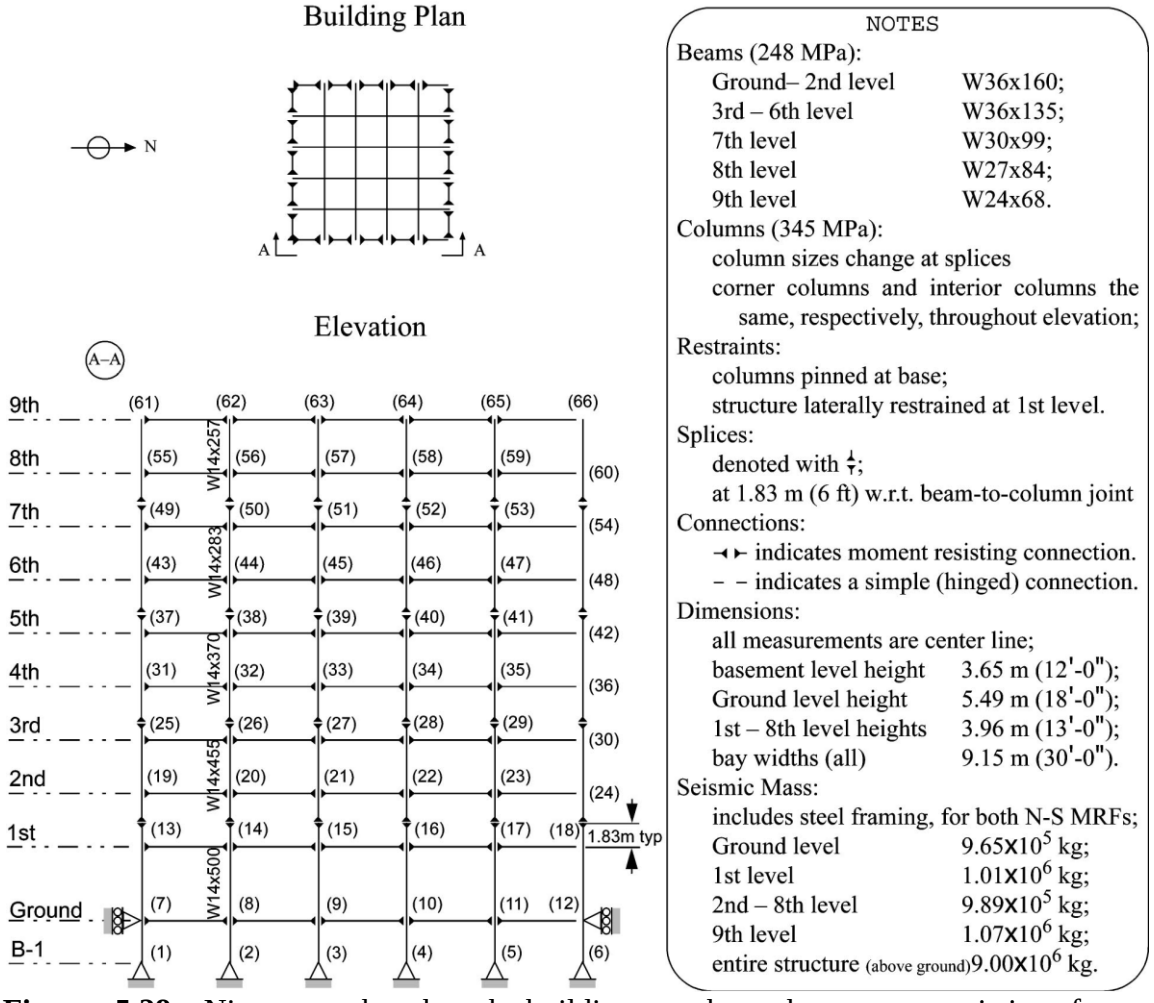


**Figure 5.28:** Nine-story benchmark building north-south moment-resisting frame (Ohtori et al. 2004)

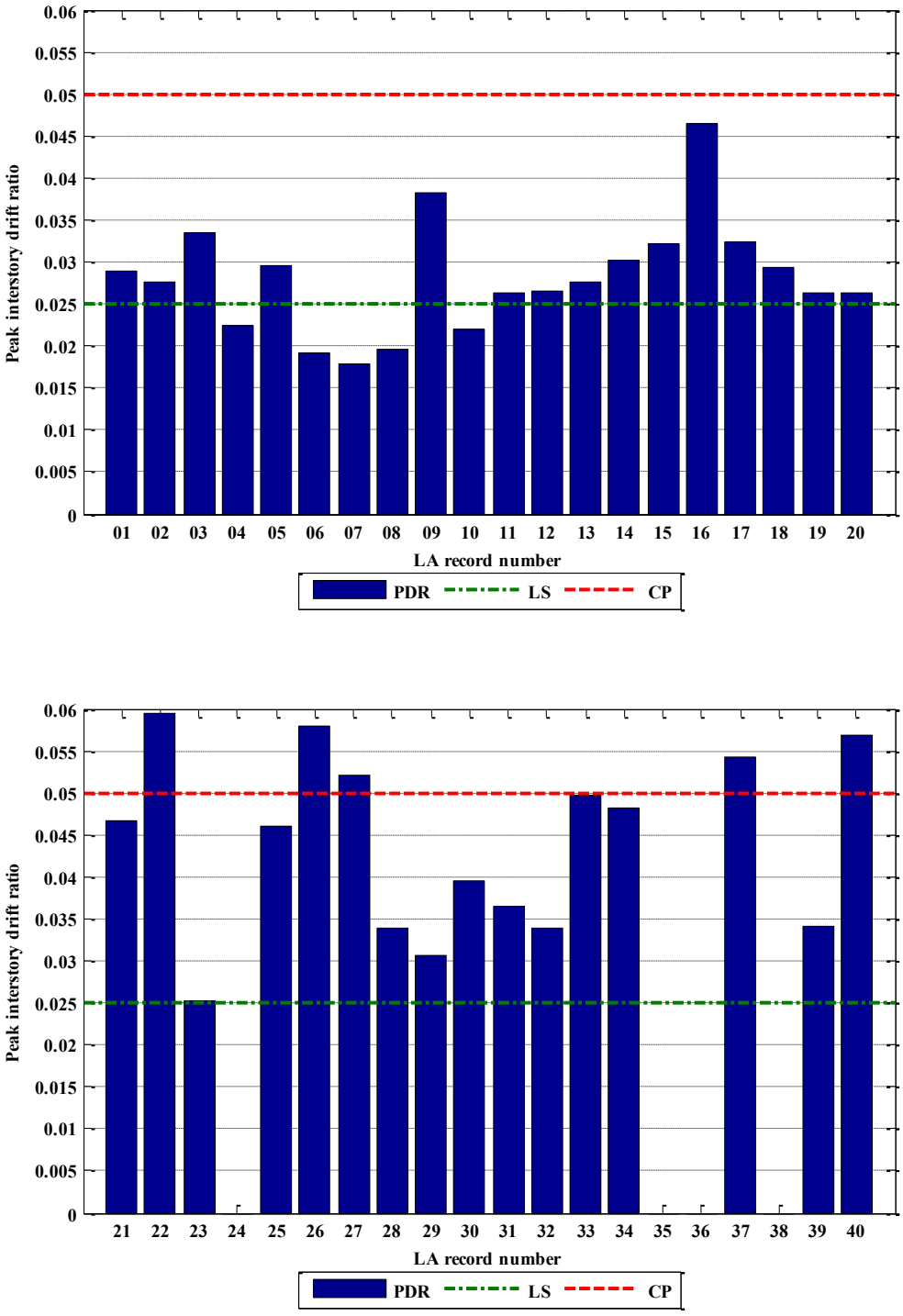


**Figure 5.29:** BSE-1 and BSE-2 interstory drift demands of 9-story benchmark building

Fig. 5.29a shows that 15 BSE-1 records cause the 9-story frame to exceed the LS limit. These form the basis for the necessary control of the structure.

As a second step, optimization of the number and location of the friction-damped braces is carried out; in this case, the use of a maximum of 36 devices in the frame (4 per story) is proposed. In this optimization process, dampers are tested in couples at a same story and inside opposite bays each time for the sake of symmetry (as can be implied, the center bay is not considered). The provisional parameters that are assigned to the FDBs are axial stiffness equal to 1600 kips/in and a slip force equal to 300 kips. The results of the optimization algorithm are presented next in Figs 5.30 to 5.33.

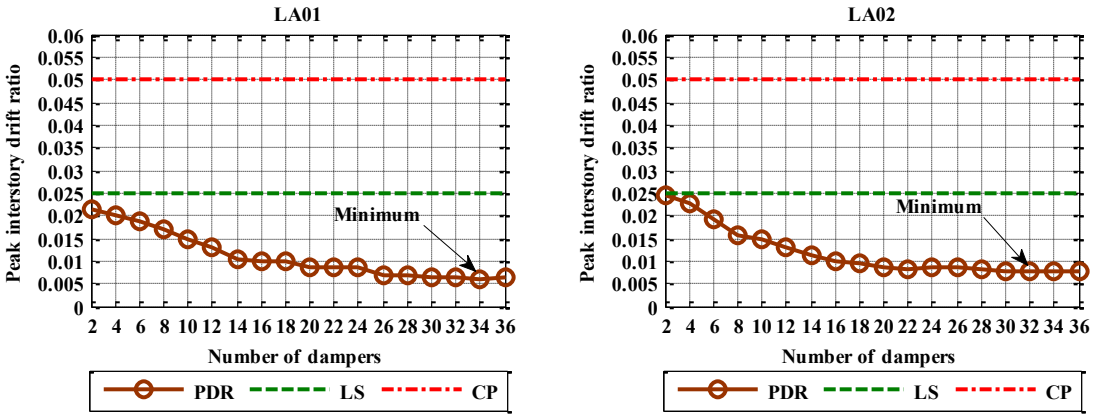


**Figure 5.30:** Performance of interstory drift ratio criterion in the 9-story building (part 1)

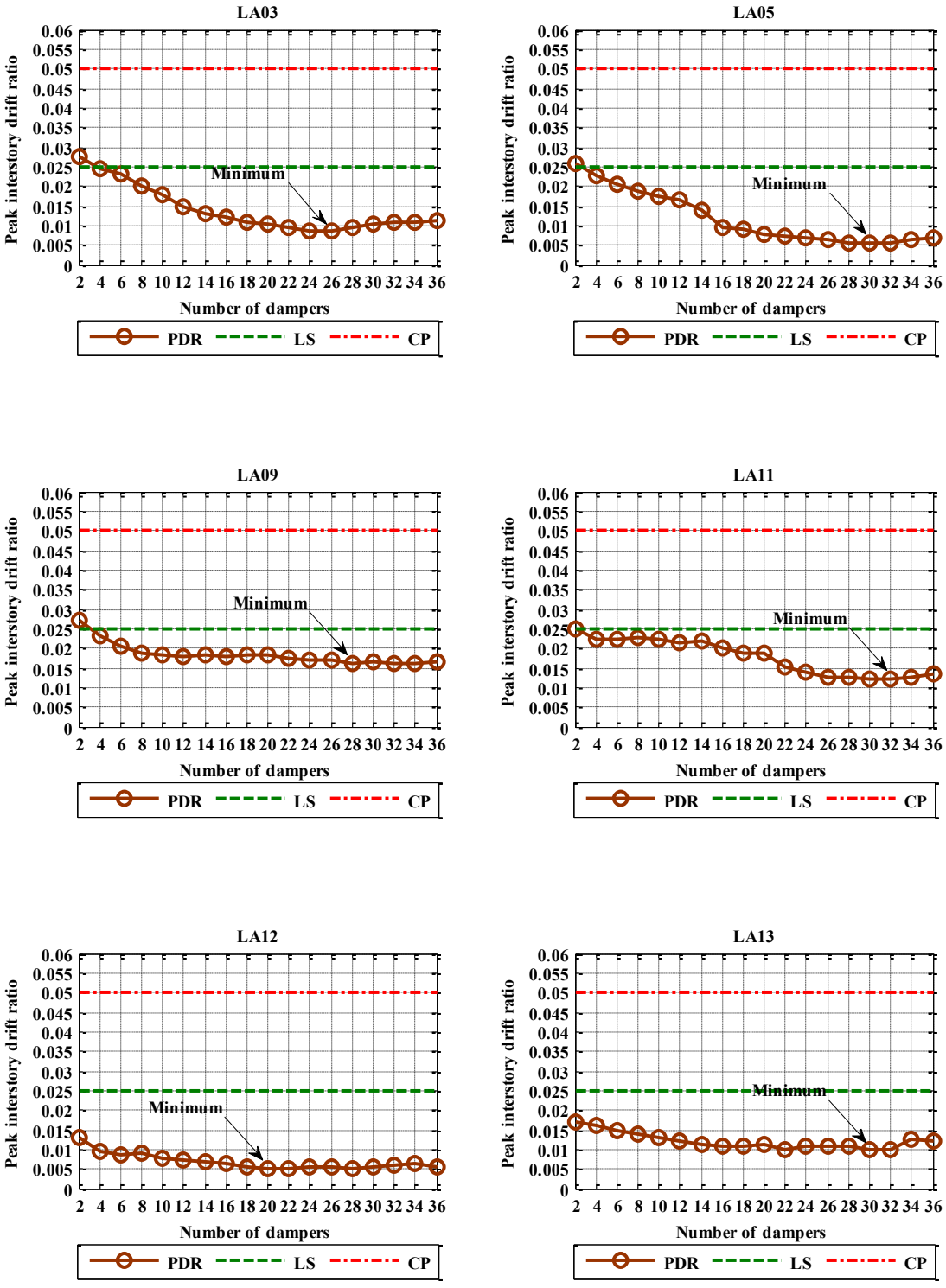


**Figure 5.31:** Performance of interstory drift ratio criterion in the 9-story building (part 2)

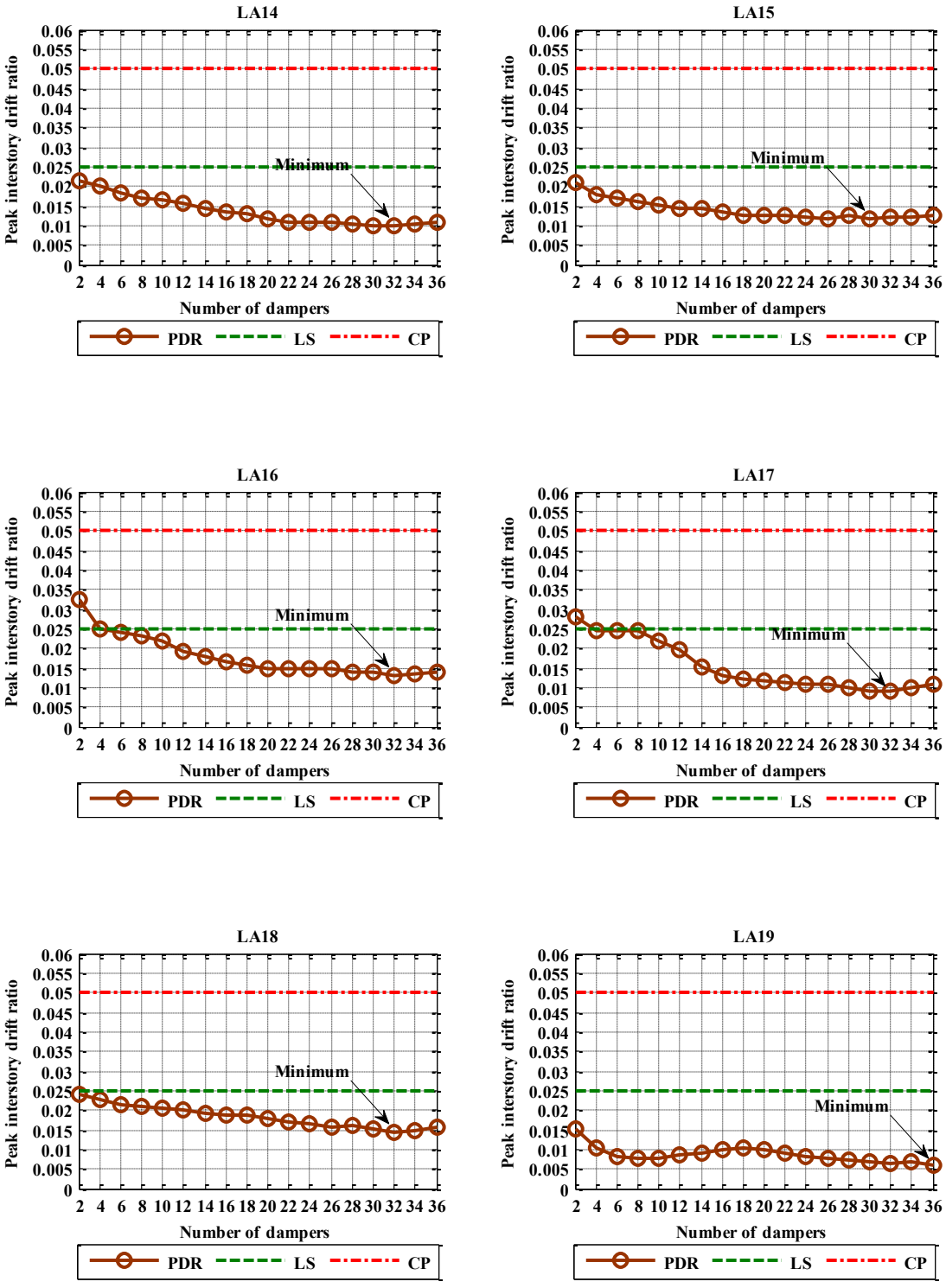


**Figure 5.32:** Performance of interstory drift ratio criterion in the 9-story building (part 3)

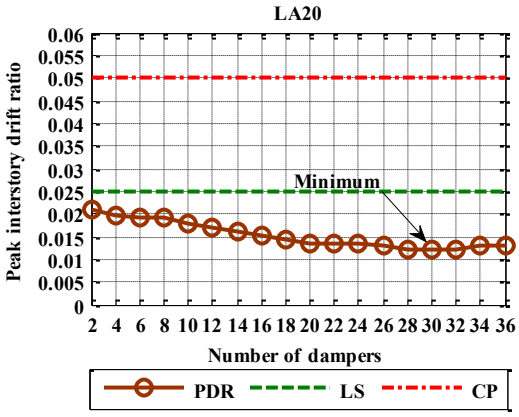


**Figure 5.33:** Performance of interstory drift ratio criterion in the 9-story building (part 4)

Once the above curves were produced, the number of dampers that yields the minimum response under each of the considered earthquakes is selected. This number of dampers corresponds, in each case, to a different and particular bracing array that will minimize the maximum response of the structure under the action of a specific earthquake. The various sub-optimal arrays resulting from the 15 different optimization processes are drawn in Fig. 5.34.

Thirteen different sub-optimal configurations were available (CLA11 and CLA17 happened to be the same as well as CLA05 and CLA20). To determine which configuration would be selected for the continuation of the work proposed for this thesis, each of the arrays in the figure was subjected to the series of 20 BSE-1 earthquakes. Later, the 20 peak interstory drift ratios obtained for each of the 13 arrays were averaged and compared; the configuration yielding the lowest average response was chosen.

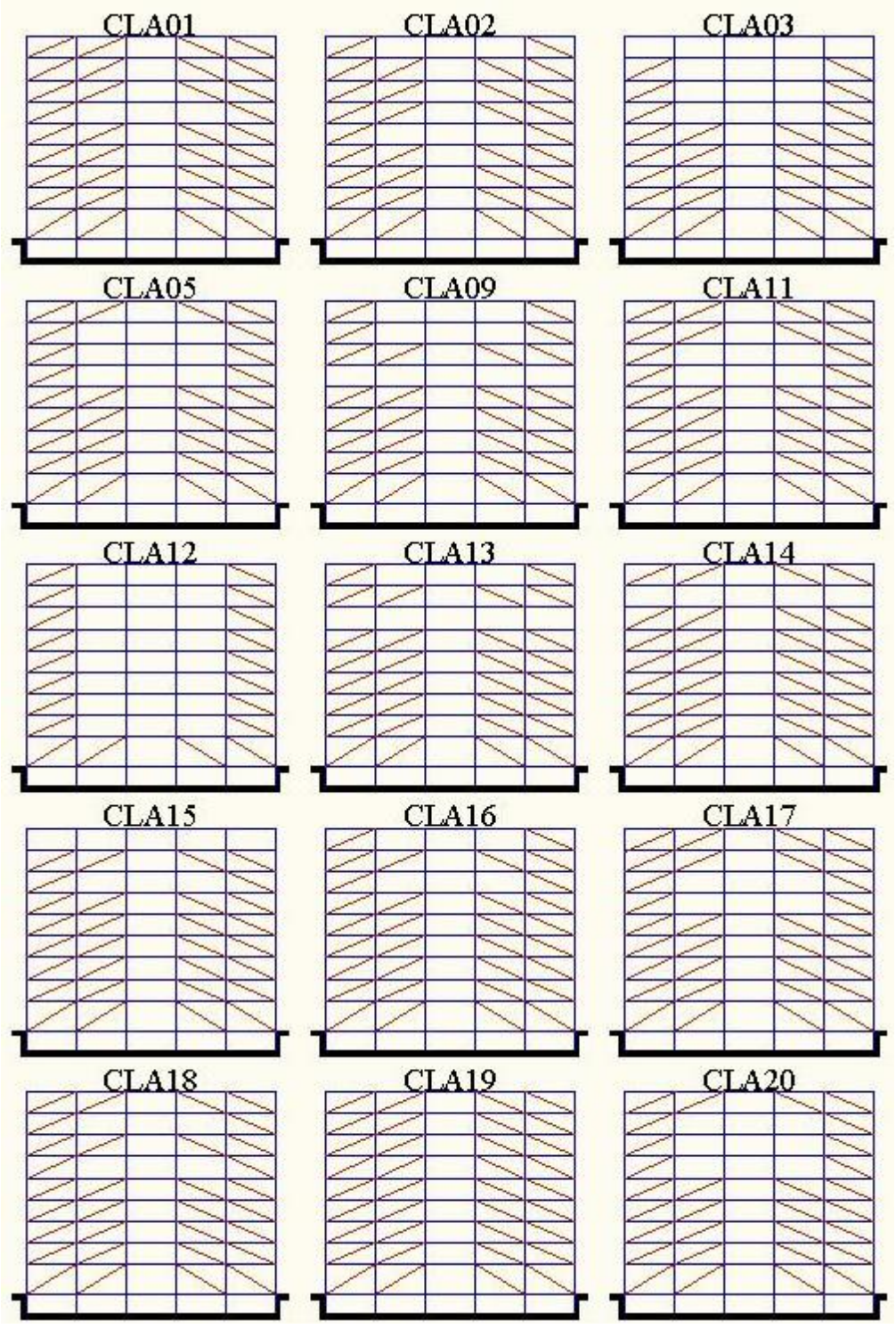


**Figure 5.34:** Sub-optimal FDBF configurations for the 9-story building

**Table 5.1:** Peak interstory drift ratio of the different damper configurations subjected to the series of BSE-1 records.

| | DAMPER CONFIGURATION | | | | | | | | | | | | |
|---|---|---|---|---|---|---|---|---|---|---|---|---|---|
| **RECORD** | **CLA01** | **CLA02** | **CLA03** | **CLA05/20** | **CLA09** | **CLA11/17** | **CLA12** | **CLA13** | **CLA14** | **CLA15** | **CLA16** | **CLA18** | **CLA19** |
| **LA01** | 0.0059 | 0.0064 | 0.0096 | 0.0065 | 0.01 | 0.0066 | 0.0084 | 0.0093 | 0.0092 | 0.0106 | 0.0063 | 0.0063 | 0.0064 |
| **LA02** | 0.0079 | 0.0077 | 0.0096 | 0.0078 | 0.0097 | 0.0077 | 0.0087 | 0.0099 | 0.0095 | 0.0103 | 0.0083 | 0.0084 | 0.0078 |
| **LA03** | 0.0104 | 0.0103 | 0.0086 | 0.0096 | 0.01 | 0.0097 | 0.0114 | 0.0103 | 0.0108 | 0.0105 | 0.0109 | 0.0101 | 0.0111 |
| **LA04** | 0.0054 | 0.0051 | 0.0096 | 0.0055 | 0.0083 | 0.0055 | 0.0067 | 0.0088 | 0.0093 | 0.0122 | 0.0047 | 0.0051 | 0.0057 |
| **LA05** | 0.0063 | 0.0062 | 0.0063 | 0.0054 | 0.0065 | 0.0056 | 0.0088 | 0.0063 | 0.0064 | 0.0064 | 0.0063 | 0.006 | 0.0069 |
| **LA06** | 0.0071 | 0.007 | 0.0077 | 0.0059 | 0.0072 | 0.0064 | 0.0056 | 0.0085 | 0.009 | 0.0088 | 0.0073 | 0.0072 | 0.0078 |
| **LA07** | 0.0077 | 0.0075 | 0.0079 | 0.0073 | 0.0075 | 0.0073 | 0.0074 | 0.0079 | 0.0079 | 0.0091 | 0.008 | 0.0079 | 0.0082 |
| **LA08** | 0.0075 | 0.0073 | 0.0074 | 0.0073 | 0.0088 | 0.0076 | 0.0077 | 0.0079 | 0.0079 | 0.0092 | 0.0082 | 0.0077 | 0.0081 |
| **LA09** | 0.0162 | 0.0171 | 0.0179 | 0.0169 | 0.016 | 0.0158 | 0.0189 | 0.0167 | 0.0177 | 0.017 | 0.0172 | 0.0163 | 0.0164 |
| **LA10** | 0.0081 | 0.0085 | 0.0083 | 0.0072 | 0.0086 | 0.0078 | 0.009 | 0.0085 | 0.0086 | 0.0101 | 0.0086 | 0.0085 | 0.0089 |
| **LA11** | 0.0124 | 0.0128 | 0.0123 | 0.0124 | 0.0136 | 0.012 | 0.0188 | 0.0139 | 0.014 | 0.0138 | 0.013 | 0.0125 | 0.0134 |
| **LA12** | 0.0057 | 0.0062 | 0.0106 | 0.0065 | 0.0075 | 0.0064 | 0.0049 | 0.0082 | 0.0088 | 0.0124 | 0.0068 | 0.0061 | 0.0054 |
| **LA13** | 0.0119 | 0.0118 | 0.0109 | 0.0109 | 0.0104 | 0.0114 | 0.0117 | 0.0097 | 0.0096 | 0.0118 | 0.0127 | 0.012 | 0.0121 |
| **LA14** | 0.01 | 0.0098 | 0.0095 | 0.0095 | 0.0115 | 0.01 | 0.0139 | 0.0105 | 0.0097 | 0.0098 | 0.0105 | 0.0103 | 0.0106 |
| **LA15** | 0.0119 | 0.0117 | 0.014 | 0.0112 | 0.0129 | 0.0117 | 0.0126 | 0.0121 | 0.0126 | 0.0116 | 0.0123 | 0.0115 | 0.0127 |
| **LA16** | 0.0138 | 0.015 | 0.0205 | 0.0165 | 0.0144 | 0.0151 | 0.0143 | 0.0155 | 0.0149 | 0.0171 | 0.0128 | 0.0132 | 0.0137 |
| **LA17** | 0.0101 | 0.01 | 0.01 | 0.0092 | 0.0097 | 0.0091 | 0.0118 | 0.0095 | 0.0099 | 0.0097 | 0.0102 | 0.0096 | 0.0109 |
| **LA18** | 0.0147 | 0.0151 | 0.0229 | 0.0174 | 0.0159 | 0.0162 | 0.0165 | 0.0171 | 0.0161 | 0.0165 | 0.0146 | 0.0143 | 0.0158 |
| **LA19** | 0.0078 | 0.0071 | 0.0106 | 0.0078 | 0.0085 | 0.0078 | 0.0068 | 0.0098 | 0.0095 | 0.0121 | 0.0068 | 0.0074 | 0.0058 |
| **LA20** | 0.0131 | 0.0134 | 0.0137 | 0.0121 | 0.0135 | 0.0125 | 0.0161 | 0.0134 | 0.0132 | 0.0132 | 0.0126 | 0.0122 | 0.013 |
| **Average** | 0.0097 | 0.0098 | 0.0114 | 0.0096 | 0.0105 | **0.0096** | 0.011 | 0.0107 | 0.0107 | 0.0116 | 0.0099 | 0.0096 | 0.01 |

Table 5.1 shows that the configuration that results in the smallest average peak interstory drift ratio is configuration CLA11/17; thus, this configuration is used in the following steps (the average response of CLA18 is actually larger if more significant figures are used).

Calibration of the FDB parameters (brace stiffness and slip force of dampers) comes now. The CLA11/17 FDBF is subjected to each of the BSE-1 earthquake records for which the bare benchmark frame was not adequate and, in each case, several combinations of stiffness and friction force are analyzed to draw the curves shown in the next graphs.

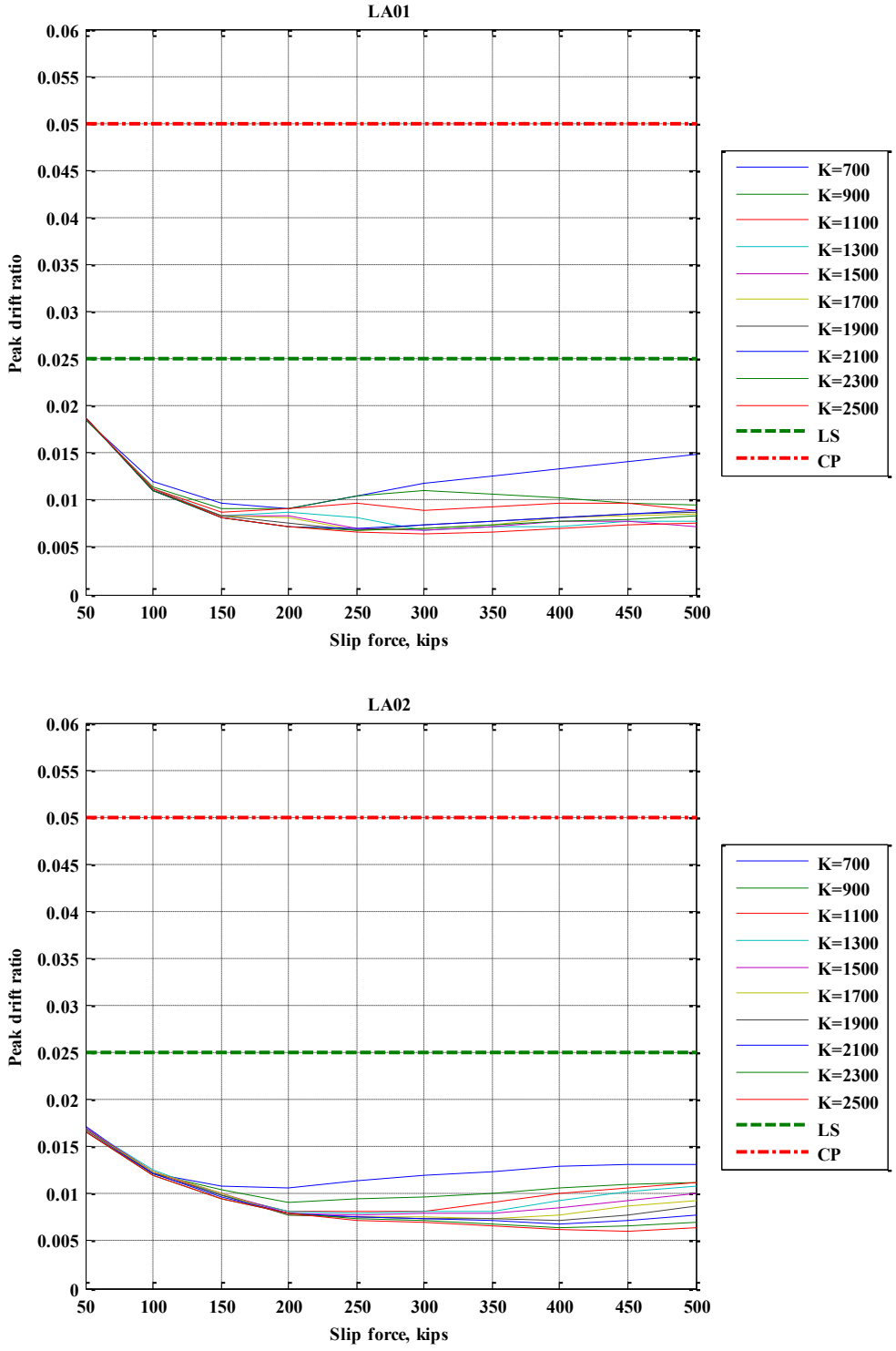


**Figure 5.35:** Effect of FDB parameters on the FDB 9-story building (part 1)

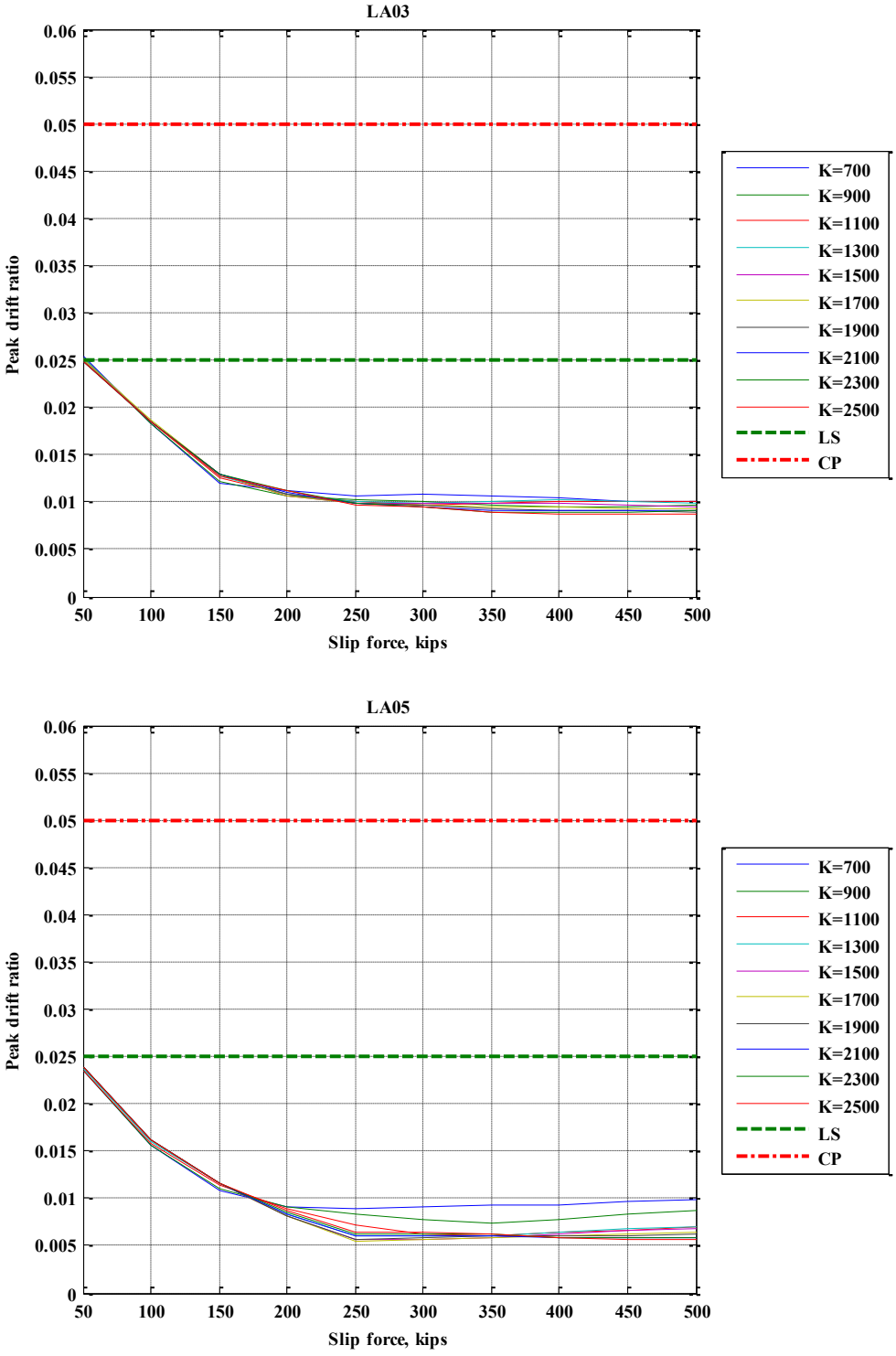


**Figure 5.36:** Effect of FDB parameters on the FDB 9-story building (part 2)

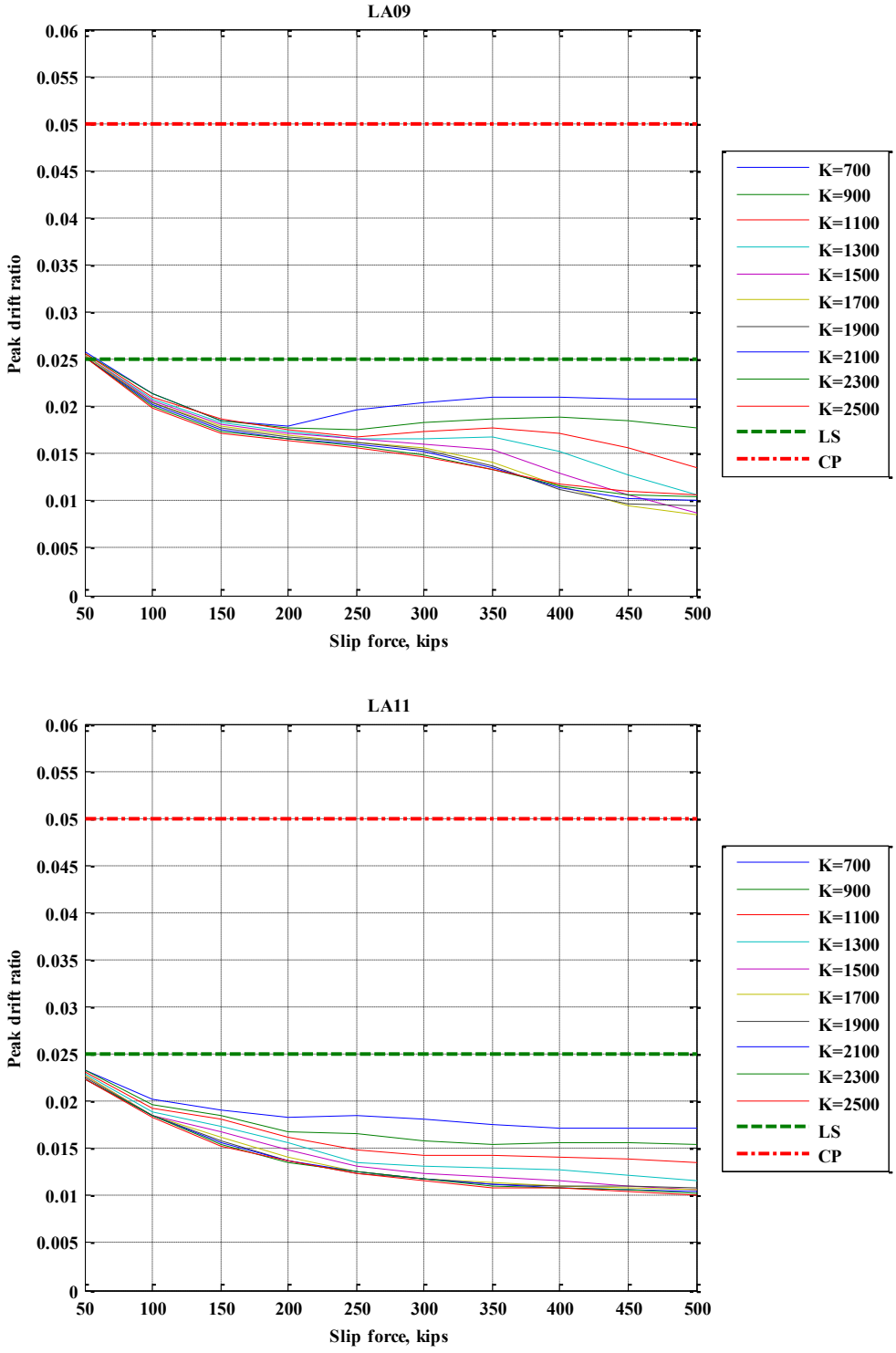


**Figure 5.37:** Effect of FDB parameters on the FDB 9-story building (part 3)

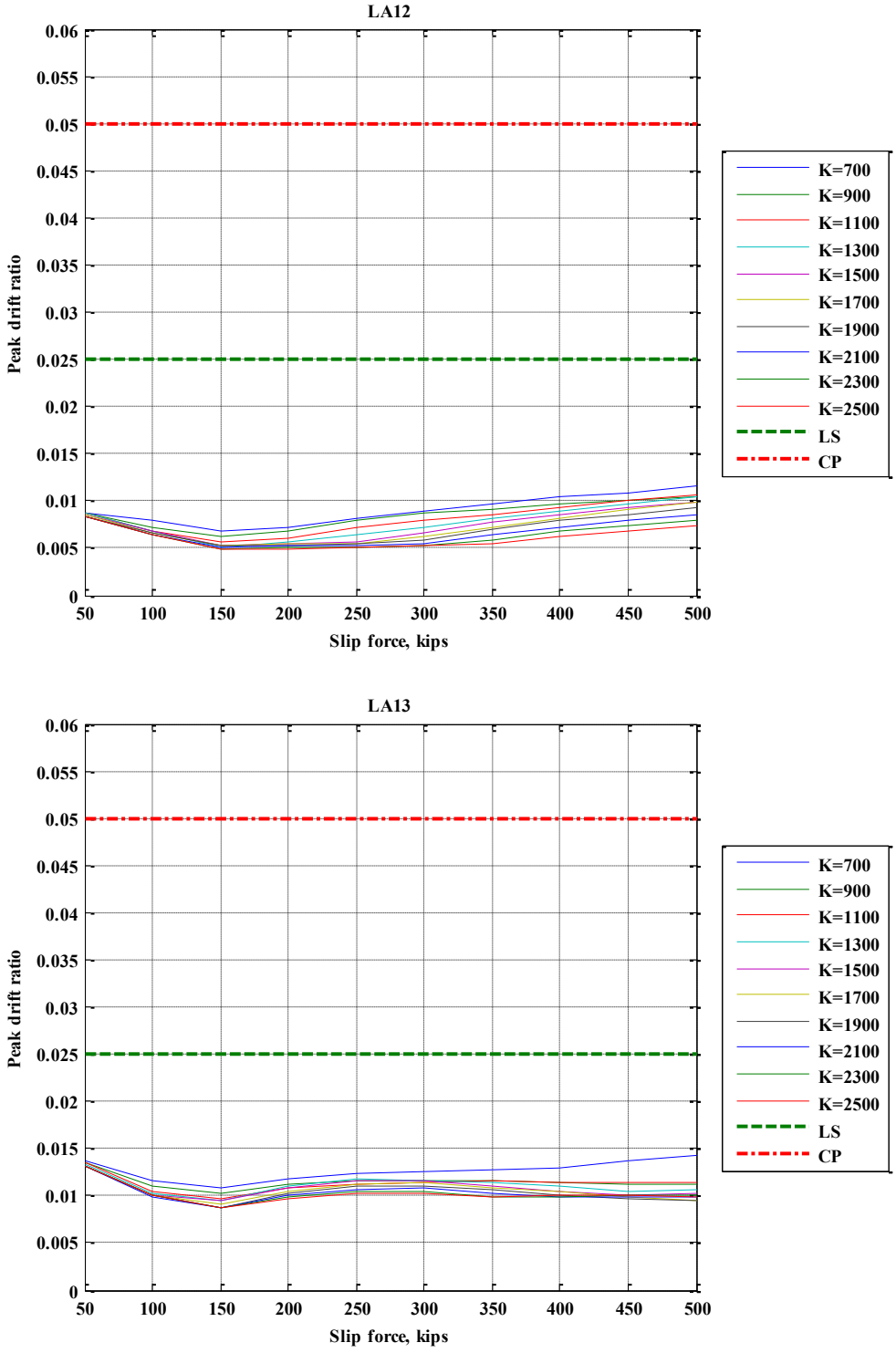


**Figure 5.38:** Effect of FDB parameters on the FDB 9-story building (part 4)

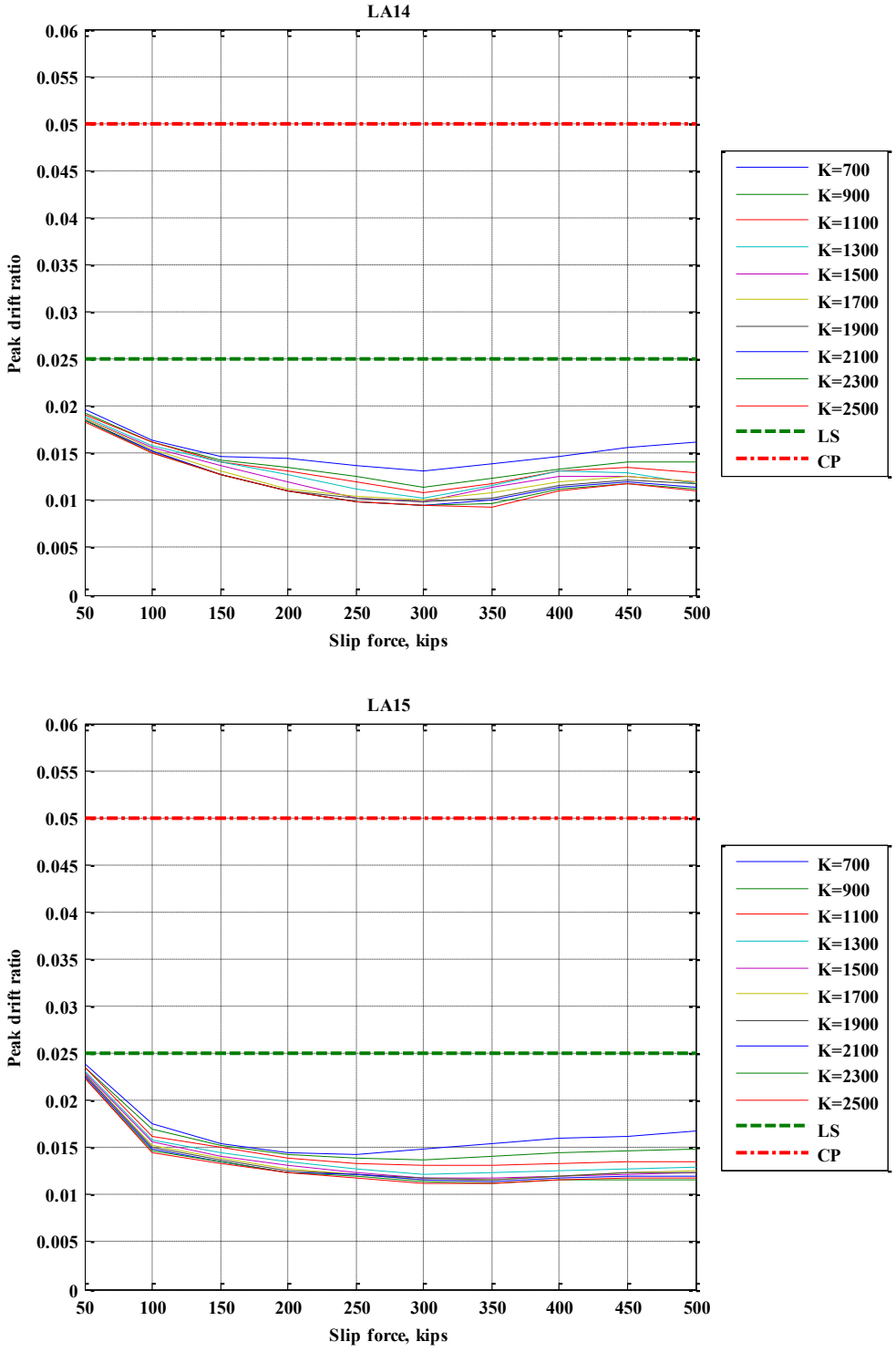


**Figure 5.39:** Effect of FDB parameters on the FDB 9-story building (part 5)

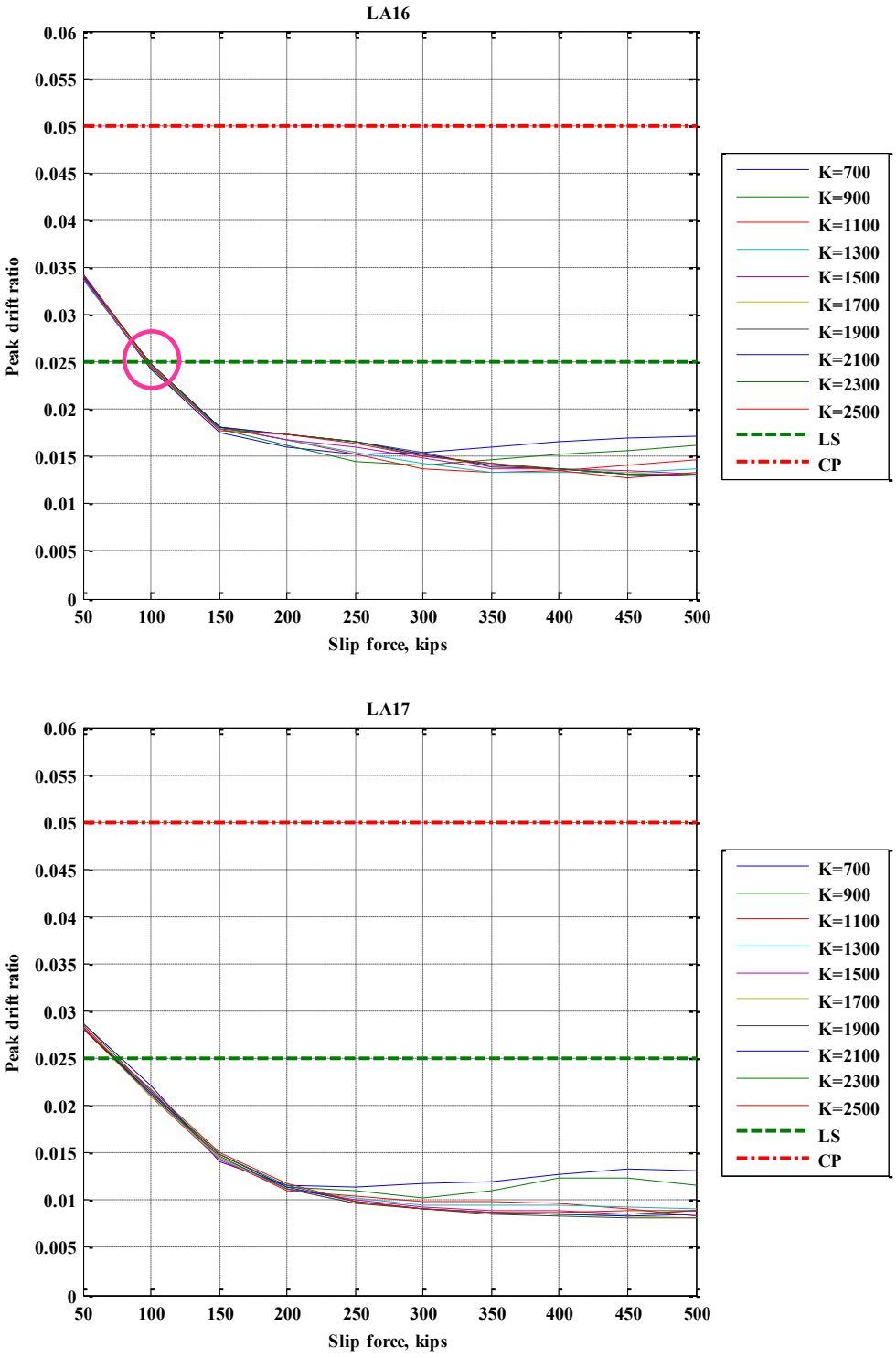


**Figure 5.40:** Effect of FDB parameters on the FDB 9-story building (part 6)

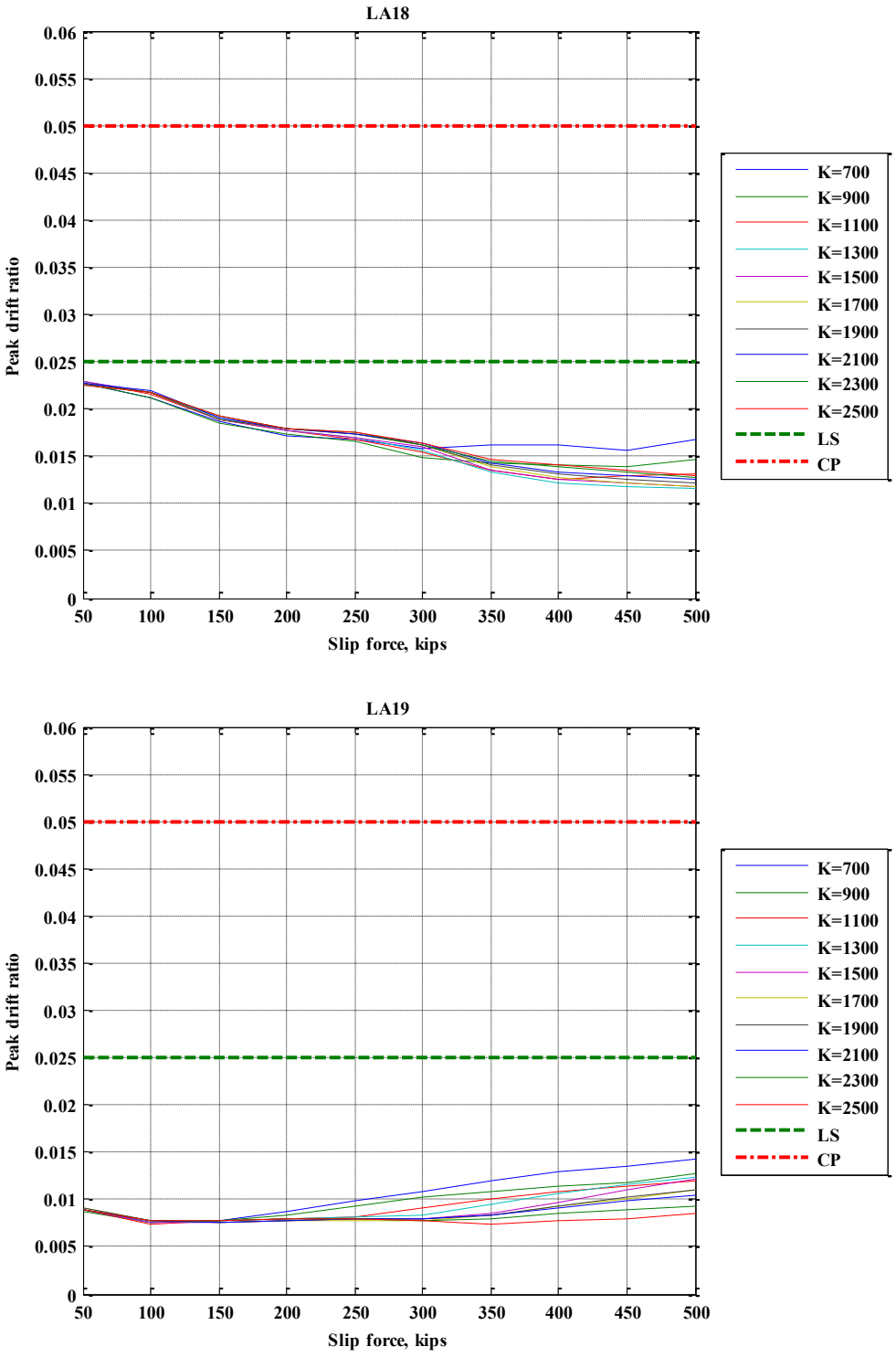


**Figure 5.41:** Effect of FDB parameters on the FDB 9-story building (part 7)

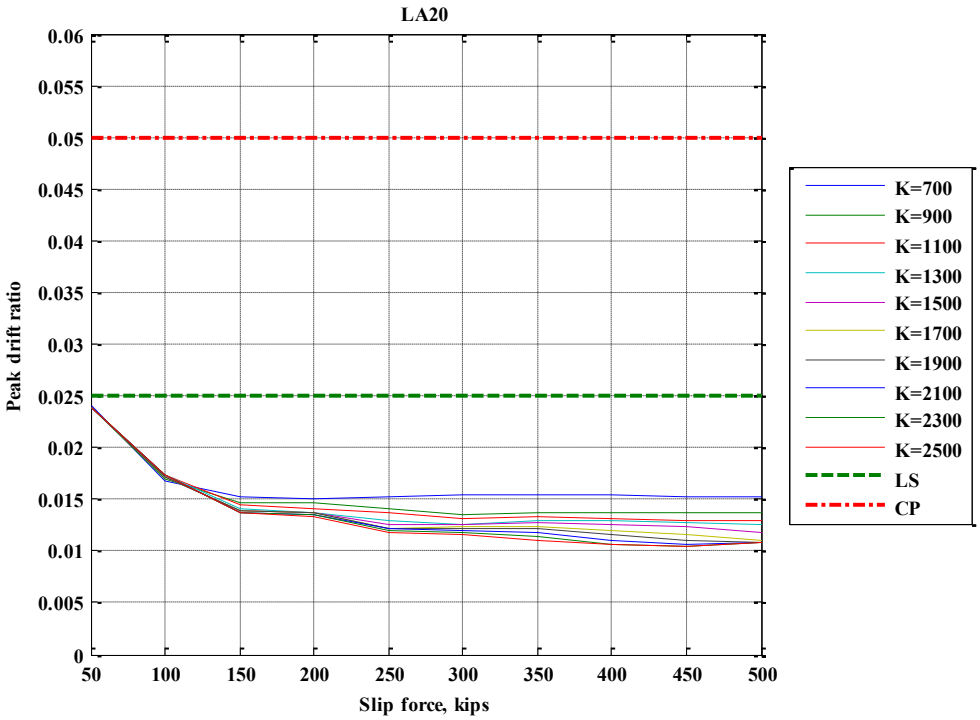


**Figure 5.42:** Effect of FDB parameters on the FDB 9-story building (part 8)

Revision of the plots shows that any value of brace stiffness acting together with friction devices with slip load equal to 100 kips will bring the peak interstory drift ratio in the building below the 0.025 threshold. Since the stiffness of the brace is, in this case, not an issue, the most economical section will be the lightest that guarantees resistance to the maximum compression load that can be developed in the brace, namely, 100 kips. Consequently, HSS9×9×5/16 shapes (K = 733 kips/in) were selected for the braces and friction devices with 100 kip slip force.

CLA11/17 is then assigned with the last obtained combination of values and, knowing that it is already adequate to guarantee compliance with the LS performance level, it is subjected to the series of 20 2% in 50 years earthquakes to determine its

suitability to fulfill also the requirements of CP. The results of these analyses are displayed in the next figure.

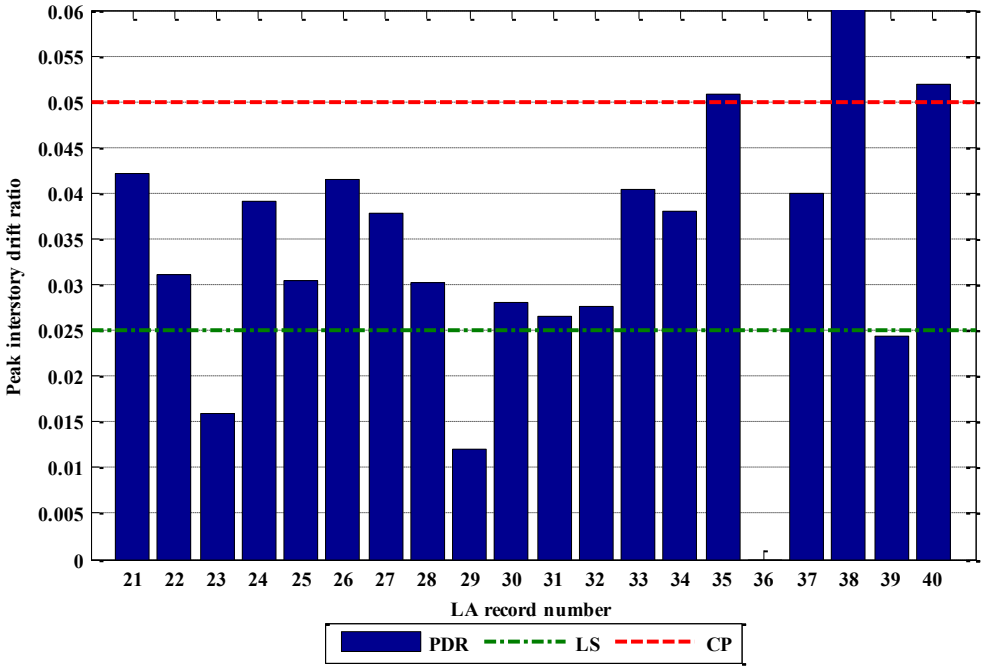


**Figure 5.43:** BSE-2 peak interstory drift ratios of the first proposed FDBF

The graph shows that the FDBF is not adequate to resist all the BSE-2 earthquakes in the series, which implies the need for further improvement. The process of trying combinations of stiffness and friction force is repeated, now considering only those BSE-2 earthquakes for which the preliminary FDBF design is not yet adequate. The results are as follows.

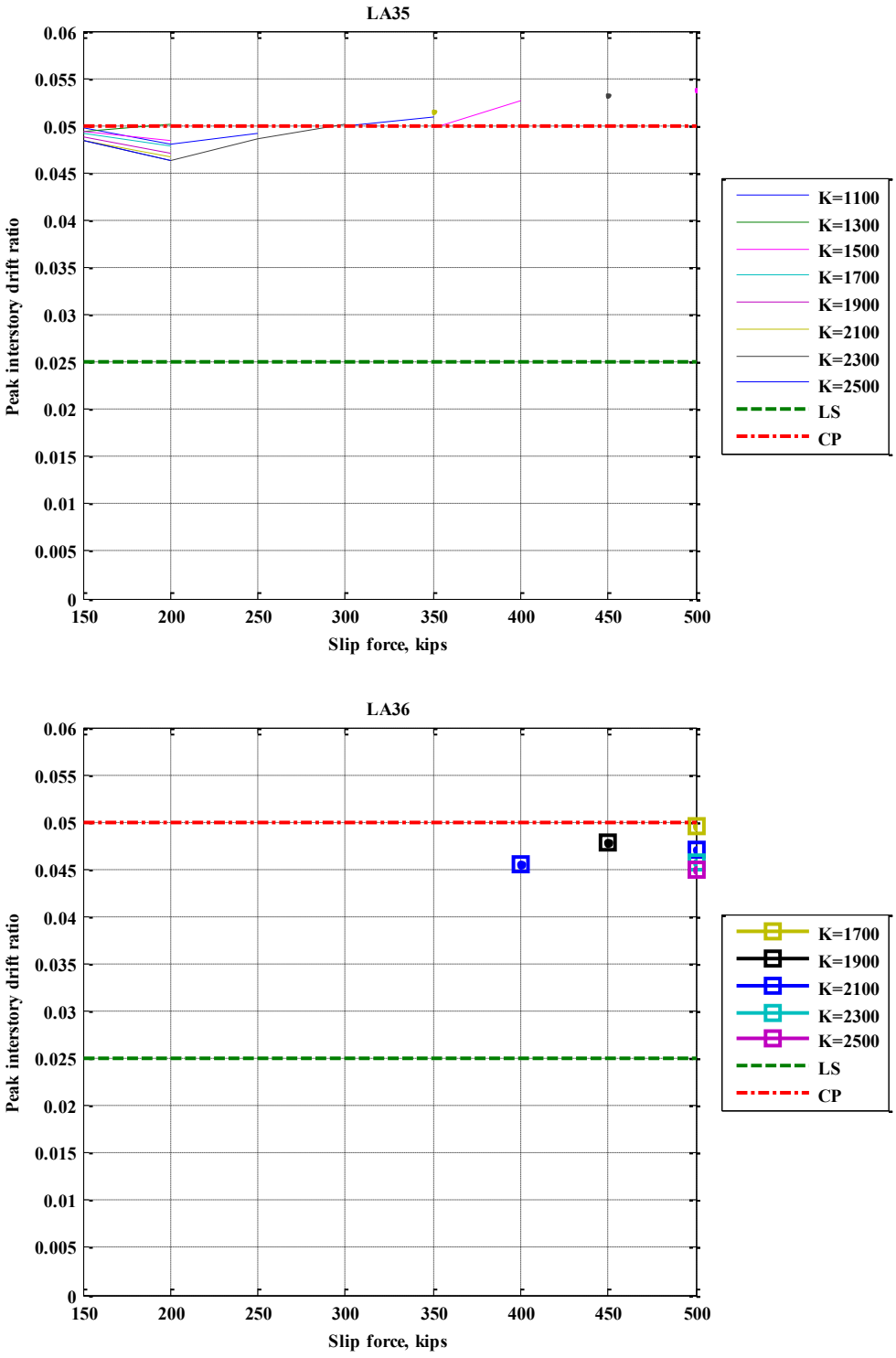


**Figure 5.44:** Effect of FDB parameters on the FDB 9-story building (part 9)

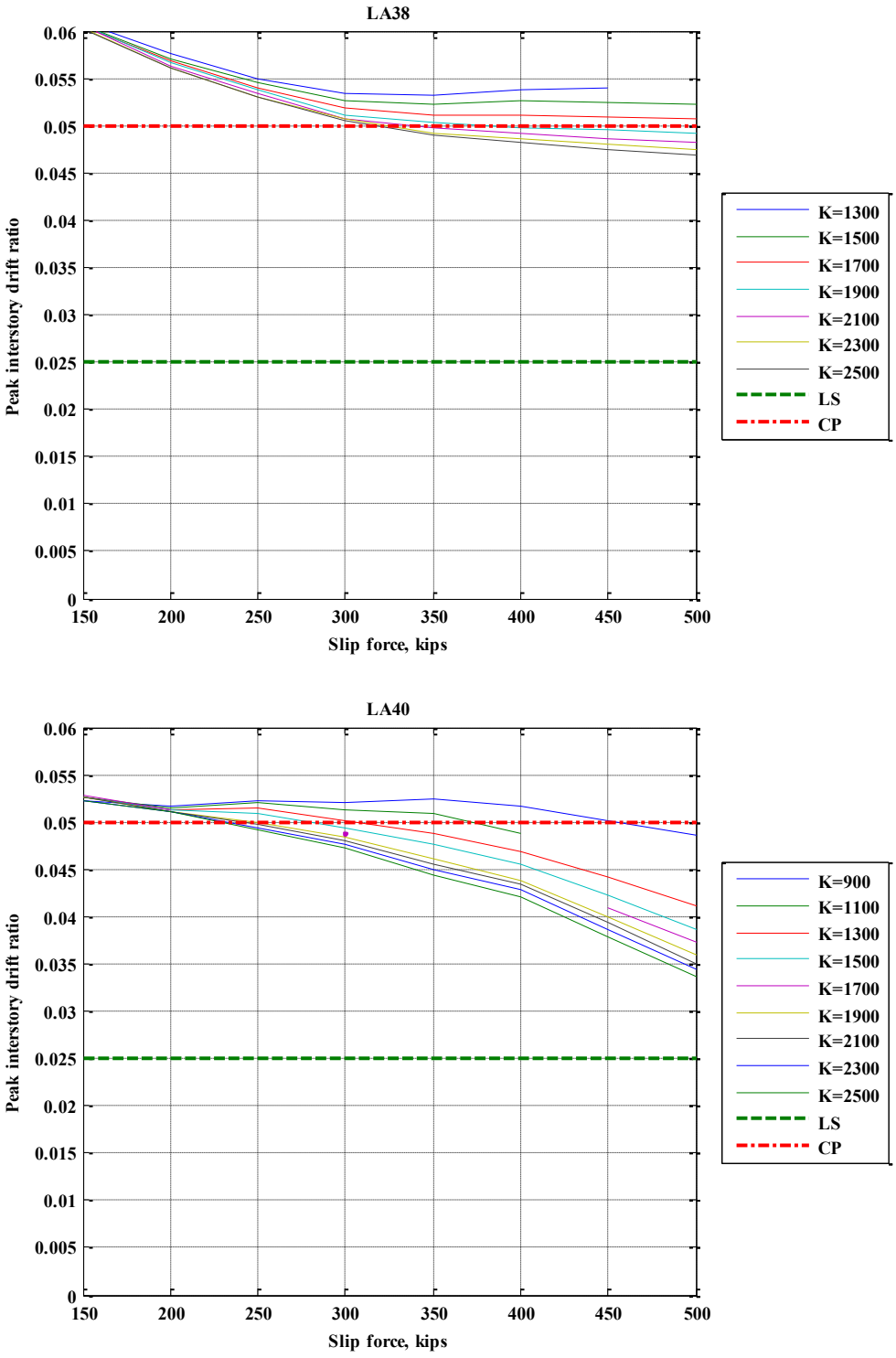


**Figure 5.45:** Effect of FDB parameters on the FDB 9-story building (part 10)

While smooth continuous curves are drawn for the LA38 and LA 40 records, the structure shows clear sensitivity and vulnerability to the LA35 and LA36 records (both derived from the same source ground accelerations); actually, for the case of the LA36 record, only discrete combinations of stiffness and friction force are successful in avoiding the collapse of the structure. As can be seen in Fig. 5.44b, the combination K = 2100 kips/in and Slip force = 400 kips yields converging results for LA35 and LA36; simultaneously, this combination of values represents points below the CP limit in the graphs corresponding to the LA38 and LA40 earthquakes and, thus, is chosen for the final design.

The use of HSS16×16×1/2 sections for the steel braces (K = 2092 kips/in) and a 400 kip slip force for the devices provides the required combination of parameters. Consequently, these refinements were made to the CLA11/17 brace configuration. This updated design is finally subjected to all the BSE-1 and BSE-2 earthquakes to evaluate its adequacy and to assess the reductions in interstory drifts. The results are shown in the next set of graphs.

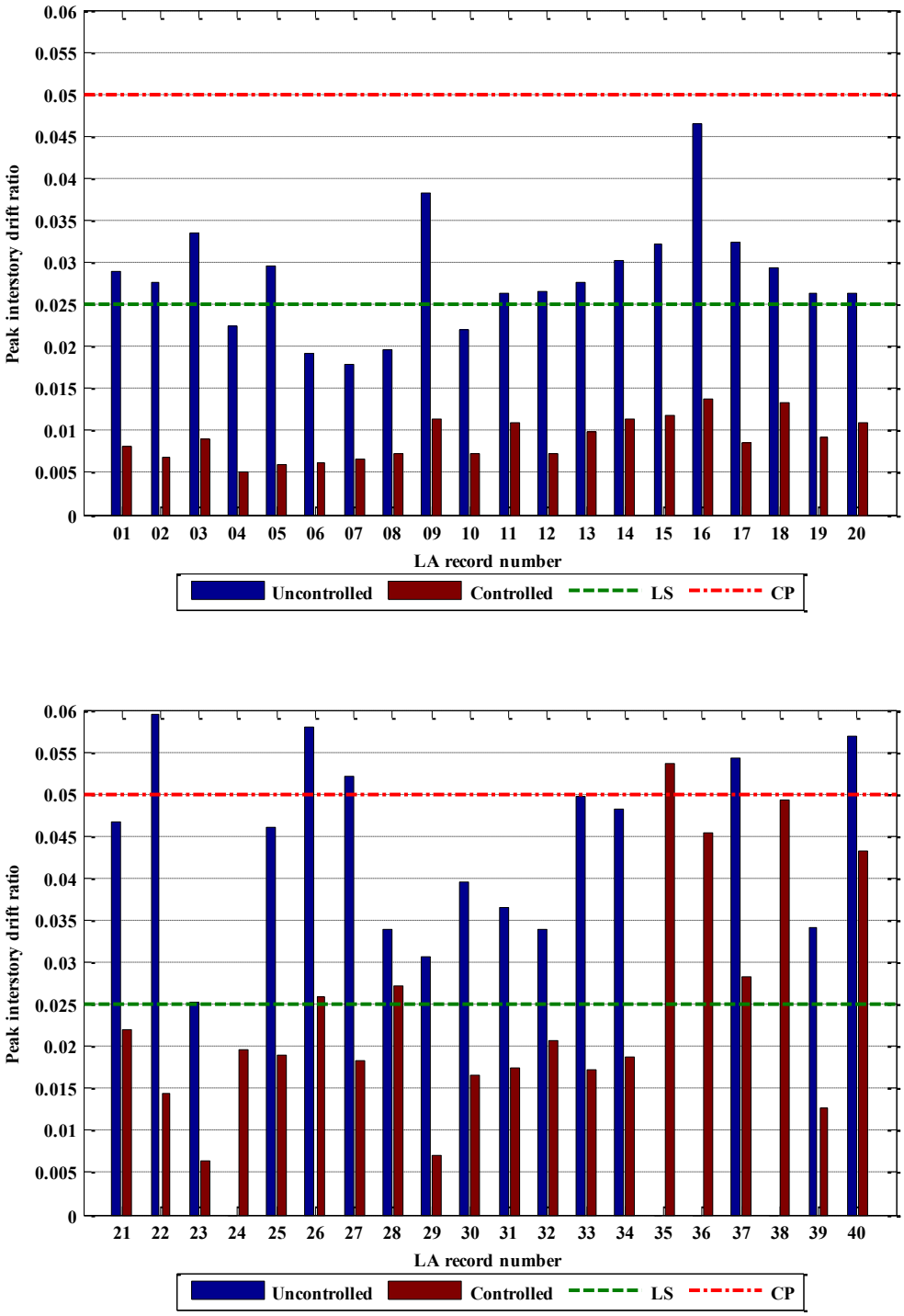


**Figure 5.46:** Comparative peak interstory drift ratios of 9-story FDBF and benchmark

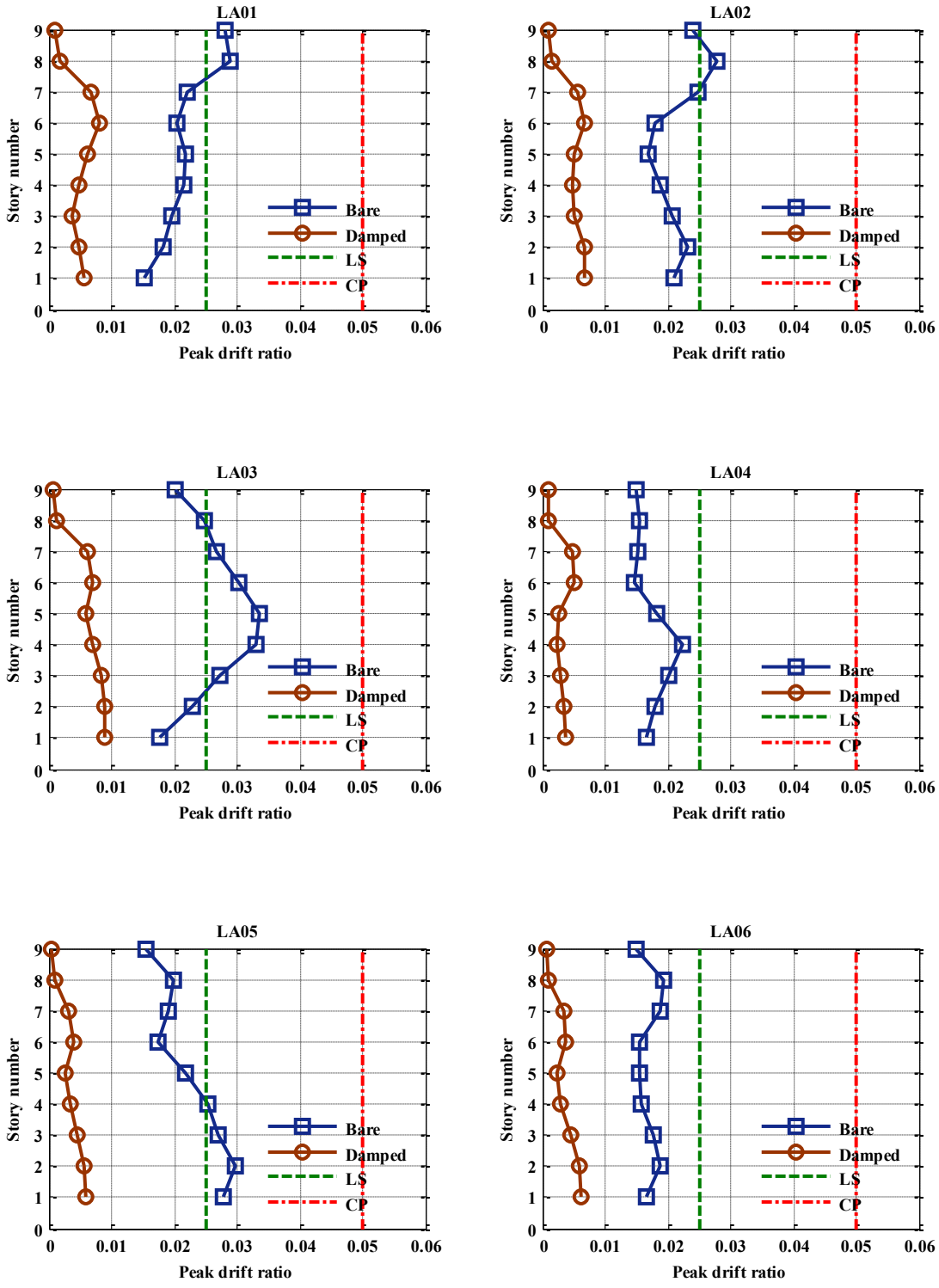


**Figure 5.47:** Comparative interstory drift ratios of 9-story FDBF and benchmark (part 1)

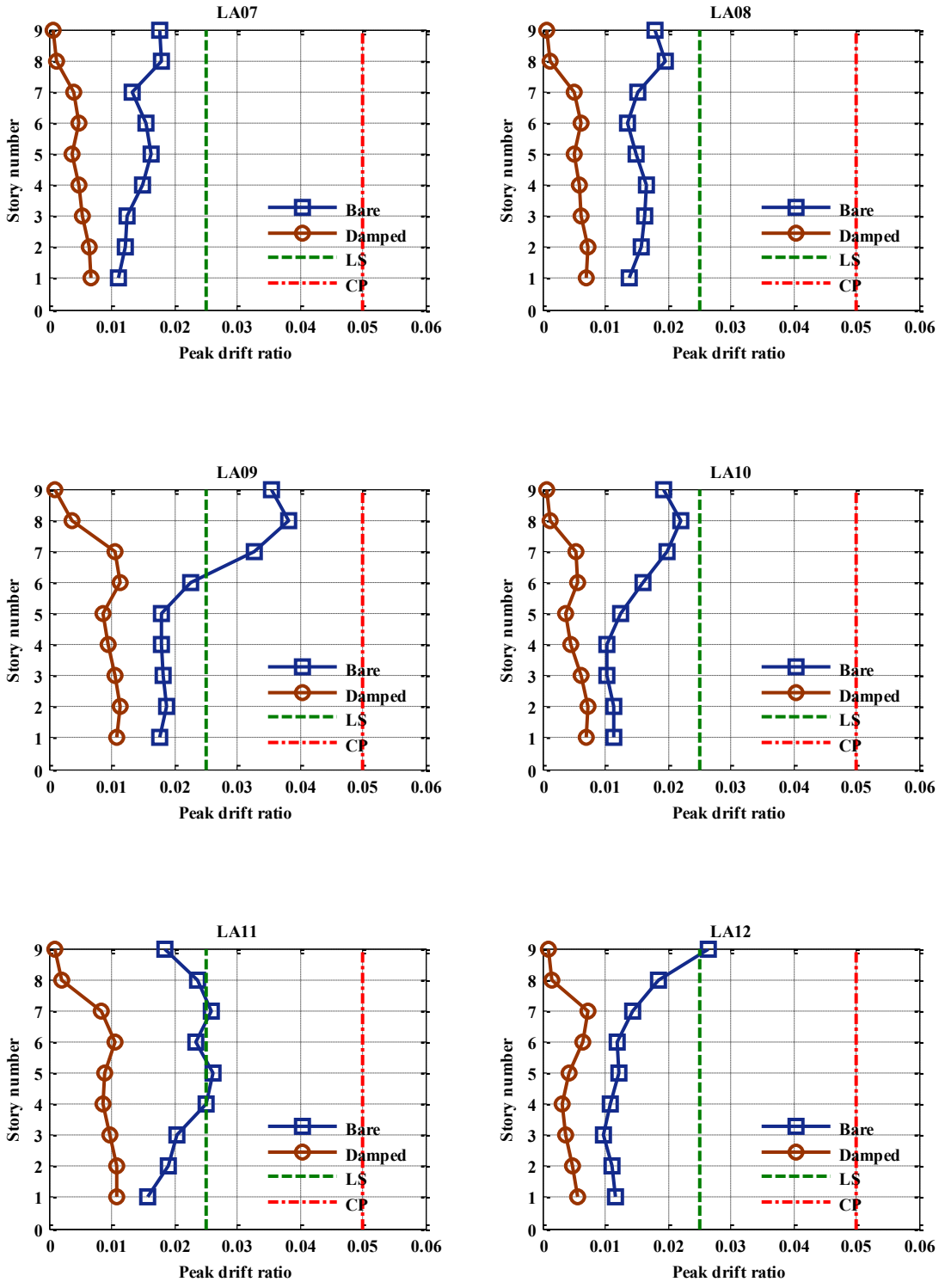


**Figure 5.48:** Comparative interstory drift ratios of 9-story FDBF and benchmark (part 2)

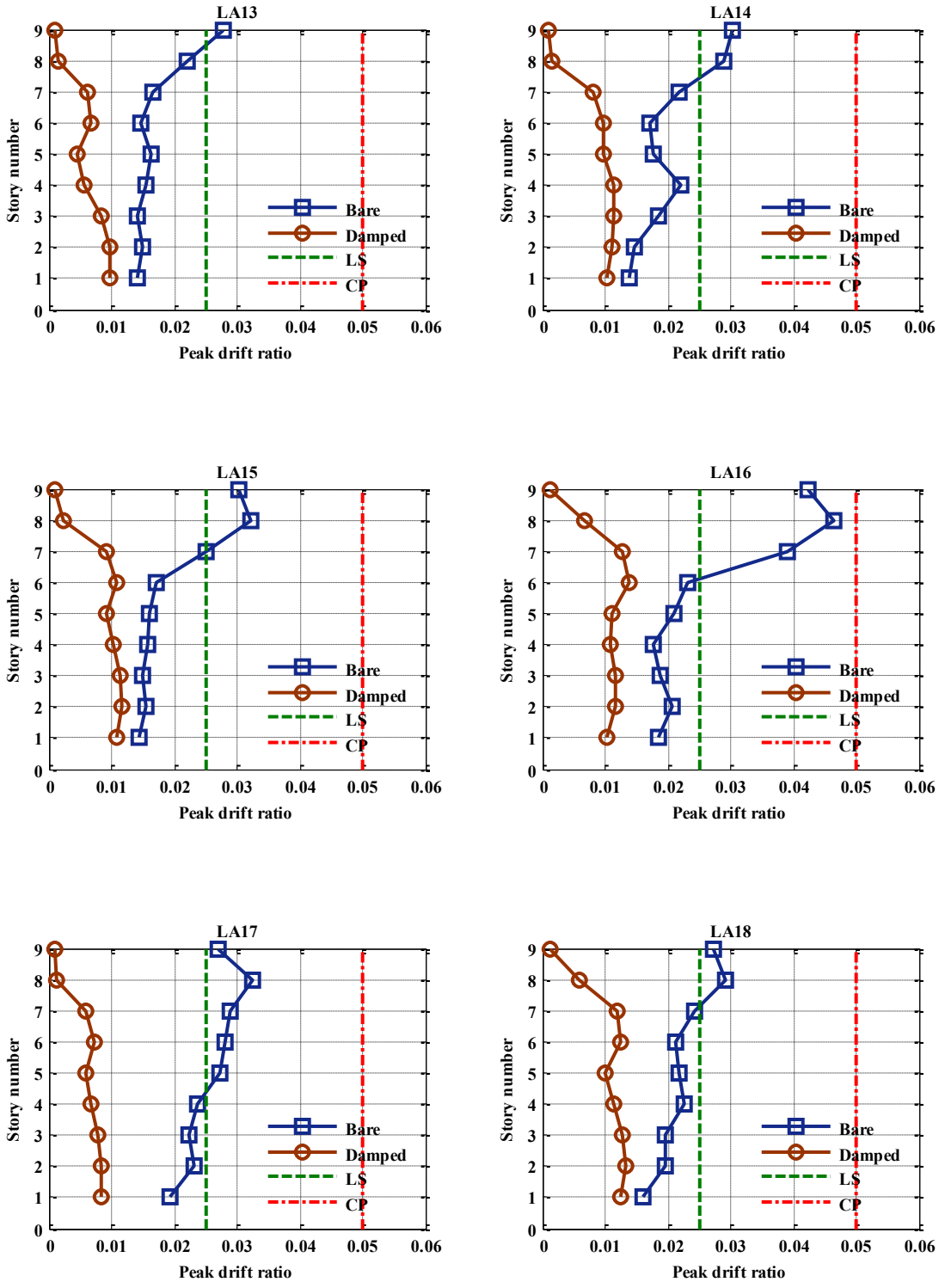


**Figure 5.49:** Comparative interstory drift ratios of 9-story FDBF and benchmark (part 3)

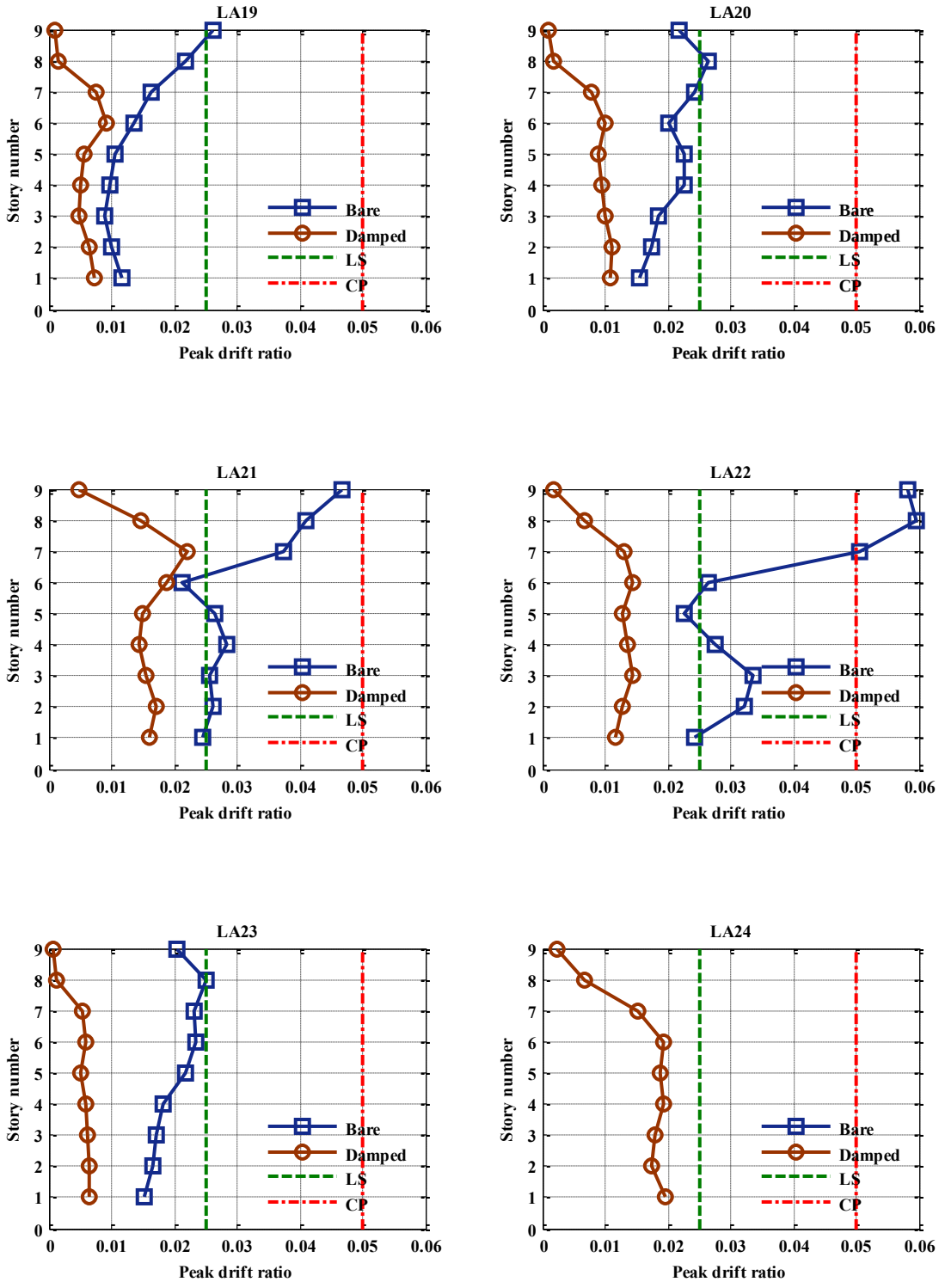


**Figure 5.50:** Comparative interstory drift ratios of 9-story FDBF and benchmark (part 4)

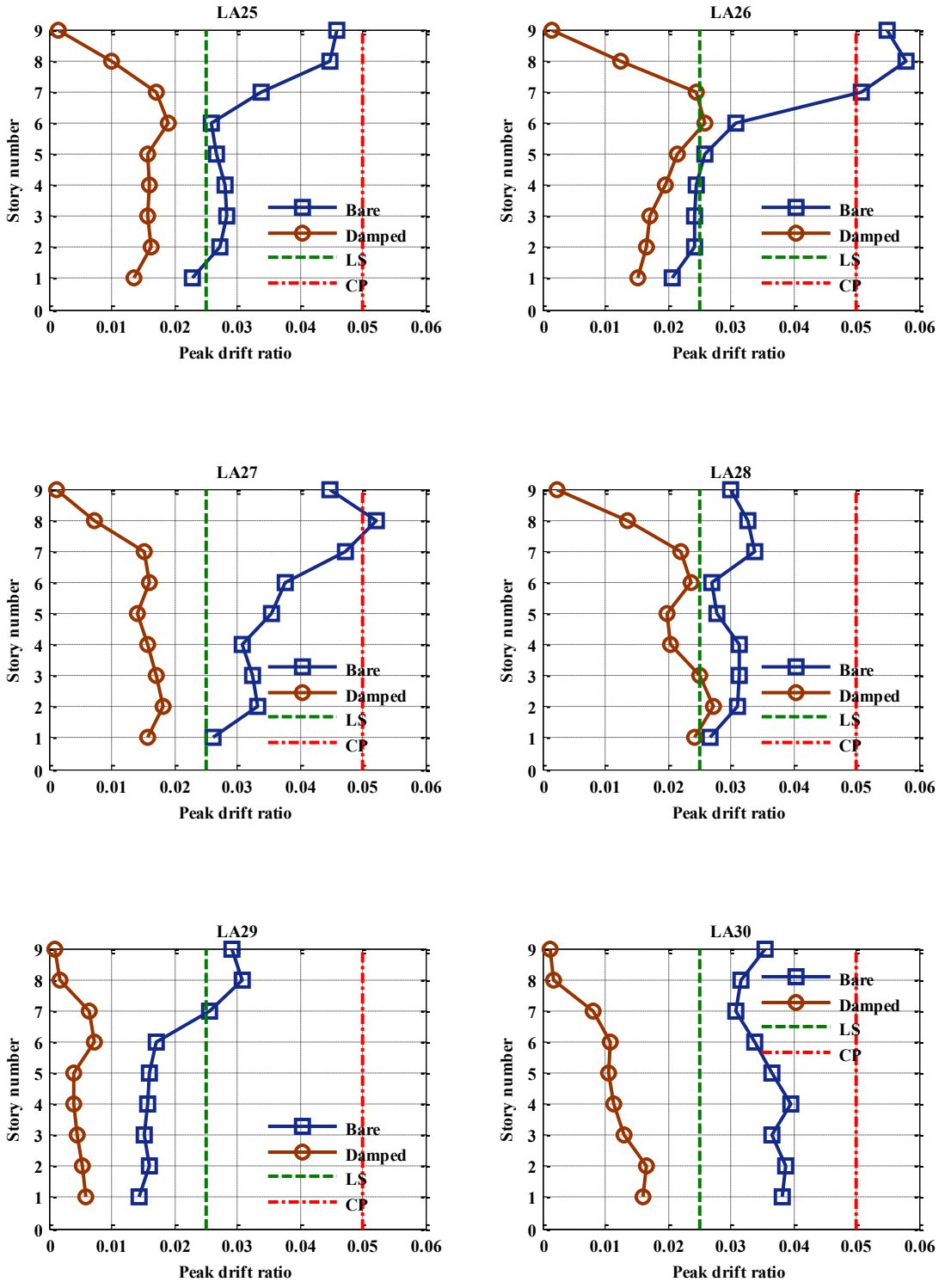


**Figure 5.51:** Comparative interstory drift ratios of 9-story FDBF and benchmark (part 5)

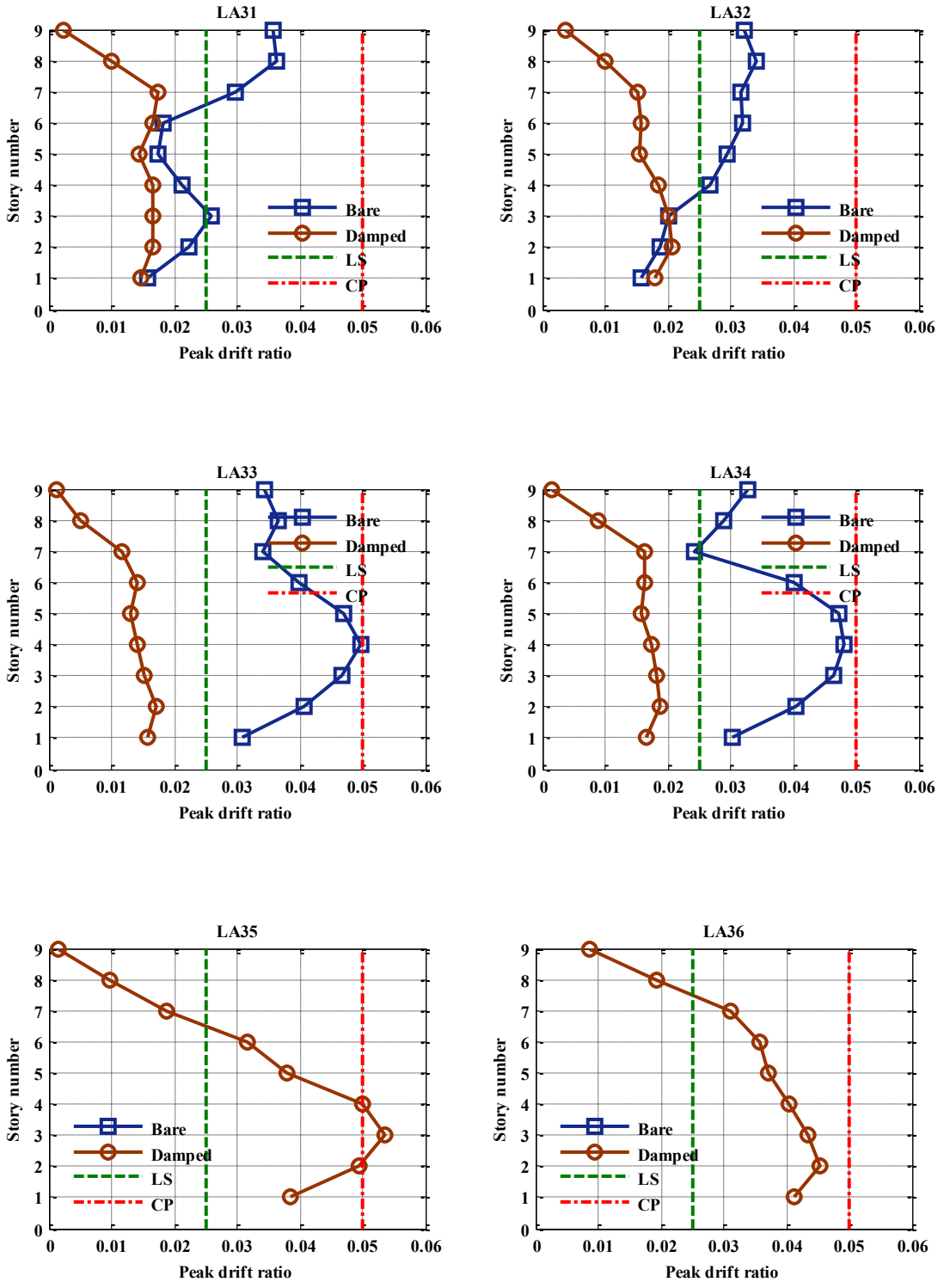


**Figure 5.52:** Comparative interstory drift ratios of 9-story FDBF and benchmark (part 6)

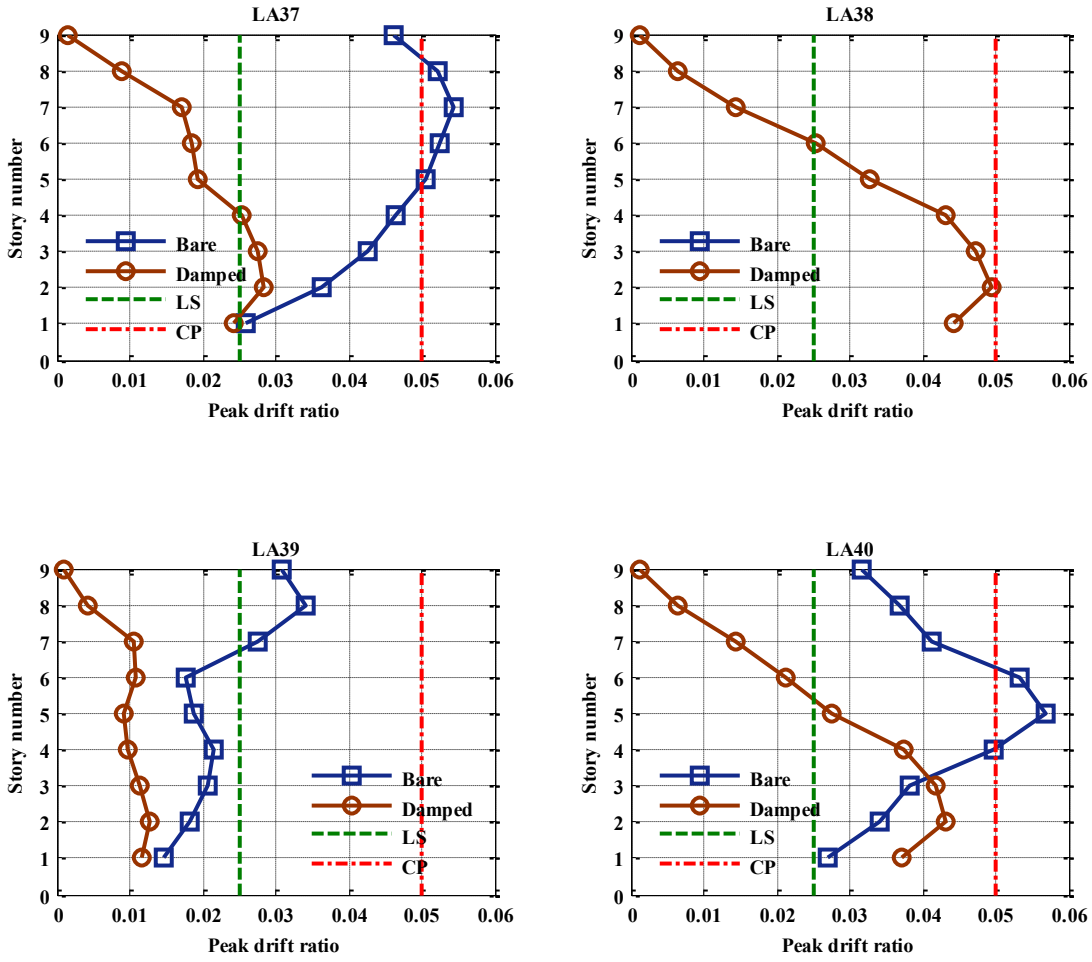


**Figure 5.53:** Comparative interstory drift ratios of 9-story FDBF and benchmark (part 7)

## 5.3 20-Story Building

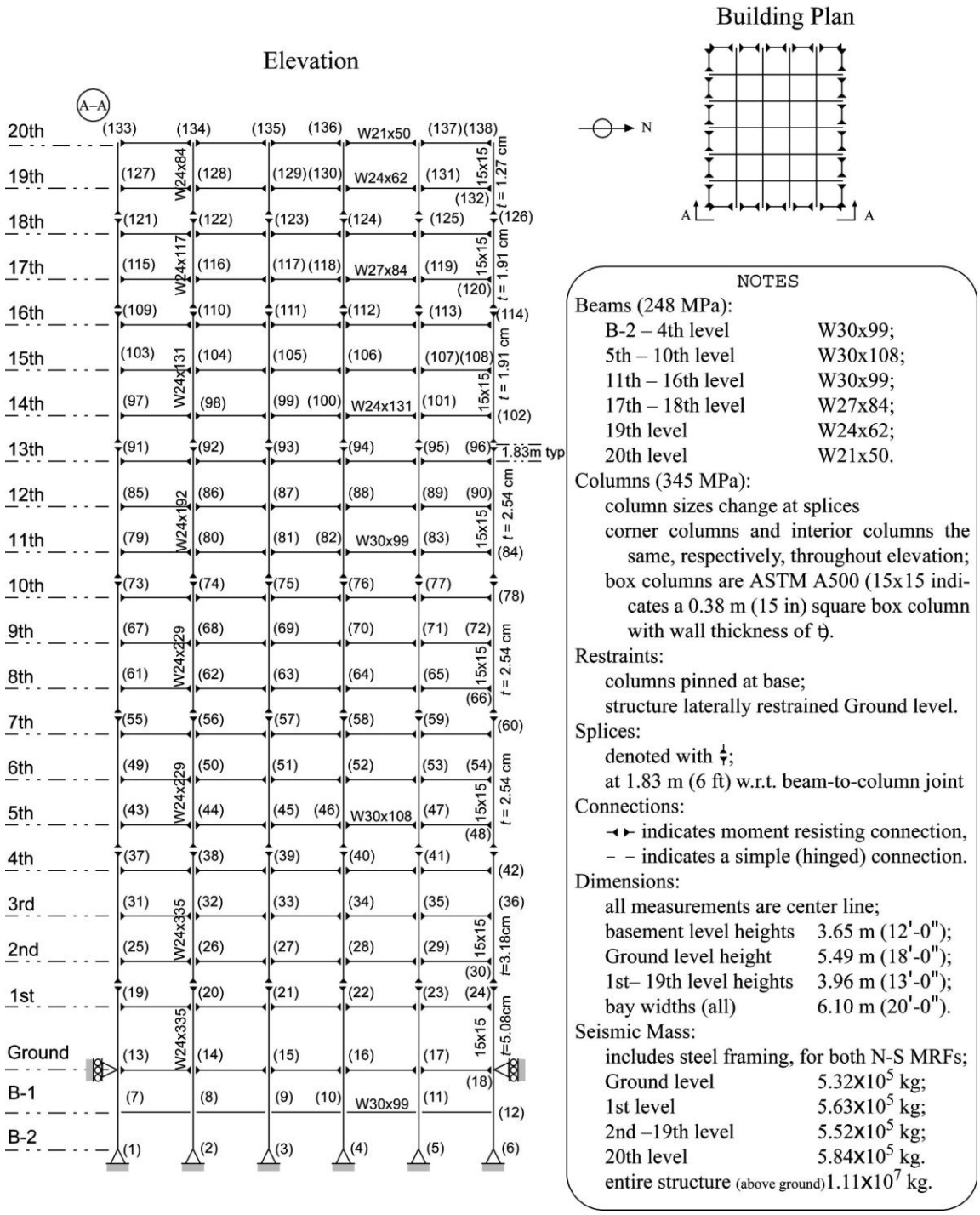


**Figure 5.54:** Twenty-story benchmark building north-south moment resisting frame (Ohtori et al. 2004)

The evaluation of the capacity of the 20-story benchmark building is performed. That is, the frame is subjected to the 20 10% in 50 years and the 20 2% in 50 years earthquake records and the values obtained for the peak interstory drift ratios (Figs. 5.55 and 5.56) are saved for their eventual comparison, but used first, as starting point, for retrofitting of the 20-story benchmark frame.

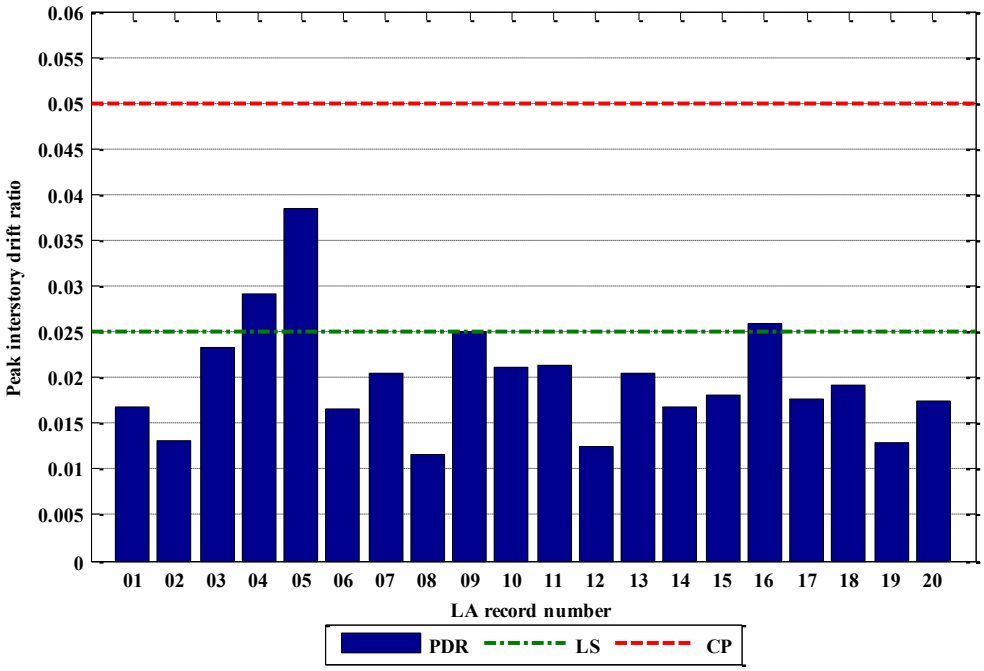


**Figure 5.55:** BSE-1 interstory drift demands of 20-story benchmark building

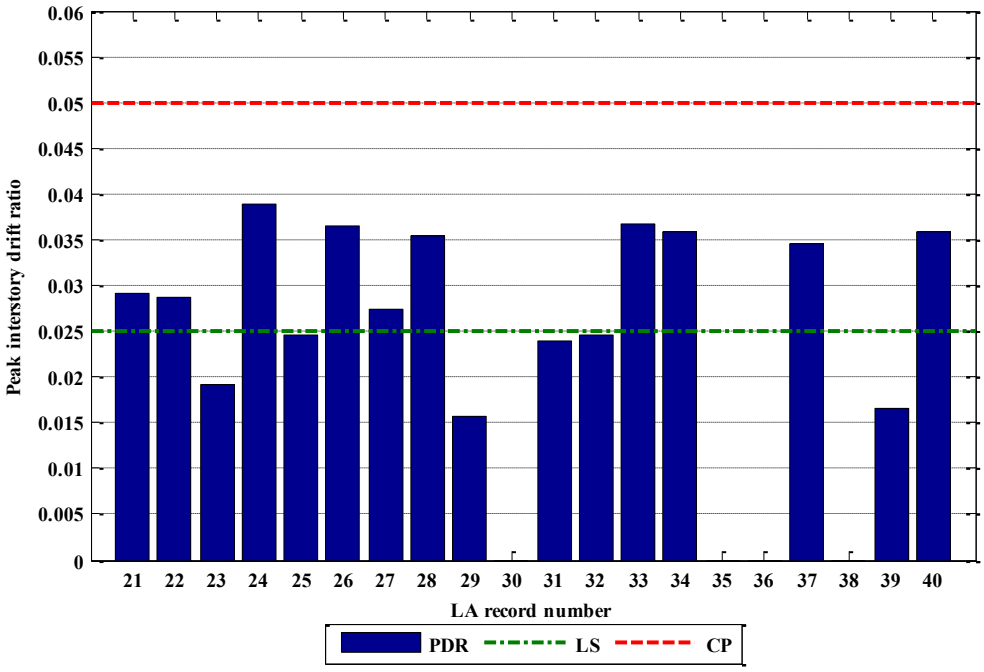


**Figure 5.56:** BSE-2 interstory drift demands of 20-story benchmark building

The 20-story benchmark building is capable of keeping the peak interstory drift ratio below the LS limit for 17 out of the 20 BSE-1 records. Thus, placement of FDBs is necessary only for the case of 3 earthquakes. Like in the case of the other benchmark frames, these 3 acceleration time histories serve as a basis for the determination of the suboptimal bracing configurations. The same optimization algorithm that has been described and used before is employed with FDBs having provisionally 1600 kips/in stiffness and 300 kips friction force. The results it yields concerning the response of the building as a function of the number of FDBs are shown in the next 3 figures.

For strengthening of the building, consideration of symmetry and neglect of the interstory drift ratio of the B-1 level suggests the use of a maximum of 80 FDBs in the

earthquake resisting frame. For the determination of the optimal number and location of the FDBs, instead of testing the dampers in pairs at a time during the optimization process, this time they are tested in groups of 4 in the same story. This number is chosen not only considering symmetry, but also to reduce the number of analyses required to determine the suboptimal configurations. This becomes an issue in the case of the 20-story frame since the algorithm could require more than 6 times the number of analyses required for the case of the 9-story building to find a sub-optimal configuration. This enormous increase in the number of analyses together with the obvious increase in computational time needed to analyze a larger structure would require an unpractical amount of time to complete the optimization procedure.

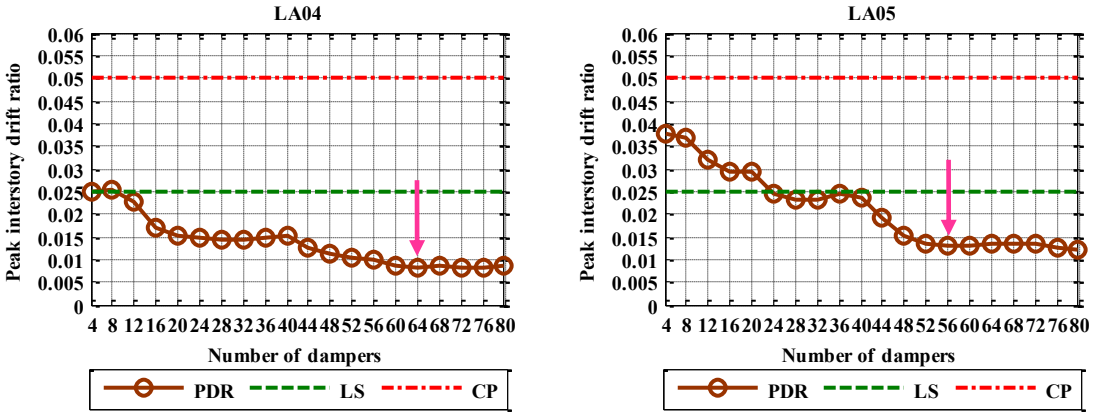


**Figure 5.57:** Performance of interstory drift ratio criterion in the 20-story building (part 1)

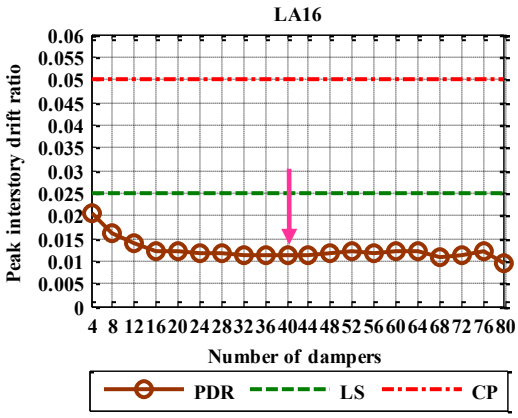


**Figure 5.58:** Performance of interstory drift ratio criterion in the 20-story building (part 2)

Taking a look at the plots, it is possible to determine a point after which, an increase in the number of friction-damped braces does not correspond to a significant reduction in the response anymore; therefore, the addition of more dampers beyond this point not justified. This situation is clearly displayed on the last three graphs and, in an almost perfect example, on the graph concerning the LA16 record. Hence, for this building, the criterion for selecting the number of dampers to be placed in the frame was not only the number of dampers that would yield the minimum response, but also consideration was given to the minimum number of dampers that would bring the maximum response of the building to that point after which the response is no longer significantly reduced.

Although a similar situation occurs in the case of the 9-story building, the consideration of this additional criterion takes more importance in the case of the present building since, here, a considerably greater number of dampers is involved and a smaller reduction in the response with their installation. Stepwise, this issue becomes also

economically more important here than in the previous frame because the number of dampers added at each step is twice. Furthermore, the need for achieving the maximum reduction in the peak response was more important in the case of the 9-story building.

In consideration of the aforementioned, the following configurations were selected (note that they are not necessarily the ones that yielded the minimum peak interstory drift value): CLA04 for the LA04 record (64 FDBs), CLA05 for the LA05 (56 FDBs) and CLA16 for the LA16 (40 FDBs).

Repeating the procedure used for the 9-story building, to make a decision on which of the 3 arrays to use, all 3 were subjected to the series of 20 BSE-1 earthquake records. The 20 maximum interstory drift ratios that were obtained were averaged and, finally, the array that yielded the lowest average peak interstory drift ratio was selected. As table 5.2 demonstrates, in this case it was configuration CLA05.

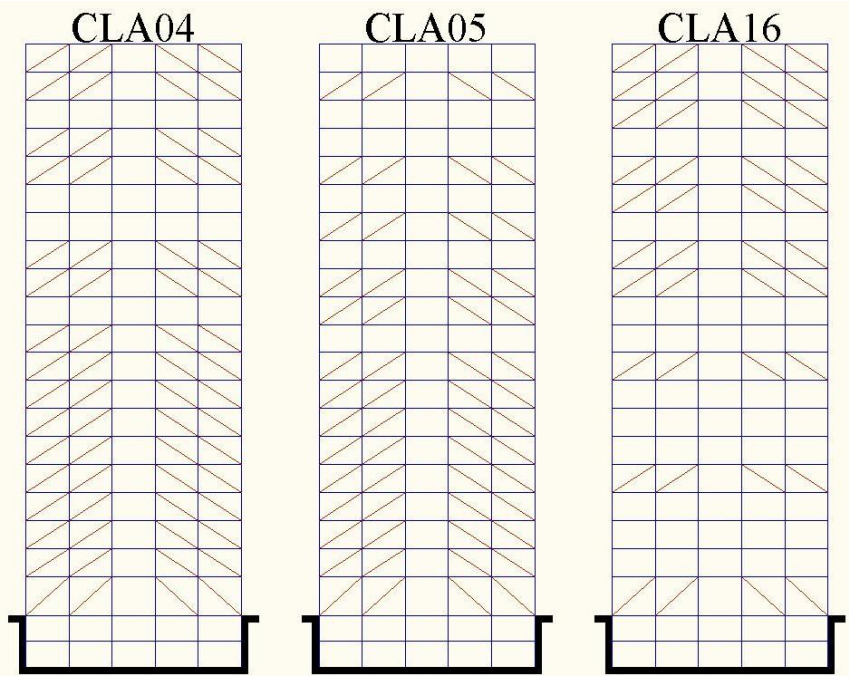


**Figure 5.59:** Sub-optimal FDBF configurations for the 20-story building

**Table 5.2:** Peak interstory drift ratio of the different damper configurations subjected to the series of BSE-1 records.

| | DAMPER CONFIGURATION | | |
|---|---|---|---|
| **RECORD** | **CLA04** | **CLA05** | **CLA16** |
| **LA01** | 0.0111 | 0.0098 | 0.0194 |
| **LA02** | 0.0119 | 0.0119 | 0.0130 |
| **LA03** | 0.0164 | 0.0144 | 0.0278 |
| **LA04** | 0.0083 | 0.0122 | 0.0240 |
| **LA05** | 0.0154 | 0.0130 | 0.0350 |
| **LA06** | 0.0088 | 0.0085 | 0.0170 |
| **LA07** | 0.0116 | 0.0111 | 0.0162 |
| **LA08** | 0.0126 | 0.0123 | 0.0137 |
| **LA09** | 0.0130 | 0.0133 | 0.0177 |
| **LA10** | 0.0106 | 0.0096 | 0.0135 |
| **LA11** | 0.0125 | 0.0113 | 0.0142 |
| **LA12** | 0.0101 | 0.0096 | 0.0083 |
| **LA13** | 0.0132 | 0.0109 | 0.0126 |
| **LA14** | 0.0144 | 0.0114 | 0.0133 |
| **LA15** | 0.0116 | 0.0095 | 0.0132 |
| **LA16** | 0.0153 | 0.0135 | 0.0113 |
| **LA17** | 0.0128 | 0.0123 | 0.0177 |
| **LA18** | 0.0123 | 0.0117 | 0.0144 |
| **LA19** | 0.0123 | 0.0117 | 0.0091 |
| **LA20** | 0.0114 | 0.0116 | 0.0162 |
| **Average** | 0.0123 | **0.0115** | 0.0164 |

For the selection of the stiffness and slip force of the FDBs, the chosen FDBF was analyzed under the LA04, LA05, and LA16 records trying 100 different combinations of stiffness and slip force analyses, in each case, to determine the effects of the variations these parameters on the response of the buildings. The next 3 graphs display the results of these analyses.

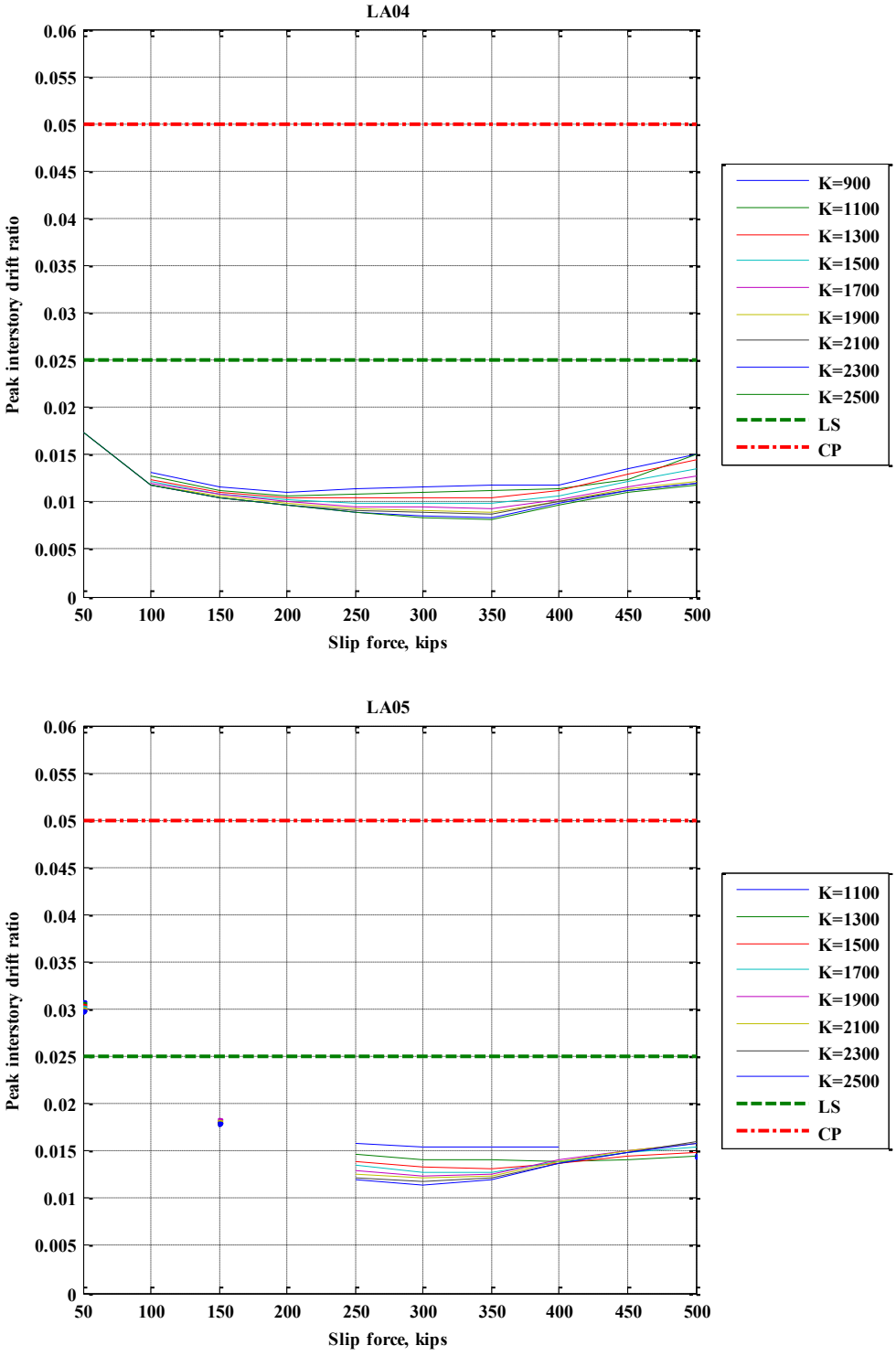


**Figure 5.60:** Effect of FDB parameters on the FDB 20-story building (part 1)

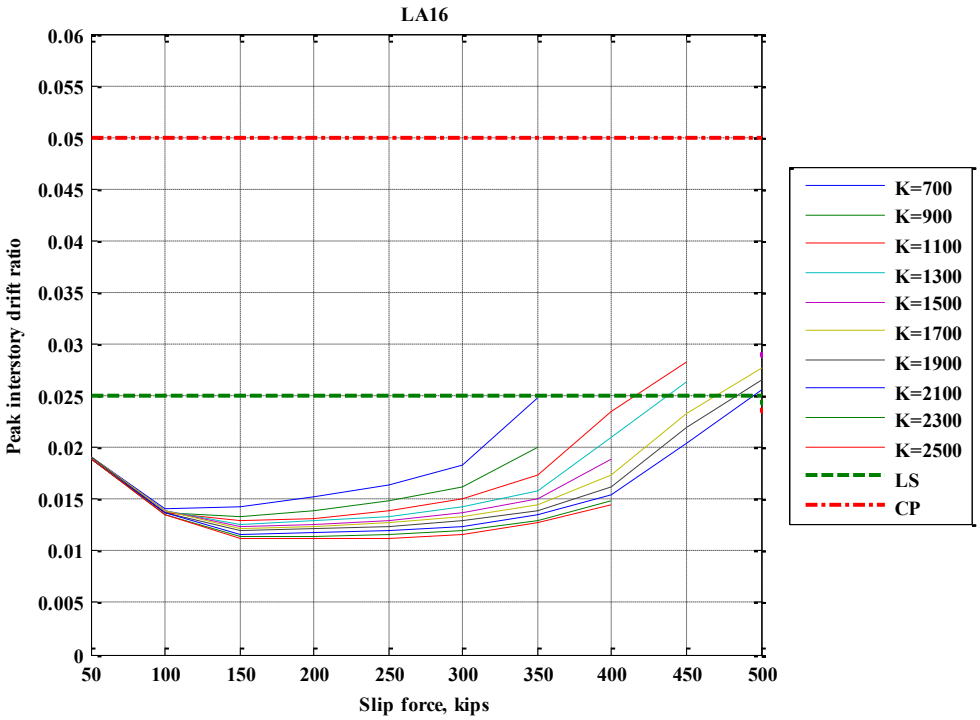


**Figure 5.61**: Effect of FDB parameters on the FDB 20-story building (part 2)

All 3 graphs show that the stiffness of the brace will not govern the design of the FDBs as long as the slip force is kept below 350 kips. Considering that 350 kips is actually a "typical" value for the slip load (it has already been used in a number of practical applications) along with the experience obtained from the analyses of the previous buildings which always showed the necessity for greater values of stiffness and friction forces to cope with the BSE-2 earthquakes, a slip load of 350 kips, which is not the minimum required, was chosen to anticipate the larger friction force that could be necessary anyway.

HSS16×12×5/16 steel shapes were used for the brace sections, which will provide a stiffness equal to 1591 kips/in and will be able to resist the maximum

compression force of 350 kips in the brace. This stiffness and the force of 350 kips properties were assigned to the analytical model of the building and, subsequently, the model was subjected to the series of BSE-2 earthquakes to evaluate its capability to stay below the CP limit.

The above defined preliminary design becomes the final one after it satisfactorily brings the peak interstory drift ratio under the action of all the 2% in 50 years earthquake records below 5%. Finally, the frame is also subjected to the series of 10% in 50 years records (LA01 to LA20) and the "before and after" results are shown and compared in the plots that follow.

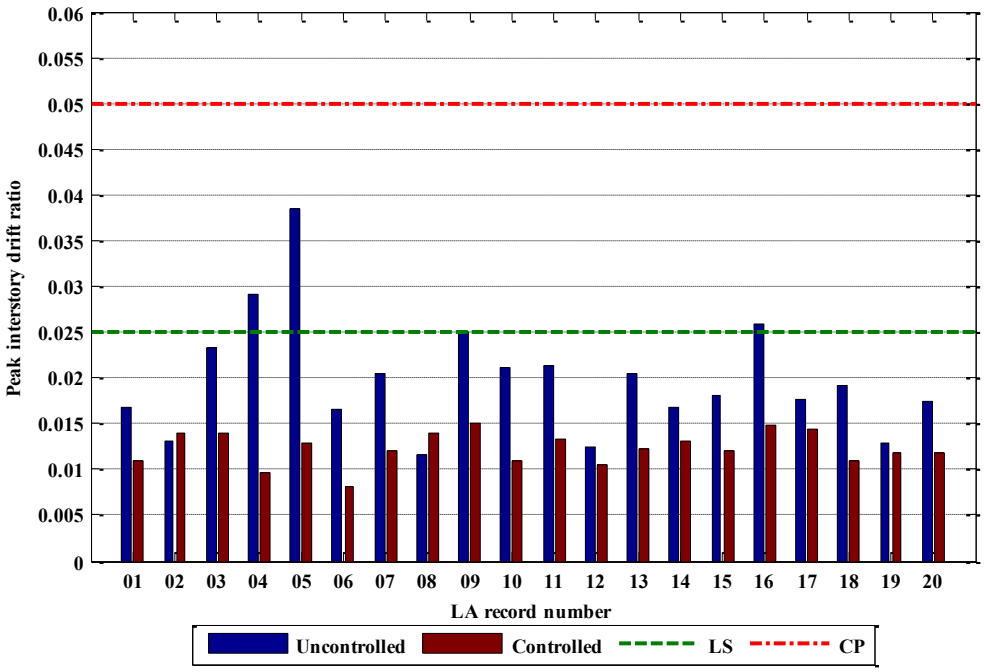


**Figure 5.62:** Comparative peak interstory drift ratios of 20-story FDBF and benchmark (part 1)

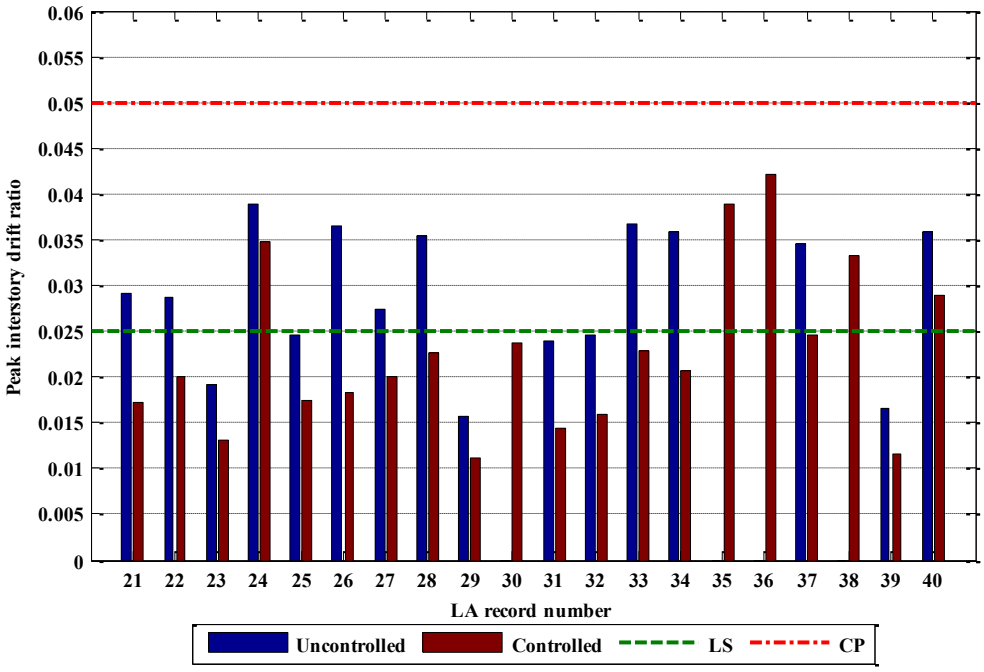


**Figure 5.63:** Comparative peak interstory drift ratios of 20-story FDBF and benchmark (part 2)

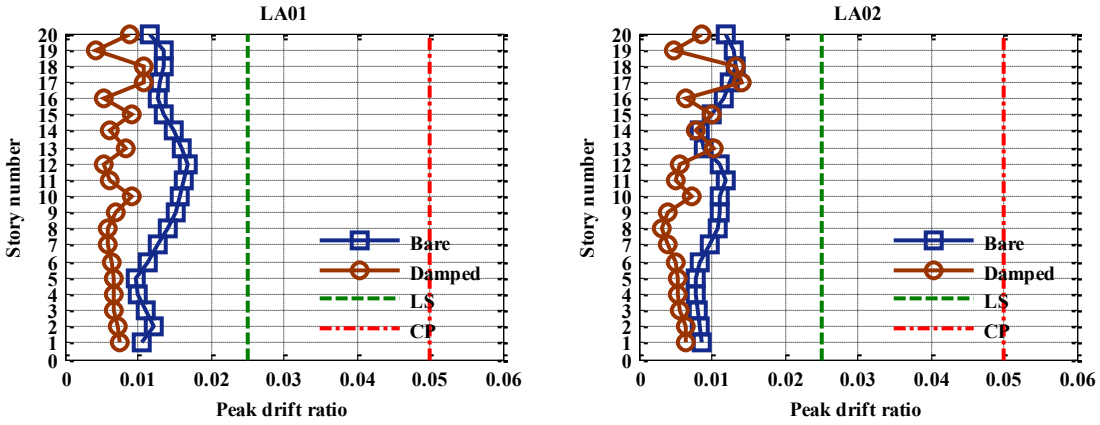


**Figure 5.64:** Comparative interstory drift ratios of 20-story FDBF and benchmark (part 1)

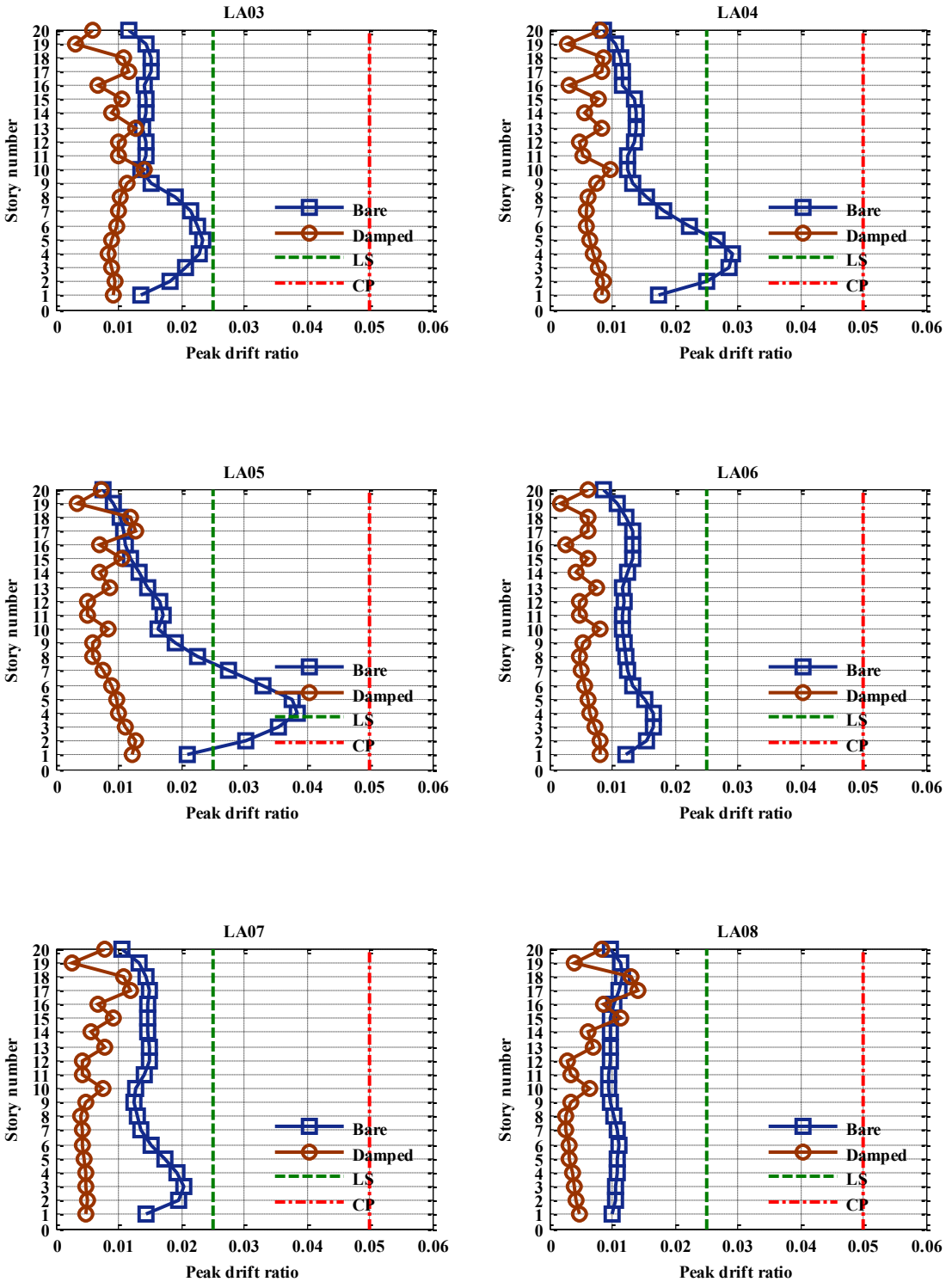


**Figure 5.65:** Comparative interstory drift ratios of 20-story FDBF and benchmark (part 2)

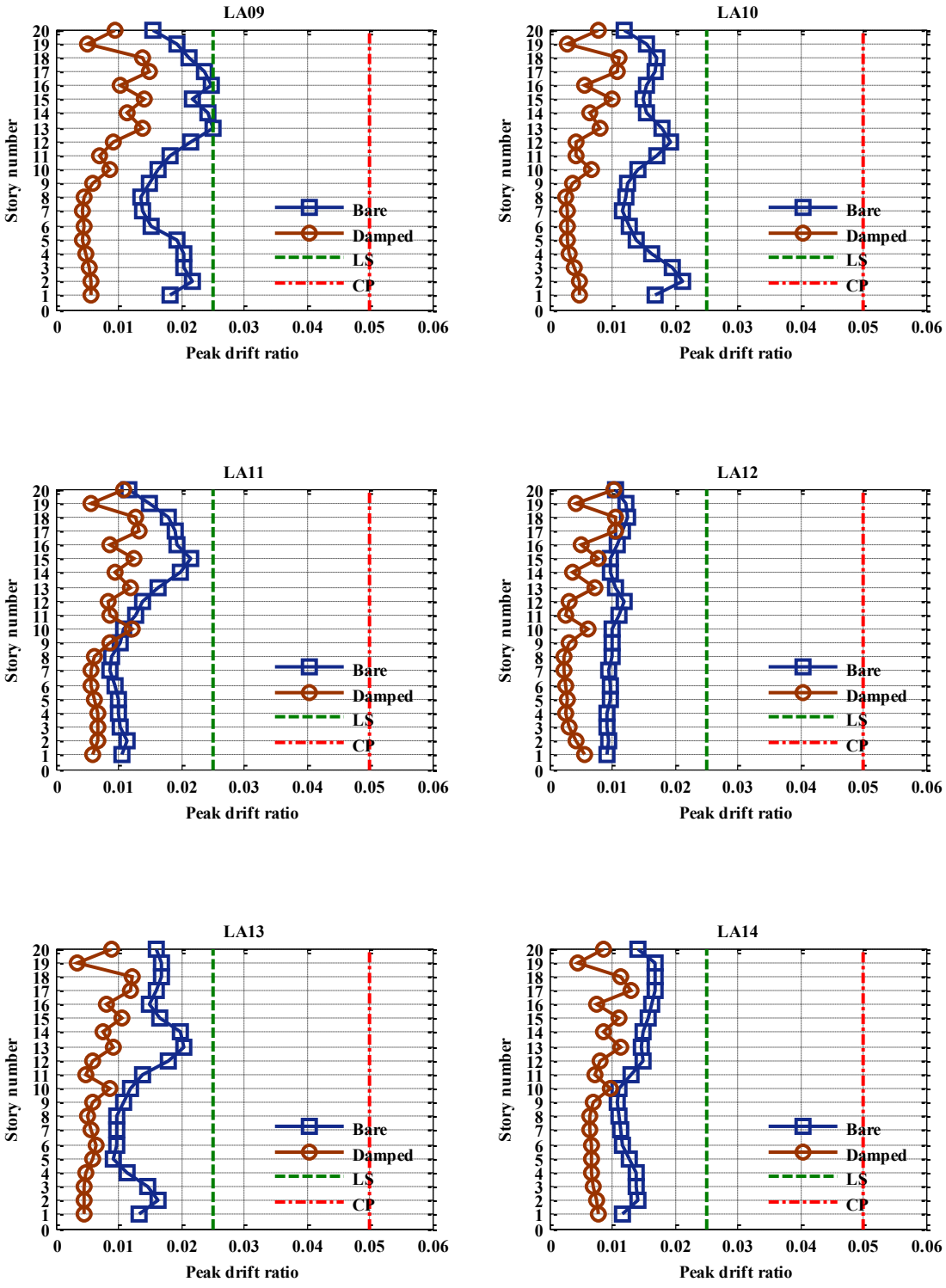


**Figure 5.66:** Comparative interstory drift ratios of 20-story FDBF and benchmark (part 3)

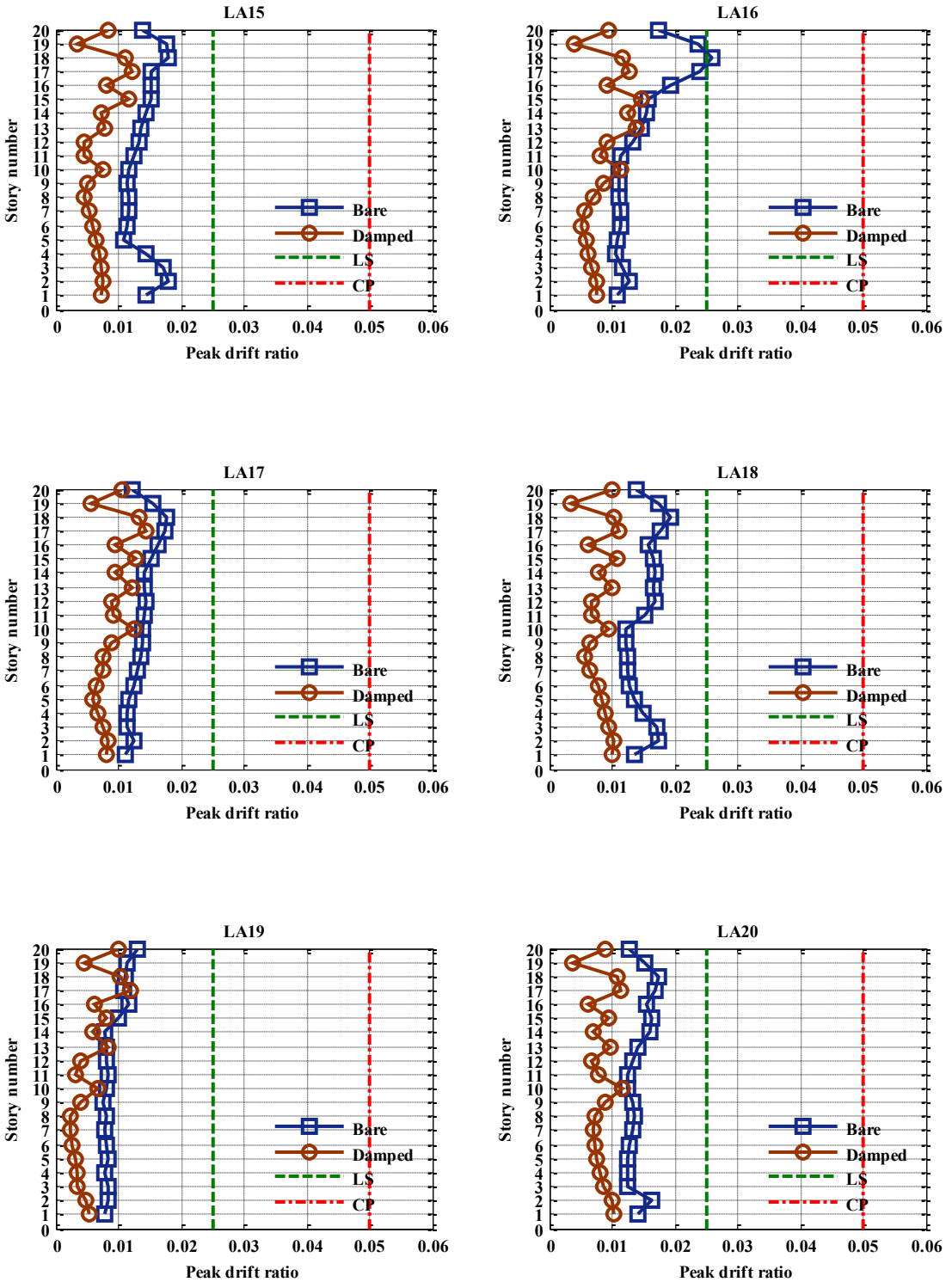


**Figure 5.67:** Comparative interstory drift ratios of 20-story FDBF and benchmark (part 4)

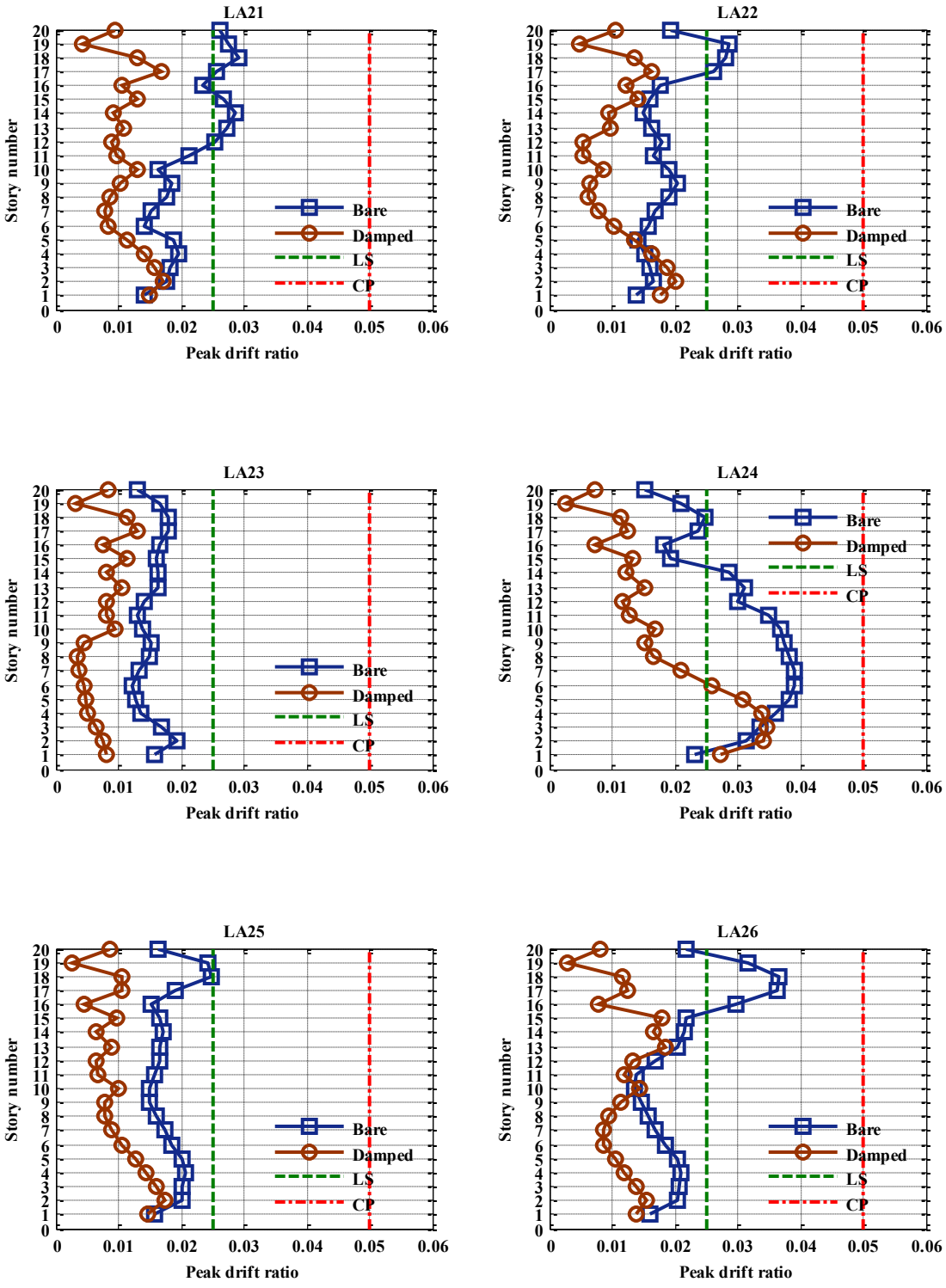


**Figure 5.68:** Comparative interstory drift ratios of 20-story FDBF and benchmark (part 5)

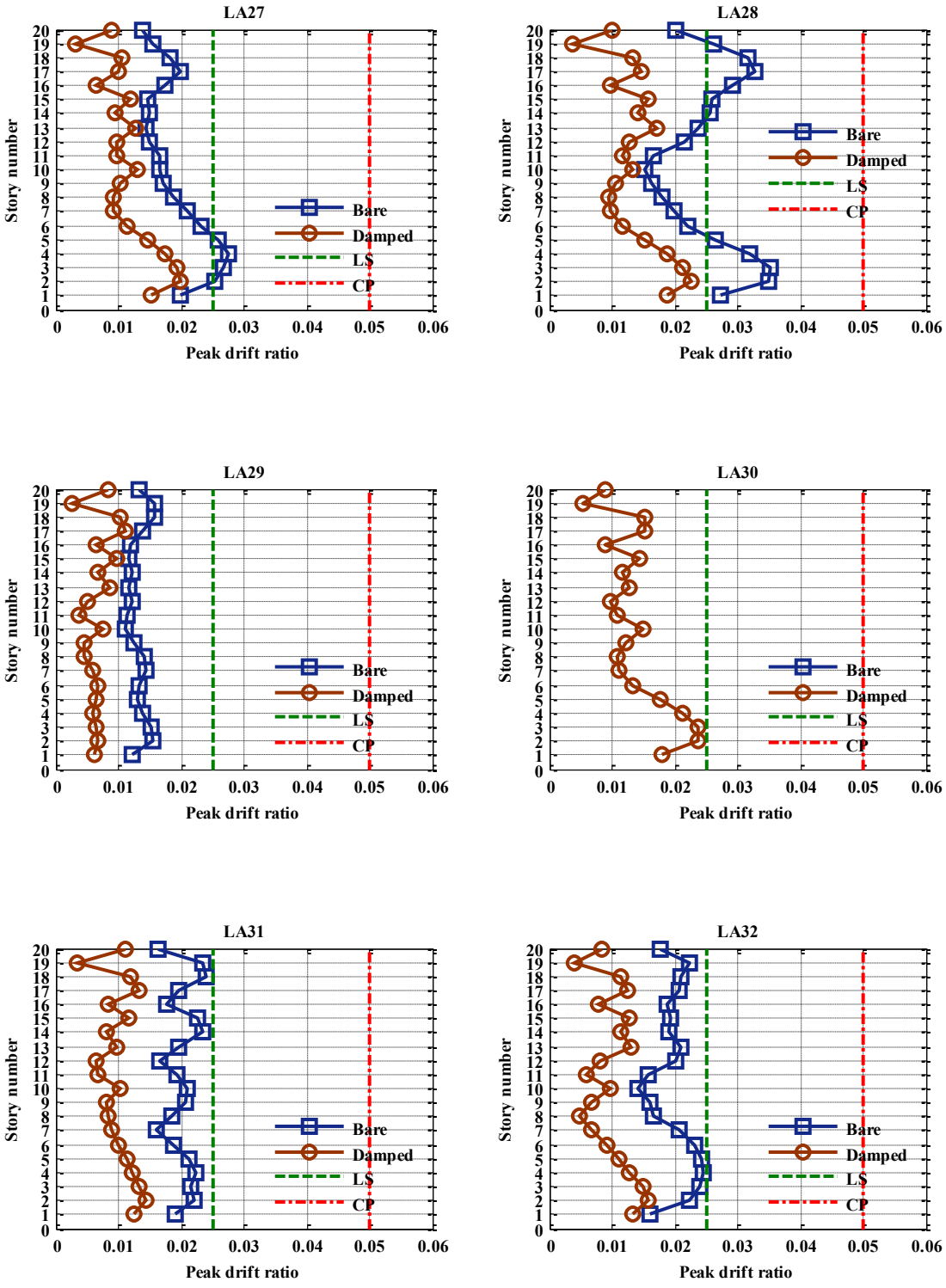


**Figure 5.69:** Comparative interstory drift ratios of 20-story FDBF and benchmark (part 6)

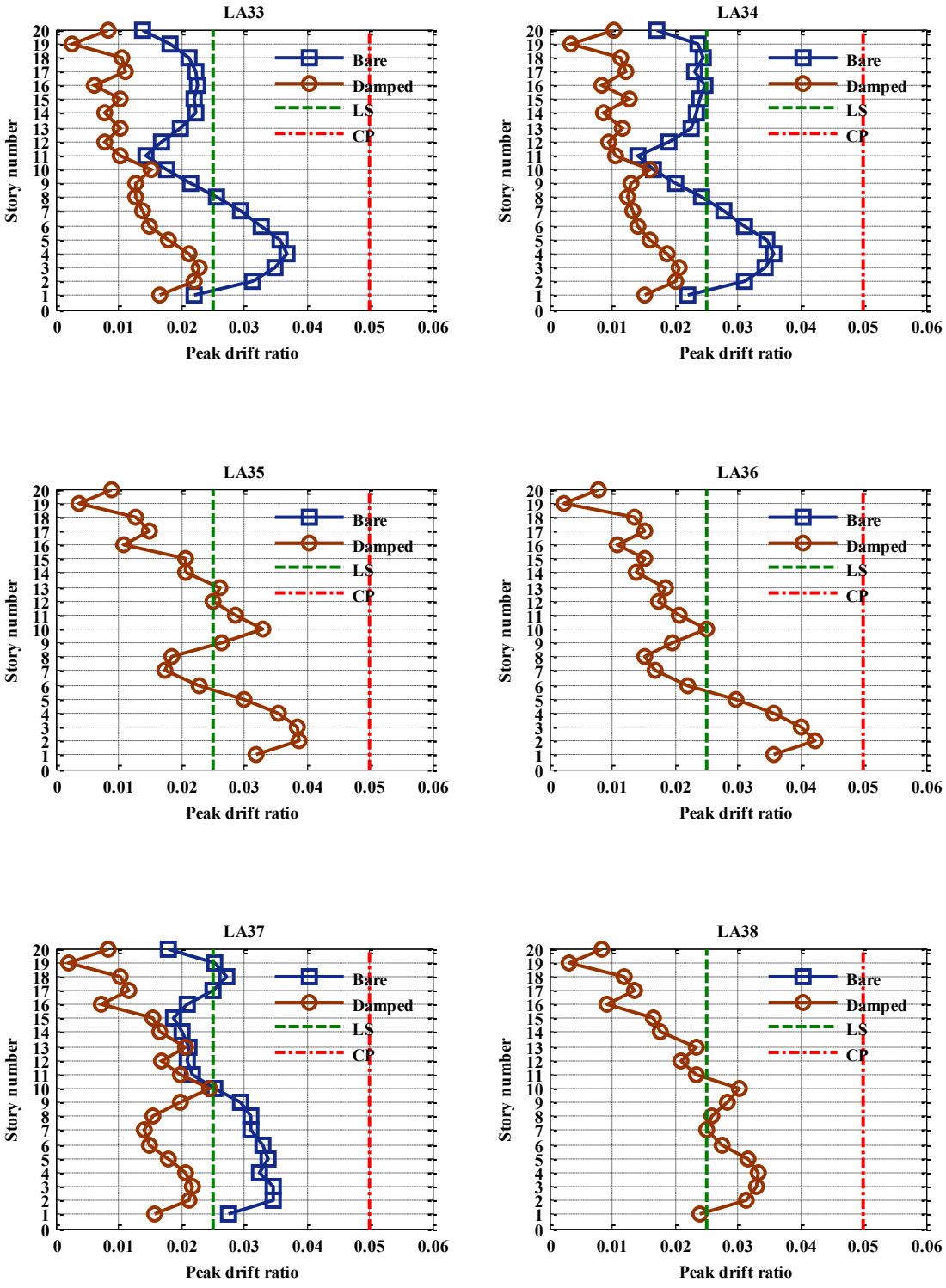


**Figure 5.70:** Comparative interstory drift ratios of 20-story FDBF and benchmark (part 7)

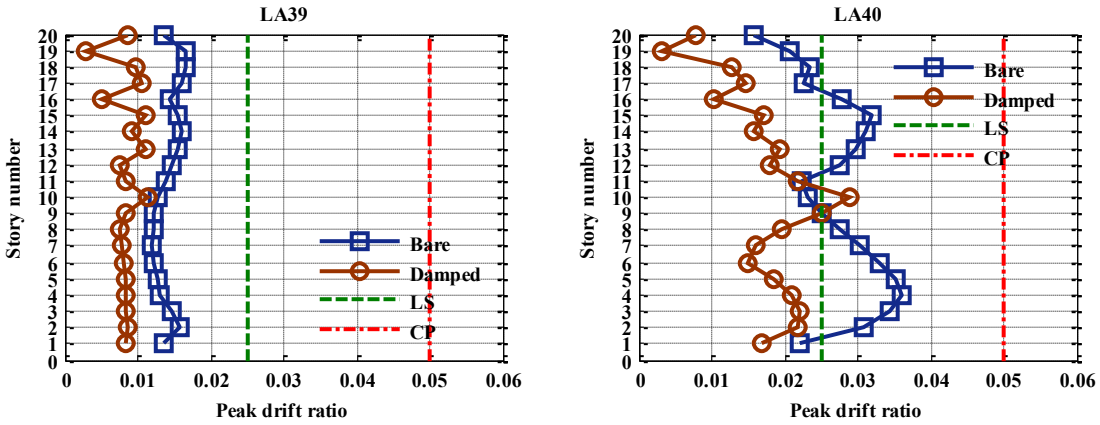


**Figure 5.71:** Comparative interstory drift ratios of 20-story FDBF and benchmark (part 8)

# 6. REDESIGN OF THE BENCHMARK BUILDINGS

Use of friction devices as a means of passive vibration control has been made and its technical effectiveness has been measured, compared and shown. In order to provide more arguments that allow a better assessment of the convenience of installing FDBs in a building either for its seismic strengthening or as part of its original design, the original benchmark buildings have been redesigned to comply with the ASCE-41 BSO without having to resort to any means of structural control. These redesigns are compared with the designs of the 3 FDBFs.

The designs given below were carried out by testing available W- and box-shapes in the frames and, eventually, selecting the lightest ones that made the building in question comply with the ASCE-41 BSO requirements. For this, the computer software SAP2000 was used. The designs were also made assuming that the original benchmark frames are already the most economical designs that satisfy the requirements of lower performance levels and/or that they satisfy a series of architectural requirements. That is why, while redesigning the frames, the philosophy was to keep modifications of the original benchmark buildings to the minimum. In other words, the overall arrangement and geometry of the frames was kept; end conditions, orientations and, whenever possible, depths of the frame elements were also respected.

Since the increase of the member sizes of only the earthquake MRFs does not represent a significant increase of the total (seismic) mass of the (3-D) building (around 3%), the seismic masses were kept the same. While attention was given to meeting

general code requirements, the technical designs of the new buildings could be subject of further improvement.

Finally, it is worth to mention that, for their analysis and design, all MRF models included all the additional features that were assigned to the original benchmark frames, namely, panel zones, clear span lengths, ASCE/FEMA nonlinear hinges, p-delta and large displacements effects, etc. The designs are provided in the next 3 parts.

## 6.1 3-Story Building

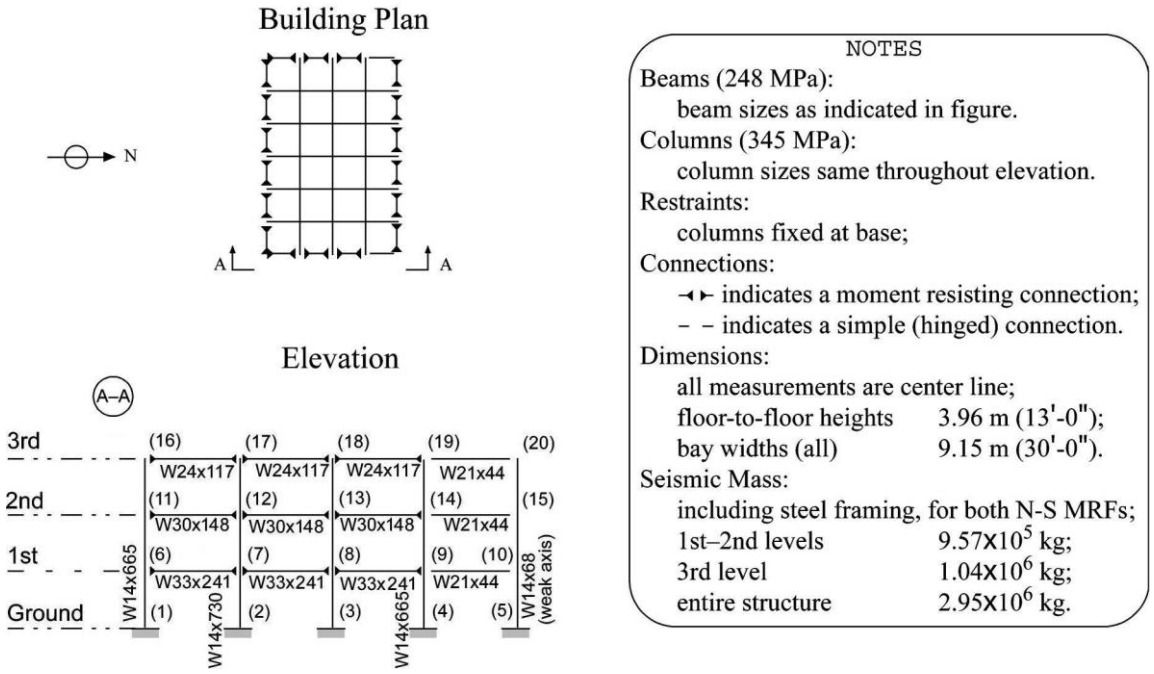


**Figure 6.1:** Redesigned 3-story building north-south moment-resisting frame (modified from (Ohtori et al. 2004))

## 6.2 9-Story Building

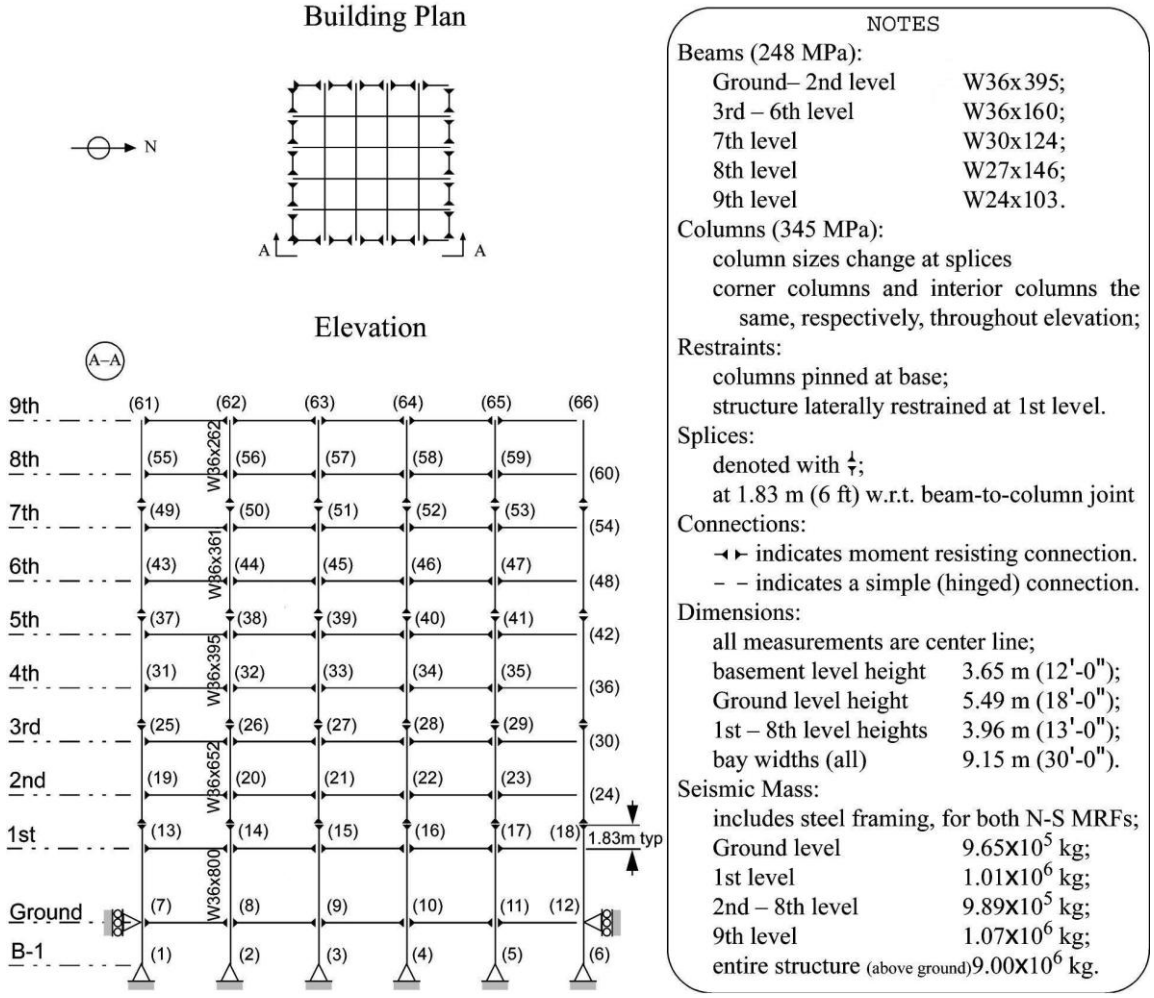


**Figure 6.2:** Redesigned 9-story building north-south moment-resisting frame (modified from (Ohtori et al. 2004))

## 6.3 20-Story Building

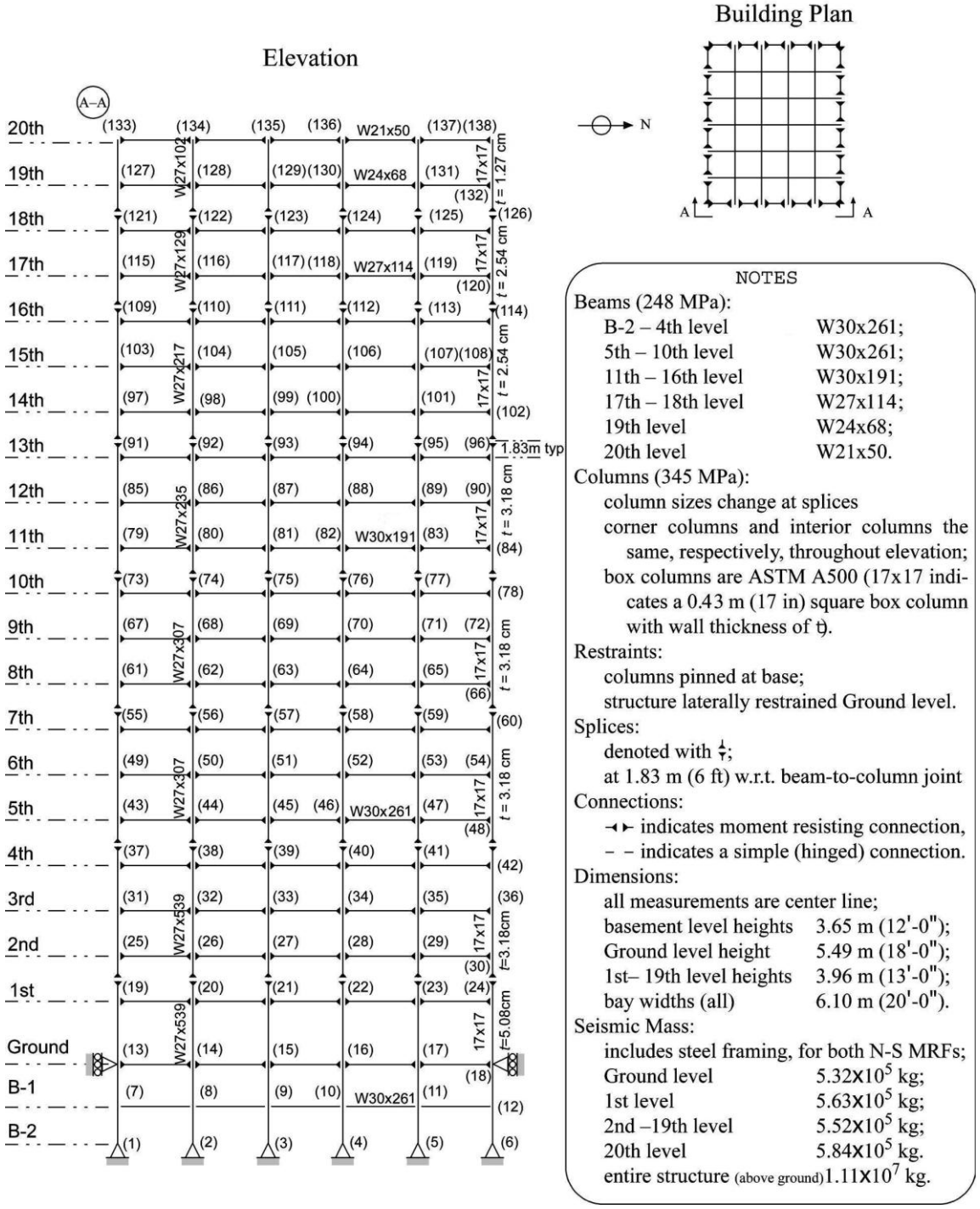


**Figure 6.3:** Redesigned 20-story building north-south moment-resisting frame (modified from (Ohtori et al. 2004))

## 6.4 Weights of the Original, Braced and Redesigned Buildings

In this section, the weights of the benchmark frames, the designed friction damped braced frames and the redesigned moment-resisting frames are calculated. The weight increase with respect to the benchmark frames of the FDBFs and the redesigned MRFs are compared as a means to assess the economic advantages of FDBs versus traditional MRFs.

It is worth recalling that both the FDBFs and the MRFs were designed to comply with the Basic Safety Objective drift requirements. Fulfillment of these requirements will imply fulfillment of the AISC strength requirements in the case of the MRFs, provided sufficient bracing of the column flanges is provided to preclude lateral torsional buckling. However, in the case of the FDBFs, the incorporation of the diagonal braces can cause overstressing of some of the structural members, especially the beams in the unbraced bays and some of the columns. Of course, a complete design of the FDBFs should account for this and include sections that resist the increased forces. This will obviously increase the weight of the FDBFs which, in turn, implies that the calculated weight savings of FDBFs versus MRFs are actually not as large as when the reductions in interstory drifts are considered as the only criterion for design.

**Table 6.1:** Structural weight of the 3-story benchmark building moment-resisting frame

**ORIGINAL 3-STORY FRAME**

**BEAMS**

**RIGID FRAMING**

| | Unit weight | Length | Number | Weight |
|---|---|---|---|---|
| **3rd level** | 68 | 30 | 3 | 6,120 |
| **2nd level** | 116 | 30 | 3 | 10,440 |
| **1st level** | 118 | 30 | 3 | 10,620 |

**SIMPLE FRAMING**

| | Unit weight | Length | Number | Weight |
|---|---|---|---|---|
| **1st-3rd level** | 44 | 30 | 3 | 3,960 |

**COLUMNS**

**RIGID FRAMING**

| | Unit weight | Length | Number | Weight |
|---|---|---|---|---|
| **1st-3rd story** | 257 | 39 | 2 | 20,046 |
| | **Unit weight** | **Length** | **Number** | **Weight** |
| **1st-3rd story** | 311 | 39 | 2 | 24,258 |

**SIMPLE FRAMING**

| | Unit weight | Length | Number | Weight |
|---|---|---|---|---|
| **1st-3rd story** | 68 | 13 | 3 | 2,652 |

TOTAL WEIGHT = **78,096** lb

**Table 6.2:** Structural weight of the 9-story benchmark building moment-resisting frame

**ORIGINAL 9-STORY FRAME**

**BEAMS**

| | Unit weight | Length | Number | Weight |
|---|---|---|---|---|
| **9th level** | 68 | 30 | 5 | 10,200 |
| **8th level** | 84 | 30 | 5 | 12,600 |
| **7th level** | 99 | 30 | 5 | 14,850 |
| **3rd-6th level** | 135 | 30 | 20 | 81,000 |
| **Ground-2nd** | 160 | 30 | 15 | 72,000 |

**COLUMNS**

| | Unit weight | Length | Number | Weight |
|---|---|---|---|---|
| **8th-9th story** | 257 | 20 | 6 | 30,840 |
| **6th-8th story** | 283 | 26 | 6 | 44,148 |
| **4th-6th story** | 370 | 26 | 6 | 57,720 |
| **2nd-4th story** | 455 | 26 | 6 | 70,980 |
| **B1-2nd story** | 500 | 36 | 6 | 108,000 |

TOTAL WEIGHT = **502,338** lb

**Table 6.3:** Structural weight of the 20-story benchmark building moment-resisting frame

**ORIGINAL 20-STORY FRAME**

**BEAMS**

| | Unit weight | Length | Number | Weight |
|---|---|---|---|---|
| **20th level** | 50 | 20 | 5 | 5,000 |
| **19th level** | 62 | 20 | 5 | 6,200 |
| **17th-18th level** | 84 | 20 | 10 | 16,800 |
| **11th-16th level** | 99 | 20 | 30 | 59,400 |
| **5th-10th level** | 108 | 20 | 30 | 64,800 |
| **B2-4th level** | 99 | 20 | 30 | 59,400 |

**COLUMNS**

**EXTERIOR**

| | Unit weight | Length | Number | Weight |
|---|---|---|---|---|
| **19th-20th story** | 99 | 20 | 2 | 3,960 |
| **14th-19th story** | 146 | 65 | 2 | 18,980 |
| **5th-14th story** | 191 | 117 | 2 | 44,694 |
| **2nd-5th story** | 234 | 39 | 2 | 18,252 |
| **B2-2nd story** | 354 | 48 | 2 | 33,984 |

**INTERIOR**

| | Unit weight | Length | Number | Weight |
|---|---|---|---|---|
| **19th-20th story** | 84 | 20 | 4 | 6,720 |
| **17th-19th story** | 117 | 26 | 4 | 12,168 |
| **14th-17th story** | 131 | 39 | 4 | 20,436 |
| **11th-14th story** | 192 | 39 | 4 | 29,952 |
| **5th-11th story** | 229 | 78 | 4 | 71,448 |
| **B2-5th story** | 335 | 87 | 4 | 116,580 |

TOTAL WEIGHT = **529,374** lb

**Table 6.4:** Structural weight of the FDBs in the 3-, 9- and 20- FDBFs

**WEIGHT OF BRACES**

**3-STORY FRAME**

| | Unit weight | Length | Number | Weight |
|---|---|---|---|---|
| **1st-3rd story** | 103 | 33 | 7 | 23,634 |
| | | TOTAL WEIGHT = | **23,634** | lb |

**9-STORY FRAME**

| | Unit weight | Length | Number | Weight |
|---|---|---|---|---|
| **1st story** | 96 | 35 | 4 | 13,497 |
| **2nd-9th story** | 96 | 33 | 28 | 88,294 |
| | | TOTAL WEIGHT = | **101,791** | lb |

**20-STORY FRAME**

| | Unit weight | Length | Number | Weight |
|---|---|---|---|---|
| **1st story** | 54 | 27 | 4 | 5,759 |
| **2nd-20th story** | 54 | 24 | 52 | 66,368 |
| | | TOTAL WEIGHT = | **72,127** | lb |

**Table 6.5:** Structural weight of the redesigned 3-story building moment-resisting frame

**REDESIGNED 3-STORY FRAME**

**BEAMS**

**RIGID FRAMING**

| | Unit weight | Length | Number | Weight |
|---|---|---|---|---|
| **3rd level** | 117 | 30 | 3 | 10,530 |
| **2nd level** | 148 | 30 | 3 | 13,320 |
| **1st level** | 241 | 30 | 3 | 21,690 |

**SIMPLE FRAMING**

| | Unit weight | Length | Number | Weight |
|---|---|---|---|---|
| **1st-3rd level** | 44 | 30 | 3 | 3,960 |

**COLUMNS**

**RIGID FRAMING**

| | Unit weight | Length | Number | Weight |
|---|---|---|---|---|
| **1st-3rd story** | 665 | 39 | 2 | 51,870 |
| | **Unit weight** | **Length** | **Number** | **Weight** |
| **1st-3rd story** | 730 | 39 | 2 | 56,940 |

**SIMPLE FRAMING**

| | Unit weight | Length | Number | Weight |
|---|---|---|---|---|
| **1st-3rd story** | 68 | 13 | 3 | 2,652 |

TOTAL WEIGHT = **160,962** lb

**Table 6.6:** Structural weight of the redesigned 9-story building moment-resisting frame

**REDESIGNED 9-STORY FRAME**

**BEAMS**

| | Unit weight | Length | Number | Weight |
|---|---|---|---|---|
| **9th level** | 103 | 30 | 5 | 15,450 |
| **8th level** | 146 | 30 | 5 | 21,900 |
| **7th level** | 124 | 30 | 5 | 18,600 |
| **3rd-6th level** | 160 | 30 | 20 | 96,000 |
| **Ground-2nd** | 395 | 30 | 15 | 177,750 |

**COLUMNS**

| | Unit weight | Length | Number | Weight |
|---|---|---|---|---|
| **8th-9th story** | 262 | 20 | 6 | 31,440 |
| **6th-8th story** | 361 | 26 | 6 | 56,316 |
| **4th-6th story** | 395 | 26 | 6 | 61,620 |
| **2nd-4th story** | 652 | 26 | 6 | 101,712 |
| **B1-2nd story** | 800 | 36 | 6 | 172,800 |

TOTAL WEIGHT = **753,588** lb

**Table 6.7:** Structural weight of the redesigned 20-story building moment-resisting frame

**REDESIGNED 20-STORY FRAME**

**BEAMS**

| | Unit weight | Length | Number | Weight |
|---|---|---|---|---|
| **20th level** | 50 | 20 | 5 | 5,000 |
| **19th level** | 68 | 20 | 5 | 6,800 |
| **17th-18th level** | 114 | 20 | 10 | 22,800 |
| **11th-16th level** | 191 | 20 | 30 | 114,600 |
| **5th-10th level** | 261 | 20 | 30 | 156,600 |
| **B2-4th level** | 261 | 20 | 30 | 156,600 |

**COLUMNS**

**EXTERIOR**

| | Unit weight | Length | Number | Weight |
|---|---|---|---|---|
| **19th-20th story** | 112 | 20 | 2 | 4,480 |
| **14th-19th story** | 218 | 65 | 2 | 28,340 |
| **5th-14th story** | 268 | 117 | 2 | 62,712 |
| **2nd-5th story** | 268 | 39 | 2 | 20,904 |
| **B2-2nd story** | 409 | 48 | 2 | 39,264 |

**INTERIOR**

| | Unit weight | Length | Number | Weight |
|---|---|---|---|---|
| **19th-20th story** | 102 | 20 | 4 | 8,160 |
| **17th-19th story** | 129 | 26 | 4 | 13,416 |
| **14th-17th story** | 217 | 39 | 4 | 33,852 |
| **11th-14th story** | 235 | 39 | 4 | 36,660 |
| **5th-11th story** | 307 | 78 | 4 | 95,784 |
| **B2-5th story** | 539 | 87 | 4 | 187,572 |

TOTAL WEIGHT = **836,944** lb

**Table 6.8:** Additional weights of the 3-, 9-, and 20-story FDBFs and redesigned moment-resisting frames

**ADDITIONAL WEIGHT TO ACHIEVE COMPLIANCE WITH ASCE-41**

**3-STORY FRAME**

| | Total weight | Weight increment | Percent increment | Percent savings |
|---|---|---|---|---|
| **Orignal** | 78,096 | — | — | — |
| **Friction damped** | 101,730 | 23,634 | 30 | 71 |
| **Redesigned MRF** | 160,962 | 82,866 | 106 | 0 |

**9-STORY FRAME**

| | Total weight | Weight increment | Percent increment | Percent savings |
|---|---|---|---|---|
| **Orignal** | 502,338 | — | — | — |
| **Friction damped** | 604,129 | 101,791 | 20 | 59 |
| **Redesigned MRF** | 753,588 | 251,250 | 50 | 0 |

**20-STORY FRAME**

| | Total weight | Weight increment | Percent increment | Percent savings |
|---|---|---|---|---|
| **Orignal** | 529,374 | — | — | — |
| **Friction damped** | 601,501 | 72,127 | 14 | 77 |
| **Redesigned MRF** | 836,944 | 307,570 | 58 | 0 |

# 7. DISCUSSION

The graphs concerning the optimization of the slip force and stiffness of the FDBs confirmed that the slip load is the parameter that has the largest influence on the response of FDBFs. For small friction forces, differences in the stiffness of the braces have negligible effects. It is only when the force of the friction device takes larger values that the stiffness of the braces gains relevance; however, the consideration of this fact should be used with discretion as is explained in the next paragraph.

If the slip load of a particular FDB is too high, the friction device might not slide and the FDB would act as a simple brace. If this happens, it is logical that the stiffness of the brace becomes, artificially, the only one design variable. In order to achieve sliding (and proper functioning) of a FDB having a large design force, it is necessary to use braces with large stiffness values, i.e. if the evaluation of a FDBF suggests the use of strong friction devices to cope with seismic forces, the design of the FDBs must include an appropriately chosen stiffness. The plots for optimization of the slip load and stiffness show which values of stiffness should be used with each friction force; these are those that permit the drawing of smooth curves; any separation of the curves could be an indication that energy dissipation has stopped occurring in the friction devices or, at least, in some of them.

The optimum slip load of the FDBs is easier to spot when low brace stiffness values are used, since the largest dissipation of energy will occur at lower friction forces. A (partial/localized) brace-like behavior will also occur at lower slip loads as well as a potential full brace-only behavior, which is displayed as a horizontally asymptotic value.

By the use of larger stiffness values, these behaviors are delayed and a broader spectrum of appropriate slip loads is obtained.

If large slip forces are used, the (ductility) demands in the primary structural members could become significantly larger after the friction devices reach their slip state. This is also why, often, larger slip forces do not guarantee lower peak interstory drifts. Selection of large slip loads can also cause large demands in the primary structural members when the FDBs are not placed uniformly throughout the height of the building.

The determination of the optimum friction force of the dampers becomes more difficult as the strength of the earthquake that is used in the process is increased. In fact, if a given earthquake record takes the response of a building close to its collapse, it becomes more challenging to find optimal values. These could also not be as reliable as those obtained using a relatively less severe earthquake. In general, the determination of the optimum slip load becomes more difficult when energy dissipation simultaneously takes place in the primary structural elements.

Filiatrault and Cherry (1987) suggested that the optimum value of the slip force of the friction dampers could be a mere structural property independent of the ground motions. After a couple of years of study they revealed that their assumption proved to be wrong. In this thesis, many graphs clearly show that the ground motions play a role in the selection of the optimum friction load. This is not clearly seen in previous research, but is shown in this thesis because of advancements in computer technology, which allowed undertaking a more extensive study that made this phenomenon more evident. Also, the use, in this work, of the benchmark buildings allowed carrying out the present

parametric study on real full scale analytical building models. It is probable that the small scale of the experimental and analytical models used in past research, together with the utilization of a smaller range of friction forces and stiffness values hid this issue to the authors of the studies.

# 8. CONCLUSIONS

A complete study on the behavior of friction damped braced frames has been developed to using recent trends, codes and evaluation criteria. Hence, it can be used to revise, standardize, update, enhance and supplement results of previously available research on the subject.

The way the work is outlined, both in its literature review and in the technical part, provides sufficient theoretical and analytical background, which can be used to better understand the problem of the application of friction damped braced frames as earthquake resisting system. Hence, this thesis should also be useful for achieving improved designs and evaluations of new or already existing FDBFs.

Conclusions made by other researchers regarding the effectiveness of FDBFs were confirmed. Results of the analyses that were carried out showed average reductions in the peak interstory drift ratios of almost 70% in the case of the 3-story building, 62% in the 9-story building and 35% in the case of the 20-story building after the FDBs were incorporated. Moreover, in many cases, not only the interstory drifts were significantly reduced and brought to acceptable levels, but also collapse of the structures was avoided. It is remarkable that success was attained in all cases.

On the other hand, the clearly underdesigned benchmark frames were redesigned to meet the ASCE-41 BSO requirements. Comparison between the additional weights of the new designs and those added by the inclusion of the FDBs into the original benchmarks showed that savings of more than 75% can be made if the option of installing FDBs is chosen instead of using bare MRFs for earthquake resistance. The

aforementioned percentage considers the case of projected new structures; however, if the necessity is that of retrofitting already existing MRFs, rebuilding of new and stronger MRFs represents absolutely no competition to retrofitting using FDBs.

Despite the extensiveness of this work, a couple of issues were not addressed and should be the subject of future research. There are still some factors that should be considered in the determination of a true optimal load; for instance, in the elaboration process of the present study, it became also evident that the optimal friction force is a function of the number and location of the FDBs throughout the height of the building.

On the other hand, determination of the optimum friction force of the devices should also take into account minimizing or avoiding residual/permanent interstory drifts. Consideration of these 2 issues would be the next logical step to be taken to broaden our knowledge on the use of friction for passive energy dissipation purposes in civil structures. It is worth mentioning that none of them has been addressed yet adequately.

Finally, taking into account variations of friction dampers and/or FDBs other than the type considered in this thesis would permit a more specialized assessment of the advantages of using a particular friction device over another.

# REFERENCES

Aiken, I., Kelly, J., and Pall, A. (1988). "Seismic response of a nine-story steel frame with friction damped cross-bracing." *Rep. No. UCB/EERC-88/17*, University of California, Berkeley, CA.

Aiken, I. D., and Kelly, J. M. (1990). "Earthquake simulator testing and analytical studies of two energy-absorbing systems for multistory structures." *Rep. No. UCB/EERC-90/03*, University of California, Berkeley, CA.

ASCE. (2003). "Seismic evaluation of existing buildings [ASCE-31]." American Society of Civil Engineers, Reston, VA.

ASCE. (2007). "Seismic rehabilitation of existing buildings [ASCE-41]." American Society of Civil Engineers, Reston, VA.

Booth, E., and Key, D. (2006). *Earthquake design practice for buildings*, Thomas Telford, London, England.

Chen, C. C., and Chen, G. D. (2002). "Nonlinear control of a 20-story steel building with active piezoelectric friction dampers." *Structural Engineering and Mechanics*, 14(1), 21-38.

Chen, G., and Chen, C. (2004). "Semiactive control of the 20-story benchmark building with piezoelectric friction dampers." *Journal of Engineering Mechanics*, 130(4), 393-400.

Chen, G. D., and Chen, C. C. (2003). "Semi-active control of a steel frame with piezoelectric friction dampers." *Proc., SPIE*, S.-C. Liu, ed., SPIE, Bellingham, WA, 207-217.

Chen, J. C., ed. (1996). *Proc., 2nd Int. Workshop on Structural Control: Next Generation of Intelligent Structures*, International Association for Structural Control (IASC) in conjunction with the Japan Panel on Structural Response Control and the U.S. Panel on Structural Control Research, The Hong Kong Univ. of Science and Technology, Hong Kong.

Chopra, A. (2001). *Dynamics of structures - Theory and applications to earthquake engineering*, Prentice Hall, Upper Saddle River, NJ.

Coburn, A., and Spence, R. (2002). *Earthquake protection*, Wiley, Chichester, England.

Constantinou, M., Reinhorn, A., Mokha, A., and Watson, R. (1991a). "Displacement control device for base isolated bridges." *Earthquake Spectra*, 7(2), 179-200.

Constantinou, M. C., Kartoum, A., Reinhorn, A. M., and Bradford, P. (1991b). "Experimental and theoretical study of a sliding isolation system for bridges." *Rep. No. NCEER 91-0027*, National Center for Earthquake Engineering Research, Buffalo, N.Y.

CSI. (2007a). *CSI analysis reference manual for SAP2000, ETABS and SAFE*, Computers and Structures Inc, Berkeley, CA.

CSI. (2007b). "SAP2000 Advanced." Computer and Structures Inc, Berkeley, CA.

FEMA. (2000). "Prestandard and Commentary for the Seismic Rehabilitation of Buildings." Federal Emergency Management Agency, Washington, DC.

Filiatrault, A., and Cherry, S. (1987). "Performance evaluation of friction damped braced steel frames under simulated earthquake loads." *Earthquake Spectra*, 3(1), 57-78.

FitzGerald, T. F., Anagnos, T., Goodson, M., and Zsutty, T. (1989). "Slotted bolted connections in aseismic design for concentrically braced connections." *Earthquake Spectra*, 5(2), 383-391.

Fu, Y., and Cherry, S. (1999). "Simplified seismic code design procedure for friction-damped steel frames." *Canadian Journal of Civil Engineering*, 26(1), 55-71.

Ghobarah, A. (2001). "Performance-based design in earthquake engineering: state of development." *Engineering Structures*, 23(8), 878-884.

Grigorian, C. E., and Popov, E. P. (1993). "Slotted bolted connections for energy dissipation." *Proc., ATC-17-1 Seminar on Seismic Isolation, Passive Energy Dissipation and Active Control*, ATC, San Francisco, CA, 545-556.

Guglielmino, E., and Edge, K. A. (2003). "The problem of controlling a friction damper: a robust approach." *Proc., American Control Conference*, AACC, Dayton, OH, 2827-2832.

Gupta, A., and Krawinkler, H. (1999). "Seismic demands for performance evaluation of steel moment resisting frame structures (SAC Task 5.4.3)." *Rep. No. 132*, The John A. Blume Earthquake Engineering Center, Stanford, CA.

Keightley, W. (1977). "Building damping by Coulomb friction." *Proc., 6th WCEE*, New Delhi, India, 3043-3048.

Keightley, W. (1979). *Prestressed walls for damping earthquake motions in buildings*, Montana State University, Dept. of Civil Engineering and Mechanics.

Kiggins, S., and Uang, C. M. (2006). "Reducing residual drift of buckling-restrained braced frames as a dual system." *Engineering Structures*, 28(11), 1525-1532.

Krinitzsky, E., Gould, J., and Edinger, P. (1993). *Fundamentals of earthquake-resistant construction*, John Wiley and Sons, New York.

Lane, J. S., Ferri, A. A., and Heck, B. S. (1992). "Vibration control using semi-active friction damping." *American Society of Mechanical Engineers, Design Engineering Division*, 49, 165-171.

Mead, D. (1998). *Passive vibration control*, John Wiley & Sons, Chichester, England.

Moehle, J. P. (1996). "Displacement-based seismic design criteria." *Proc., 11th World Conference on Earthquake Engineering*, Pergamon, Acapulco, Mexico.

Moreschi, L. M., and Singh, M. P. (2003). "Design of yielding metallic and friction dampers for optimal seismic performance." *Earthquake Engineering and Structural Dynamics*, 32(8), 1291-1311.

Mualla, I., and Belev, B. (2002). "Performance of steel frames with a new friction damper device under earthquake excitation." *Engineering Structures*, 24(3), 365-371.

Ng, C. L., and Xu, Y. L. (2004). "Seismic response control of a complex structure using semi-active friction dampers." *Proc., SPIE*, S.-C. Liu, ed., SPIE, Bellingham, WA, 177-188.

Nishitani, A., Nitta, Y., Ishibashi, Y., and Itoh, A. (1999). "Semi-active structural control with variable friction dampers." *Proc., American Control Conference*, AACC, Dayton, OH, 1017-1021.

Ohtori, Y., Spencer Jr, B. F., and Dyke, S. J. (2004). "Benchmark control problems for seismically excited nonlinear buildings." *Journal of Engineering Mechanics*, 130(4), 366-385.

Pall, A., and Marsh, C. (1982). "Seismic response of friction damped braced frames." *Journal of the Structural Division*, 108(6), 1313-1323.

Pall, A., Marsh, C., and Fazio, P. (1980). "Friction joints for seismic control of large panel structures." *Journal of Prestressed Concrete Institute*, 25(6), 38-61.

Pall, A., and Pall, R. T. (2004). "Performance-based design using Pall friction dampers - An economical design solution." *Proc., 13th World Conference on Earthquake Engineering*, Vancouver, B. C., Canada.

PDL. "Pall Dynamics Ltd."

Sabelli, R., Mahin, S., and Chang, C. (2003). "Seismic demands on steel braced frame buildings with buckling-restrained braces." *Engineering Structures*, 25(5), 655-666.

SAC_Steel_Project. (1994). Technical Office, Richmond, CA 94804-4698.

Somerville, P. G. (1997). "Development of ground motion time-histories for phase 2 of the FEMA/SAC steel project." *Rep. No. SAC/BD-97/04*, SAC Joint Venture, Sacramento, CA.

Soong, T. T., and Constantinou, M. C., eds. (1994). *Passive and active structural vibration control in civil engineering*, CISM Courses and Lectures, Springer, New York.

Soong, T. T., and Dargush, G. F. (1997). *Passive energy dissipation systems in structural engineering*, Wiley, New York.

Spencer, B. F., Christenson, R. E., and Dyke, S. J. (1999). "Next generation benchmark control problem for seismically excited buildings." *Proc., 2nd World Conf. on Structural Control*, T. Kobori et al., eds., Vol. 2, Wiley, New York, 1135-1360.

Spencer, B. F., Dyke, S. J., and Deoskar, H. S. (1998a). "Benchmark problems in structural control: part I - active mass driver system." *Earthquake Engineering & Structural Dynamics*, 27(11), 1127-1139.

Spencer, B. F., Dyke, S. J., and Deoskar, H. S. (1998b). "Benchmark problems in structural control: part II - active tendon system." *Earthquake Engineering & Structural Dynamics*, 27(11), 1141-1147.

TheMathWorks. (2008). "SIMULINK." The MathWorks, Natick, MA.

Wen, Y. (1976). "Method for random vibration of hysteretic systems." *Journal of the Engineering Mechanics Division*, 102(2), 249-263.

Zhu, S., and Zhang, Y. (2008). "Seismic analysis of concentrically braced frame systems with self-centering friction damping braces." *Journal of Structural Engineering*, 134(1), 121-131.

# VITA

**Name:** Luis Eduardo Peternell Altamira

**Address:** Zachry Department of Civil Engineering,

Texas A&M University,

3136 TAMU

College Station, Texas 77843-3136

**E-mail:** lepa@tamu.edu

**Education:** B.S., Civil Engineering, Universidad de las Américas, Puebla, Mexico, 2005

M.S., Civil Engineering, Texas A&M University, 2009